

1 **Comparative transcriptomics analyses across species, organs and developmental stages reveal**
2 **functionally constrained lncRNAs**

3

4 Fabrice Darbellay^{1,§,*} and Anamaria Necsulea^{1,2,*}

5

6

7 ¹School of Life Sciences, École Polytechnique Fédérale de Lausanne (EPFL), Lausanne, Switzerland

8 ²Université de Lyon, Université Lyon 1, CNRS, Laboratoire de Biométrie et Biologie Évolutive UMR

9 5558, F-69622 Villeurbanne, France

10

11 [§]Present address: Environmental Genomics and Systems Biology Division, Lawrence Berkeley

12 National Laboratory, 1 Cyclotron Road, Berkeley, California 94720, USA.

13

14

15 *Corresponding authors:

16 Fabrice Darbellay (fabrice.darbellay@epfl.ch)

17 Anamaria Necsulea (anamaria.necsulea@univ-lyon1.fr)

18

19 Running title: Functionally constrained lncRNAs in embryonic development

20

21 Keywords: long non-coding RNAs; evolution; development; comparative transcriptomics.

22

23

24

25 **Abstract**

26 **Background** Transcription of long non-coding RNAs (lncRNAs) is pervasive, but their functionality is
27 disputed. As a class, lncRNAs show little selective constraint and negligible phenotypic effects upon
28 perturbation. However, key biological roles were demonstrated for individual lncRNAs. Most validated
29 lncRNAs were implicated in gene expression regulation, in pathways related to cellular pluripotency,
30 differentiation and organ morphogenesis, suggesting that functional lncRNAs may be more abundant
31 in embryonic development, rather than in adult organs.

32 **Results** Here, we perform a multi-dimensional comparative transcriptomics analysis, across five
33 developmental time-points (two embryonic stages, newborn, adult and aged individuals), four organs
34 (brain, kidney, liver and testes) and three species (mouse, rat and chicken). Overwhelmingly, lncRNAs
35 are preferentially expressed in adult and aged testes, consistent with the presence of permissive
36 transcription during spermatogenesis. lncRNAs are often differentially expressed among
37 developmental stages and are less abundant in embryos and newborns compared to adult individuals,
38 in agreement with a requirement for tighter expression control and less tolerance for noisy
39 transcription early in development. However, lncRNAs expressed during embryonic development
40 show increased levels of evolutionary conservation, both in terms of primary sequence and of
41 expression patterns, and in particular at their promoter regions. We find that species-specific lncRNA
42 transcription is frequent for enhancer-associated loci and occurs in parallel with expression pattern
43 changes for neighboring protein-coding genes.

44 **Conclusions** We show that functionally constrained lncRNA loci are enriched in developing organ
45 transcriptomes, and propose that many of these loci may function in an RNA-independent manner.

46

47 **Background**

48 Long non-coding RNAs (lncRNAs, loosely defined as transcripts that lack protein-coding potential, at
49 least 200 nucleotides long) are an excellent illustration of the ongoing conceptual tug-of-war between
50 biochemical activity and biological function (Graur et al. 2013; Doolittle 2018). The development of
51 sensitive transcriptome exploration techniques led to the identification of thousands of lncRNA loci in
52 vertebrates (Guttman et al. 2009; Khalil et al. 2009; Iyer et al. 2015; Pertea et al. 2018). While this ever
53 wider class of transcripts includes well-studied lncRNAs with undisputed biological roles, such as *Xist*
54 (Brown et al. 1991) or *H19* (Brannan et al. 1990), experimental validations are lacking for the great
55 majority of lncRNAs and their functionality is controversial.

56
57 The first functional characterizations of individual lncRNAs forged the idea that these non-coding
58 transcripts are important contributors to gene expression regulatory networks. This has been
59 unequivocally proven for some lncRNAs, such as *Xist*, whose transcription and subsequent coating of
60 the X chromosome triggers a complex chain of molecular events leading to X inactivation in placental
61 mammals (Gendrel and Heard 2014). Additional proposed mechanisms for gene expression regulation
62 by lncRNAs included directing chromatin-modifying complexes at specific genomic locations, to control
63 gene expression in *trans* (Rinn et al. 2007); providing decoy targets for microRNAs (Cesana et al. 2011);
64 enhancing expression of neighboring genes through an RNA-dependent mechanism (Ørom et al. 2010).
65 These initial studies generally asserted that the biological function of lncRNA loci is directly carried out
66 by the transcribed RNA molecule. However, it was shown early on that in some cases the function
67 resides in the act of transcription at a given genomic location, rather than in the product of
68 transcription (Latos et al. 2012). Moreover, several recent publications showed that lncRNA transcripts
69 are not required, and that instead biological functions are carried out by other elements embedded in
70 the lncRNA genomic loci (Bassett et al. 2014). For example, it was recently shown that transcription of
71 the *Linc-p21* gene, originally described as a *cis*-acting enhancer lncRNA, is not needed to regulate
72 neighboring gene expression (Groff et al. 2016). Genetic engineering of multiple lncRNA loci in mouse

73 likewise showed that lncRNA transcripts are dispensable, and that gene expression regulation by
74 lncRNA loci is instead achieved by the process of lncRNA transcription and splicing, or by additional
75 regulatory elements found in lncRNA promoters (Engreitz et al. 2016; Anderson et al. 2016).
76 Furthermore, some attempts to look for lncRNA function through genetic engineering approaches
77 showed that the tested lncRNA loci are altogether dispensable (Amândio et al. 2016; Zakany et al.
78 2017; Goudarzi et al. 2019). These recent observations signal a paradigm shift in lncRNA biology, as it
79 is increasingly acknowledged that, even when phenotypic effects can be unambiguously mapped to
80 lncRNA loci, the underlying biological processes are not necessarily driven by the lncRNA transcripts
81 themselves.

82
83 Importantly, this new perspective on lncRNA biology had been predicted by evolutionary analyses,
84 which have long been used to evaluate the functionality of diverse genomic elements (Haerty and
85 Ponting 2014; Ulitsky 2016). Evolutionary studies of lncRNAs in vertebrates all agree that the extent of
86 selective constraint on lncRNA primary sequences is very low, though significantly above the genomic
87 background (Ponjavic et al. 2007; Kutter et al. 2012; Necsulea et al. 2014; Washietl et al. 2014; Hezroni
88 et al. 2015). These observations are compatible with the hypothesis that many of the lncRNAs detected
89 with sensitive transcriptomics techniques may be non-functional noise (Ponjavic et al. 2007), but may
90 also indicate that lncRNA functionality does not reside in the primary transcribed sequence. In
91 contrast, mammalian lncRNA promoters show higher levels of sequence conservation, similar to
92 protein-coding gene promoters (Necsulea et al. 2014), as expected if they carry out enhancer-like
93 regulatory functions independently of the transcribed RNA molecule. Moreover, it was previously
94 reported that, in multi-exonic lncRNAs, splicing regulatory elements are more conserved than the rest
95 of the exonic sequence (Schüler et al. 2014; Haerty and Ponting 2015), which is compatible with the
96 recent finding that lncRNA splicing can contribute to neighboring gene regulation (Engreitz et al. 2016).
97 Thus, detailed evolutionary analyses of lncRNA loci can bring important insights into their functionality,
98 and can help to prioritize candidates for experimental validation.

99

100 At present, comparative transcriptomics analyses in vertebrates indicate that the extent of
101 evolutionary conservation of lncRNA sequences and expression patterns is very limited. However,
102 these studies were so far restricted to adult organ transcriptomes. In particular, it was shown that
103 most known vertebrate lncRNAs are active in adult testes and thus likely during spermatogenesis, a
104 process characterized by a permissive chromatin environment, which can promote non-functional
105 transcription (Soumillon et al. 2013). The resulting lncRNA datasets may thus be enriched in non-
106 functional transcripts. Additional lines of evidence suggest that the search for functional lncRNAs
107 should be extended beyond adult organ transcriptomes. For example, involvement in developmental
108 phenotypes was proposed for many experimentally-tested lncRNAs (Sauvageau et al. 2013; Ulitsky et
109 al. 2011; Grote et al. 2013), and an enrichment for developmental transcription factor binding was
110 reported for the promoters of highly conserved lncRNAs (Necsulea et al. 2014). These observations
111 motivated us to add a temporal dimension to comparative lncRNA transcriptomics studies. Therefore,
112 here we characterize the lncRNA transcriptomes of two model mammalian species (mouse and rat), in
113 four major organs (brain, kidney, liver and testes), across five developmental stages that cover the
114 entire lifespan of the individuals (including two embryonic stages, newborn, young adult and aged
115 individuals). To gain a deeper evolutionary perspective, we generate similar data for embryonic stages
116 of chicken somatic organs. We analyze the spatial and temporal expression patterns of protein-coding
117 and lncRNA genes, in conjunction with their evolutionary conservation. We find that, while lncRNAs
118 are overall poorly conserved among species in terms of primary sequence or expression patterns,
119 higher frequencies of evolutionarily constrained lncRNAs are observed in embryonic transcriptomes.
120 For many of these loci, biological function may be RNA-independent, as the highest levels of sequence
121 conservation are observed on promoter regions and on splice signals, rather than on lncRNA exonic
122 sequence. Our results are thus compatible with unconventional, RNA-independent functions for
123 lncRNA loci, in particular for those that are expressed during embryonic development.

124 **Results**

125 *Comparative transcriptomics across species, organs and developmental stages*

126 To study protein-coding and lncRNA expression patterns across both developmental and evolutionary
127 time, we generated RNA-seq data for mouse and rat, for four major organs (brain, kidney, liver and
128 testes) and five developmental time points, including two embryonic stages, newborn, young and aged
129 adult individuals (Figure 1A, Supplementary Table 1, Methods). The selected time points allow us to
130 obtain a broad view of major organ ontogenesis and to capture drastic physiological changes during
131 development (Theiler 1989). We chose to include in our study both young adult (8-10 weeks old) and
132 aged adult individuals (12 to 24 months old), to investigate transcriptomic changes that occur later in
133 life, thus completing our overview of the temporal patterns of gene expression variation. At the
134 earliest embryonic stage (day 13.5 post-conception for mouse, day 15 for rat), only three of the four
135 studied organs, with the exception of the testes, are well differentiated and large enough to be readily
136 dissected. Our experimental design for mouse and rat thus comprises 19 organ / developmental stage
137 combinations. Although most of our study relies on mouse-rat comparisons, to obtain a broader
138 evolutionary perspective we generated comparable RNA-seq data for the chicken, for the two earliest
139 developmental stages (Figure 1A, Supplementary Table 1). We obtained between 2 and 4 biological
140 replicates for each species/organ/developmental stage combination (Supplementary Table 1).
141 Additional RNA-seq samples from previous publications were included in the lncRNA annotation
142 pipeline, to increase detection sensitivity (Supplementary Table 2, Methods).

143
144 The organs and developmental stages included in our study differ greatly in terms of their cellular
145 composition diversity. To verify that our whole-organ RNA-seq data reflects cellular composition
146 heterogeneity, we assessed the expression patterns of cell population markers derived from single-
147 cell transcriptomics studies (Tabula Muris Consortium 2018; Green et al. 2018) in our samples (Figure
148 1B, Supplementary Table 3). This analysis confirms that our transcriptome collection reflects expected
149 developmental patterns. For example, mature oligodendrocyte cell markers are systematically highly

150 expressed in adult brain, while oligodendrocyte precursor markers are more highly expressed in the
151 earliest developmental stages (Figure 1B). Similarly, *Neurod6*, a gene involved in neuronal
152 differentiation (Kathleen Baxter et al. 2009), is preferentially expressed in embryonic and newborn
153 brain. Moreover, spermatogenesis-specific markers are enriched in adult but not in embryonic and
154 newborn testes, while markers for somatic cells (Leydig, Sertoli cells) are expressed earlier during
155 testes development (Figure 1B). Immune cell markers tend to be more broadly shared across organs
156 and developmental stages, but show strongest expression in the late embryo and newborn liver (Figure
157 1B), consistent with this organ's crucial role in establishing immunity (Nakagaki et al. 2018). In general,
158 adult organ transcriptomes contain higher numbers of expressed cell type-specific markers (Figure 1B).
159 However, as these genes were defined based on adult organ data, this observation may indicate that
160 cell sub-populations that are specific to embryonic organs are under-represented in this marker set,
161 rather than reflecting the true cellular diversity at different developmental stages.

162

163 We note that, in some cases, the cell type-specific markers predicted by single-cell transcriptomics
164 studies have seemingly unexpected expression patterns in our whole-organ RNA-seq collection. For
165 example, the expression of *Parvalbumin (Pvalb)*, which was proposed as a marker for collecting duct
166 epithelial cells in the kidney (Tabula Muris Consortium 2018), is highest in the adult and aged brain,
167 for both mouse and rat (Figure 1B). Likewise, cellular retinoic acid binding protein 1 (*Crabp1*), which
168 was predominantly detected in spermatogonia in a single-cell transcriptomics study of mouse testes
169 (Green et al. 2018), is preferentially expressed in mid-stage embryonic kidney in our samples (Figure
170 1B). These apparent discrepancies likely reflect the pleiotropic nature of genes, as well as the presence
171 of similar cell types across organs with distinct physiological functions (Arendt et al. 2016). In general,
172 the genes proposed as markers for major cell types behave similarly in mouse and rat, although some
173 species-specific patterns can be observed, in particular for immune cell markers (Figure 1B). Likewise,
174 for those genes that had orthologues in the chicken, expression patterns are generally similar among
175 species, with higher between-species divergence for immunity-related genes (Supplementary Figure

176 1). This observation confirms that the organs and developmental stages selected for our integrative
177 transcriptomics study are comparable across species.

178

179 We note that the cell-type specific markers that we analyzed here cannot always discriminate between
180 organs and developmental stages, as expected given that some cell sub-populations are shared among
181 tissues. To further characterize our transcriptome collection and identify the patterns that are specific
182 to each sample, we sought to identify genes that could serve as markers for organ/developmental
183 stage combinations. To do this, we selected genes that have narrow expression distributions, and for
184 which the maximum expression is observed in the same organ/developmental stage combination in
185 mouse and rat (Methods, Supplementary Table 4, Supplementary Figures 2-5). Gene ontology
186 enrichment analyses for the resulting lists of genes (Supplementary Dataset 3) are coherent with the
187 cellular composition and biological processes at work in the corresponding samples. For example, we
188 observe strong over-representation of genes involved in forebrain neuron differentiation in the mid-
189 stage embryonic brains, while processes related to synaptic transmission are enriched among genes
190 specifically expressed in adult brains (Supplementary Figure 2). In the kidney, the early developmental
191 stages are expectedly enriched in genes involved in metanephric development (Supplementary Figure
192 3). The newborn liver stands out due to its strong enrichment in genes involved in immune response,
193 while metabolic processes are over-represented in the adult livers (Supplementary Figure 4).
194 Embryonic testes samples express genes implicated in gamete generation and gene silencing by
195 miRNAs, including the *Piwi*-like genes, while adult testes transcriptomes are dominated by genes
196 involved in spermatogenesis (Supplementary Figure 5). These expected patterns confirm that our
197 whole-organ transcriptomics collection provides a good overview of the cell composition changes and
198 physiological transitions that occur during organ development.

199 *Developmental expression patterns are well conserved among species for protein-coding genes*

200 Broad patterns of transcriptome evolution are already visible in our analyses of cell type specific
201 markers and of transcriptome complexity: individual gene expression profiles and numbers of

202 expressed genes are generally similar between mouse and rat, while more divergence is observed
203 between the two rodent species and the chicken (Figure 1B-D, Supplementary Figure 1). To further
204 explore the evolution of developmental gene expression patterns, we performed a principal
205 component analysis (PCA) on normalized, log-transformed TPM values for 10,363 protein-coding
206 genes shared among the three species (Methods, Figure 2A). This analysis revealed that the main
207 source of gene expression variability among species, organs and developmental stages is the
208 distinction between adult and aged testes and the other samples, which are separated on the first PCA
209 axis (Figure 2A). In contrast, embryonic and newborn testes are grouped with kidney samples from
210 similar developmental stages, in agreement with the common developmental origin of the kidney and
211 the gonads (McMahon 2016). The first axis of the PCA, which explains 67% of the total expression
212 variance, also correlates with the developmental stage: samples derived from adult and aged
213 individuals have higher coordinates on this axis than embryonic and newborn samples, for mouse and
214 rat (Figure 2A). The second PCA axis (10% explained variability) mainly reflects the difference between
215 brain and the other organs (Figure 2A). While mouse and rat samples are generally undistinguishable,
216 the PCA confirms that there is considerably higher expression divergence between chicken and the
217 two rodent species (Figure 2A). However, differences among major organs are stronger than
218 differences among species, even at these broad evolutionary distances: brain samples all cluster
219 together, irrespective of the species of origin, and are clearly separated from kidney and liver samples
220 on the second PCA axis (Figure 2A). Interestingly, within the brain cluster, embryonic chicken samples
221 tend to be closer to adult and aged rodent brains than to embryonic or neonate samples (Figure 2A).

222
223 These broad patterns of gene expression variations among species, organs and developmental stages
224 are confirmed by a hierarchical clustering analysis based on Spearman's correlation coefficients
225 between pairs of samples (Figure 2B). The strongest clustering is observed for adult and aged testes
226 samples, followed by a robust grouping of brain samples, irrespective of the species (Figure 2B).

227

228 The grouping among samples derived from similar organs and developmental stages, irrespective of
229 the species of origin, is considerably stronger for genes that are associated with embryonic
230 development and with gene expression regulation (Methods, Figure 2C,D). For this set of genes, both
231 the principal component analysis and the hierarchical clustering analysis are characterized by a near-
232 perfect separation of organs and developmental stages, for all three species (Figure 2C,D). Chicken
233 samples, which clustered apart from rodent samples in whole transcriptome analyses, are now
234 grouped with the corresponding organs and developmental stages from mouse and rat. Our
235 transcriptome collection can thus reveal highly conserved expression patterns for key regulators of
236 embryonic development, across vertebrates.

237 *Variations in transcriptome complexity among organs and developmental stages*

238 We next sought to assess the transcriptome complexity in different organs across developmental
239 stages, for both protein-coding genes and lncRNAs. To predict lncRNAs, we used the RNA-seq data to
240 reconstruct gene models with StringTie (Pertea et al. 2015), building on existing genomic annotations
241 (Cunningham et al. 2019). We verified the protein-coding potential of newly annotated transcripts,
242 based on the codon substitution frequency score (Lin et al. 2007, 2011) and on sequence similarity
243 with known proteins, and we applied a stringent series of filters to reduce contaminations from un-
244 annotated protein-coding UTRs and other artefacts (Methods). We thus obtain a total of 18,858
245 candidate lncRNAs in the mouse, 20,159 in the rat and 5,496 in the chicken, including both newly-
246 annotated and previously known lncRNAs transcribed in our samples (Supplementary Dataset 1). We
247 note that many of these candidate lncRNAs are expressed at very low levels. When imposing a
248 minimum normalized expression level (transcript per million, or TPM) at least equal to 1, in at least
249 one sample, the numbers of candidate lncRNAs falls to 12,199, 15,319 and 2,892 in the mouse, rat and
250 chicken, respectively (Supplementary Datasets 2-3, Supplementary Table 4).

251

252 The differences in lncRNA content among species may reflect discrepancies in RNA-seq read coverage
253 and sample distribution, as well as genome sequence and annotation quality. To correct for the effect

254 of RNA-seq read coverage, we down-sampled the RNA-seq data to obtain the same number of uniquely
255 mapped reads for each organ/developmental stage combination within each species (Methods). After
256 this equalizing procedure, the number of detectable protein-coding genes (supported by at least 10
257 uniquely mapped reads) still shows broad variations among organs and developmental stages, with
258 the highest numbers of genes detected in the testes, for all time points (Figure 3A). Large numbers of
259 protein-coding genes (between 12,800 and 16,700) are detected in all samples. In contrast, for
260 lncRNAs, the pattern is much more striking: the young and aged adult testes express between 11,000
261 and 12,000 lncRNAs, in both mouse and rat, while in somatic organs and earlier developmental stages
262 we can detect only between 1,800 and 4,800 lncRNAs (Figure 3B). This observation is in agreement
263 with previous findings indicating that the particular chromatin environment of the adult testes, and in
264 particular of spermatogenesis-specific cell types, is extraordinarily permissive to transcription
265 (Soumillon et al. 2013). Interestingly, the numbers of protein-coding genes detectable in each organ
266 also varies among developmental stages. In young and aged adult individuals, the brain shows the
267 second-highest number of expressed protein-coding genes, after the testes, as previously observed
268 (Soumillon et al. 2013; Ramsköld et al. 2009). However, in embryonic and newborn samples, the kidney
269 expresses higher numbers of protein-coding genes than the brain (Figure 3B).

270 *Spatial and temporal expression pattern differences between protein-coding genes and lncRNAs*

271 We next compared spatial and temporal expression patterns between protein-coding genes and
272 lncRNAs. In agreement with previous findings (Soumillon et al. 2013), we show that lncRNAs are
273 overwhelmingly preferentially expressed in the testes (Figure 4A). Indeed, more than 68% of lncRNAs
274 reach their maximum expression level in this organ, compared to only approximately 32% of protein-
275 coding genes, for both mouse and rat (Figure 4A). Interestingly, more than 80% of lncRNAs are
276 preferentially expressed in young and aged adult samples, compared to only 62% of protein-coding
277 genes (Figure 4B).

278

279 As noted previously, between 59 and 82% of protein-coding genes are significantly differentially
280 expressed (DE) among developmental stages, at a false discovery rate (FDR) below 1%, in each organ
281 and species (Figure 4C, Supplementary Dataset 4). The proportions of DE lncRNAs are much lower in
282 somatic organs, between 18 and 40%, but are similar in the testes, around 75% (Figure 4C). However,
283 we suspected that this could be due to the low expression levels of this class of genes, as total read
284 counts are known to affect the sensitivity of DE analyses (Anders and Huber 2010). Indeed, as
285 previously observed, lncRNAs are expressed at much lower levels than protein-coding genes
286 (Supplementary Figure 7). To control for this effect, we down-sampled the read counts observed for
287 protein-coding genes, bringing them to the same average counts as lncRNAs but preserving relative
288 gene abundance (Methods). Strikingly, when performing the DE analysis on this dataset, we observe
289 higher proportions of DE loci for lncRNAs compared to protein-coding genes (Figure 4C). Moreover,
290 the amplitude of expression variation among developmental stages are more important for lncRNAs
291 than for protein-coding genes (Supplementary Figure 8A). This is expected given the lower lncRNA
292 expression levels, which preclude detecting subtle expression shifts among time points. Finally, we
293 observe that the developmental stage with maximum expression is generally different between
294 protein-coding genes and lncRNAs, even when considering genes that are significantly DE among
295 stages. For all organs, DE lncRNAs tend to show highest expression levels in the young and aged adults,
296 while DE protein-coding genes are more homogeneously distributed among developmental stages
297 (Figure 4D, Supplementary Figure 8B).

298
299 Similar conclusions are reached when performing DE analyses between consecutive time points
300 (Supplementary Dataset 4, Supplementary Figure 6). For both protein-coding genes and lncRNAs, the
301 strongest expression changes are observed between newborn and young adult individuals. Almost
302 10,000 lncRNAs are significantly up-regulated between newborn and young adult testes, confirming
303 the strong enrichment for lncRNAs during spermatogenesis (Supplementary Dataset 4). We note that,
304 as expected, the lowest numbers of DE genes are observed at the transition between young and aged

305 adult organs. At this time-point, we observe more changes for the rat than for the mouse, potentially
306 due to a higher proportion of immune cell infiltrates in rat aged organs. Genes associated with antigen
307 processing and presentation tend to be expressed at higher levels in aged adults than in young adults,
308 for mouse kidney, rat brain and liver (Supplementary Dataset 4).

309 *Stronger selective constraint on lncRNAs expressed earlier in development*

310 We next analyzed the patterns of long-term evolutionary sequence conservation for lncRNAs, in
311 conjunction with their spatio-temporal expression pattern (Supplementary Table 6). We used the
312 PhastCons score (Siepel et al. 2005) across placental mammals (Casper et al. 2018), to assess the level
313 of sequence conservation for various aspects of mouse lncRNAs: exonic promoter regions (defined as
314 1 kb regions upstream of the transcription start site, masking any exonic sequence within this region),
315 splice sites (first and last two bases of the introns, for multi-exonic loci). As approximately 20% of
316 lncRNAs overlap with exonic regions from other genes on the opposite strand (Supplementary Dataset
317 1), we masked exonic sequences from other genes before computing sequence conservation scores.
318 As previously observed (Ponjavic et al. 2007; Haerty and Ponting 2013), the amount of exonic and
319 splice site sequence conservation is much lower for lncRNAs than for protein-coding genes, but above
320 the average conservation observed for intergenic regions (Figure 5A, C). In contrast, promoter
321 sequence conservation levels are more comparable between protein-coding genes and lncRNAs
322 (Figure 5B). The highest levels of conservation are observed for bidirectional promoters, shared with
323 protein-coding genes (Figure 5B).

324

325 We next analyzed sets of protein-coding genes and lncRNAs that are expressed above noise levels
326 (TPM>=1, averaged across all replicates) in each organ / developmental stage combination. For exonic
327 sequences and splice site regions, the extent of sequence conservation is much lower for lncRNAs than
328 for protein-coding genes, irrespective of the organ and developmental stage in which they are
329 expressed (Figure 5D, F). For all examined regions and for both categories of genes, the spatio-
330 temporal expression pattern is well correlated with the level of sequence conservation. Globally,

331 sequence conservation is higher for genes that are expressed earlier in development than for genes
332 expressed later in development, and is significantly higher for somatic organs than for adult and aged
333 testes (Figure 5D-F). Interestingly, for genes that are highly expressed in mid-stage embryonic brain
334 and kidney samples, the levels of promoter sequence conservation are higher for lncRNAs than for
335 protein-coding genes (Figure 5E). However, this pattern is mainly due to those lncRNA loci that have
336 bidirectional promoters, shared with protein-coding genes or with other non-coding loci
337 (Supplementary Figure 9A-C).

338
339 Finally, we asked whether the highest level of evolutionary sequence conservation is seen at exons,
340 promoter or splice site regions, for each lncRNA locus taken individually. We show that this pattern
341 also depends on the organs and the developmental stages where the lncRNAs are expressed: for loci
342 detected in somatic organs and in the developing testes, there is significantly higher conservation for
343 the promoter and the splice sites than for exonic regions (Supplementary Figure 9D, E). However, for
344 lncRNAs that are highly transcribed in the adult and aged testes (which constitutes the great majority
345 of genes), this pattern is absent (Supplementary Figure 9D, E).

346 *Detection of homologous lncRNAs across species*

347 Having investigated the patterns of long-term sequence conservation of mouse lncRNAs, we next
348 sought to assess the conservation of lncRNA repertoires in mouse, rat and chicken. We detected
349 lncRNA separately in each species, using only RNA-seq data and existing genome annotations, as
350 previously suggested (Hezroni et al. 2015). We then searched for putative 1-to-1 orthologous lncRNAs
351 between species using pre-computed whole-genome alignments as a guide (Methods), to increase the
352 sensitivity of orthologous gene detection in the presence of rapid sequence evolution (Washietl et al.
353 2014). The orthologous lncRNA detection procedure involves several steps, including the identification
354 of putative homologous (projected) loci across species, filtering to remove large-scale structural
355 changes in the loci and intersection with predicted loci in the target species (Methods). As illustrated
356 in Figure 6, for comparisons between rodents the extent of sequence divergence is low enough that

357 more than 90% of 18,858 lncRNA loci are successfully projected from mouse to rat (Figure 6A,
358 Supplementary Dataset 5). However, only 54% of projected loci have even weak levels of detectable
359 transcription in the target species (at least 10 uniquely mapped reads). Only 26% of mouse lncRNA loci
360 have predicted 1-to-1 orthologues in the rat, and only 15% are orthologous to confirmed lncRNA loci
361 in the rat (Figure 6A, Supplementary Dataset 5). The 1,493 mouse lncRNAs that have non-lncRNAs
362 orthologues in the rat are generally matched with loci discarded because of low read coverage,
363 minimum exonic length or distance to protein-coding genes (Supplementary Dataset 5). Cases of
364 lncRNA-protein-coding orthologues are rare at this evolutionary distance (Supplementary Dataset 5),
365 and they may stem from gene classification errors. We note that, even when orthologous loci can be
366 detected, lncRNA gene structures are highly divergent across species, in terms of exonic length or
367 number of exons (Supplementary Figure 10).

368
369 At larger evolutionary distances, the rate of sequence evolution is the main factor hampering detection
370 of orthologous lncRNAs. Only 2,613 (14%) of mouse lncRNAs could be projected on the chicken
371 genome, and after subsequent filters we detect only 66 mouse – chicken lncRNA orthologues
372 (Supplementary Dataset 5). We note that our lncRNA detection power is weaker for the chicken than
373 for the rodents because of organ and developmental stage sampling, although we did strive to include
374 RNA-seq data from adult organs in the lncRNA detection process (Methods, Supplementary Table 2).
375 Conserved lncRNAs differ from non-conserved lncRNAs in terms of expression patterns. While only
376 subtle differences can be observed when comparing mouse-rat orthologous lncRNAs to the mouse-
377 specific lncRNA set, lncRNAs that are conserved across rodents and chicken (Supplementary Table 7)
378 are strongly enriched in somatic organs and early developmental stages (Figure 6B,C).

379 *Global patterns of lncRNA expression across species, organs and developmental stages*

380 We next assessed the global patterns of expression variation across species, organs and developmental
381 stages, for predicted mouse – rat lncRNA orthologues (Supplementary Dataset 6). As for protein-coding
382 genes, the main source of variability in a PCA performed on lncRNA expression levels is the difference

383 between adult and aged testes and the other samples (Figure 7A). However, for lncRNAs, samples
384 cluster according to the species of origin already on the second factorial axis (11% explained variance),
385 thus confirming that lncRNA expression patterns evolve rapidly. Overall, differences between organs
386 and developmental stages are less striking for lncRNAs, compared to the variation stemming from the
387 species factor (Figure 7A). This pattern is also visible on a hierarchical clustering analysis (performed
388 on distances derived from Spearman's correlation coefficient): in contrast with what is observed for
389 protein-coding genes, for lncRNAs samples generally cluster by species, with the exception of adult
390 and aged testes which are robustly grouped (Figure 7B).

391

392 The higher rates of lncRNA expression evolution are also visible when analyzing within-species
393 variations, through comparisons across biological replicates (Figure 8A). Both within-species and
394 between-species comparisons are affected by technical biases, such as the low expression levels of
395 lncRNAs, which hampers accurate expression estimates. To partially account for this effect, we sought
396 to measure the global extent of gene expression conservation by contrasting between-species and
397 within-species variations. Briefly, we constructed an expression conservation index by dividing the
398 between-species and the within-species Spearman's correlation coefficient, computed on all genes
399 from a category, for a given organ/developmental stage combination (Methods). The resulting
400 expression conservation values are very high for protein-coding genes, in particular for the brain and
401 the mid-stage embryonic kidney. However, there is significant less conservation between species for
402 the adult and aged testes (Figure 8B). For lncRNAs, expression conservation values are much lower
403 than those observed for protein-coding genes, with strikingly low values for adult and aged testes
404 (Figure 8C).

405 *Evolutionary divergence of individual lncRNA expression profiles*

406 For the mouse and rat, we could delve deeper into the evolutionary comparison of lncRNA expression
407 patterns, by asking whether variations among developmental stages are shared between species, for
408 individual lncRNAs. We used models from the DESeq2 (Love et al. 2014) package to detect differential

409 gene expression among developmental stages, independently for each species and organ
410 (Supplementary Dataset 4, Methods). We focused on orthologous lncRNAs that are significantly
411 differentially expressed (FDR<0.01) in both mouse and rat, and compared their patterns of expression
412 variations among developmental stages. Several hundreds of orthologous lncRNAs are DE in both
413 mouse and rat, in each organ (Figure 9). These lncRNAs show parallel patterns of variation among
414 developmental stages in mouse and rat, for all organs (Figure 9). Indeed, the developmental stage with
415 maximum expression is generally coherent across species (Figure 9A). As previously observed, few
416 genes are differentially expressed between young and aged adults (Supplementary Figure 6), hence
417 these two developmental stages are mixed in the comparative DE analysis. We clustered the relative
418 expression profiles of shared DE lncRNAs across species using the k-means algorithm (Methods). These
419 patterns further illustrate the similarity of the relative expression profiles among species (Figure 9B-
420 E). Interestingly, although temporal expression profiles are likewise similar between mouse and rat for
421 DE protein-coding genes (Supplementary Figure 11), almost 25% of shared DE protein-coding genes
422 show different trends for mouse and rat in the testes (Supplementary Figure 11). These sets of genes
423 do not show any strong functional enrichment (Supplementary Dataset 4). This pattern confirms
424 previous reports of rapid expression evolution in the adult testes (Brawand et al. 2011), and extends
425 them by showing that patterns of variations among developmental stages are often species-specific in
426 the testes, for protein-coding genes.

427

428 To further quantify lncRNA expression profile differences among species, we measured the amount of
429 expression divergence as the Euclidean distance between relative expression profiles (average TPM
430 values across biological replicates, normalized by dividing by the sum of all values for a gene, for each
431 species), for mouse and rat orthologues (Methods, Supplementary Dataset 7, Supplementary Table 8).
432 The resulting expression divergence values correlate negatively with the average expression level
433 (Figure 10A), as expected given that abundance estimation is less reliable for weakly expressed genes.
434 While the raw expression divergence values are significantly higher for lncRNAs than for protein-coding

435 genes (Figure 10B), this is largely due to the low lncRNA expression levels. Indeed, the effect disappears
436 when analyzing the residual expression divergence after regressing the mean expression level (Figure
437 10C). These patterns remain true when analyzing separately protein-coding and lncRNAs with different
438 types of promoters, bidirectional or unidirectional (Supplementary Figure 12A). For lncRNAs, we also
439 observe a weak negative correlation between expression divergence and the extent of gene structure
440 conservation (Figure 10D). We measured the relative contribution of each organ/developmental stage
441 to the expression divergence estimate (Figure 10E). For both protein-coding genes and lncRNAs, by far
442 the highest contributors are the young adult and aged testes samples, which are responsible for almost
443 30% of the lncRNA expression divergence (Figure 10E). This is visible in the expression patterns of the
444 2 protein-coding and lncRNA genes with the highest residual expression divergence: the lncRNA
445 expression divergence is mostly due to changes in adult testes, while more complex expression pattern
446 changes seem to have occurred for the protein-coding genes (Supplementary Figure 12). The most
447 divergent protein-coding genes are enriched in functions related to immunity (Supplementary Dataset
448 7), suggesting that differences in immune cell infiltrates among species could be responsible for these
449 extreme cases of expression pattern divergence.

450 Candidate species-specific lncRNAs

451 We next sought to investigate the most extreme cases of expression divergence: situations where
452 expression can be robustly detected in one species, but not in the other one, despite the presence of
453 almost perfect sequence alignment (Methods). We selected lncRNA loci that were supported by at
454 least 100 uniquely mapped reads in one species, with no reads detected in the predicted homologous
455 region in the other species. With this convention, we obtain 1,041 candidate mouse-specific and 1,646
456 candidate rat-specific loci (Supplementary Dataset 8). These lists include striking examples, such as the
457 region downstream of the *Fzd4* protein-coding gene, which contains a mouse-specific and a rat-specific
458 lncRNA candidate, each perfectly aligned in the other species (Supplementary Figure 13A). We could
459 not identify any differential transcription factor binding or transposable element enrichment in the
460 promoters of these species-specific lncRNAs (data not shown). Interestingly however, they are

461 increasingly associated with predicted expression enhancers (Supplementary Figure 14). While the
462 evolutionary and mechanistic origin of these lncRNAs is still mysterious, we could confirm that their
463 presence is associated with increased expression divergence in the neighboring genes. To test this, we
464 selected species-specific and orthologous lncRNAs that are transcribed from bidirectional promoters
465 shared with protein-coding genes, and evaluated the expression divergence of their protein-coding
466 neighbors (Supplementary Figure 13B,C). Though the difference is subtle, genes that are close to
467 species-specific lncRNAs have significantly higher expression divergence than the ones that have
468 conserved lncRNA neighbors, even after correcting for expression levels (Wilcoxon test, p-value < 10-
469 3). It thus seems that expression changes that led to the species-specific lncRNA transcription extend
470 beyond the lncRNA locus and affect the neighboring genes, as previously proposed (Kutter et al. 2012).

471 **Discussion**

472 *Assessing lncRNA functionality: current challenges and insights from evolutionary approaches*

473 More than a decade after the publication of the first genome-wide lncRNA datasets (Guttman et al.
474 2009; Khalil et al. 2009), the debate regarding their functionality is still not settled. While experimental
475 assessments of lncRNA functions are rapidly accumulating, they are lagging behind the exponential
476 increase of RNA sequencing datasets, each one revealing thousands of previously unreported
477 noncoding transcripts (Pertea et al. 2018). There is thus a need to define biologically relevant criteria
478 to prioritize lncRNAs for experimental investigation. Furthermore, *in vivo* tests of lncRNA functions
479 need to be carefully designed to account for ubiquitous confounding factors, such as the presence of
480 overlapping regulatory elements at lncRNA loci (Bassett et al. 2014). Another challenge is the fact that
481 some lncRNA loci undoubtedly have “unconventional” biological functions, that require for example
482 the presence of a transcription and splicing at a given genomic location, independently of the lncRNA
483 molecule that is produced (Latos et al. 2012; Engreitz et al. 2016).

484

485 Evolutionary approaches can provide important tools to assess biological functionality (Haerty and
486 Ponting 2014), and they have been already successfully applied to lncRNAs. Although only a few large-
487 scale comparative transcriptomics studies are available so far for vertebrate lncRNAs (Kutter et al.
488 2012; Washietl et al. 2014; Hezroni et al. 2015; Necsulea et al. 2014), they all agree that lncRNAs evolve
489 rapidly in terms of primary sequence, exon-intron structure and expression patterns, indicating that
490 there is little selective constraint and thus little functionality for these loci. However, these studies
491 have all focused on lncRNAs detected in adult organs. We hypothesized that lncRNAs expressed during
492 embryogenesis are enriched in functional loci, as suggested by the increasing number of lncRNAs with
493 proposed roles in development (Rinn et al. 2007; Sauvageau et al. 2013; Grote et al. 2013; Grote and
494 Herrmann 2015). To test this hypothesis, we performed a multi-dimensional comparative
495 transcriptomics analysis, following lncRNA and protein-coding gene expression patterns across
496 species, organs and developmental stages.

497 *Comparability of transcriptomes across species, organs and developmental stages*

498 One of main concerns was to ensure that our transcriptome collection provides a good representation
499 of the changes in cellular composition and physiological functions that occur during major organ
500 development, and that the resulting patterns are comparable across diverse vertebrate species. Our
501 analyses of cell-type specific gene markers, derived from single-cell transcriptomics analyses (Tabula
502 Muris Consortium 2018; Green et al. 2018), confirms that this is indeed the case, as we see expected
503 expression patterns in our transcriptome collection. Likewise, we observed due enrichment of
504 biological processes in the sets of genes that are specifically expressed in each organ/developmental
505 stage combination. Furthermore, we showed that protein-coding gene expression profiles across
506 major organs and developmental stages are well conserved among species, even at large evolutionary
507 distances. Although differences among rodents and chicken are visible when analyzing the full set of
508 orthologous protein-coding genes, we find that the expression profiles of genes that are known to be
509 implicated in embryonic development and in gene expression regulation processes are highly
510 conserved among species (Figure 2). Our transcriptome collection thus enables detection of ancestral

511 developmental expression patterns, shared across amniote species, for key players in developmental
512 regulatory networks.

513 *Spatio-temporal lncRNA expression patterns*

514 Our first major observation is that lncRNAs are overwhelmingly expressed in the adult and aged testes,
515 in agreement with previous data (Soumillon et al. 2013). Their relative depletion in embryonic and
516 newborn testes reinforces the association between lncRNA production and spermatogenesis, in accord
517 with the hypothesis that the particular chromatin environment during spermatogenesis is a driver for
518 promiscuous, non-functional transcription (Kaessmann 2010; Soumillon et al. 2013). Interestingly, we
519 show that lncRNAs are significantly differentially expressed among developmental stages, at least as
520 frequently as protein-coding genes, after correcting for their lower expression levels. However, in
521 contrast with protein-coding genes, the majority of lncRNAs reach their highest expression levels in
522 adult rather than in developing organs. As requirements for tight gene expression control are
523 undoubtedly higher during embryonic development (Ben-Tabou de-Leon and Davidson 2007), an
524 explanation for the relative lncRNA depletion in embryonic and newborn transcriptomes is that
525 transcriptional noise is more efficiently blocked during the early stages of development. Differences in
526 cellular composition heterogeneity may also be part of the explanation. Expression analyses of cell-
527 type specific markers suggest that adult and aged organ transcriptomes may be a mix of more diverse
528 cell types, notably including substantial immune cell infiltrates. A higher cell type diversity may explain
529 the increased abundance of lncRNAs in adult and aged organs, especially given that lncRNAs are
530 thought to be cell-type specific (Liu et al. 2016).

531 *Functionally constrained lncRNAs are enriched in developmental transcriptomes*

532 We show that, for those lncRNAs that are expressed above noise levels (TPM \geq 1) in somatic organs
533 and in the earlier developmental stages, there is a higher proportion of functionally constrained loci
534 than in testes-expressed lncRNAs. Strikingly, we find that the level of long-term sequence conservation
535 for lncRNA promoter regions is higher than the one observed for protein-coding promoters, when we

536 analyze genes that are robustly expressed (TPM \geq 1) in embryonic brain and kidney. Furthermore, we
537 show that lncRNAs that are expressed in somatic organs and in the developing testes differ from those
538 expressed in the adult testes not only in terms of overall levels of sequence conservation, but also with
539 respect to the regions of the lncRNA loci that are under selective constraint. Thus, for lncRNAs that are
540 expressed in somatic organs and in the developing testes, there is significantly more evolutionary
541 constraint on promoter and splice site sequences than on exonic regions, while these patterns are not
542 seen for the bulk of lncRNAs, expressed in adult and aged testes. We are thus able to modulate
543 previous reports of increased constraint on splicing regulatory regions in mammalian lncRNAs (Schüler
544 et al. 2014; Haerty and Ponting 2015), by showing that this pattern is specifically seen in lncRNAs that
545 are expressed in somatic organs and in the developing testes.

546

547 These results are also in agreement with a series of recent findings, suggesting that at many lncRNA
548 loci, biological function may reside in the presence of additional non-coding regulatory elements at
549 the lncRNA promoter rather than in the production of a specific transcript (Engreitz et al. 2016; Groff
550 et al. 2016). While the elevated sequence conservation at splicing regulatory signals could in principle
551 indicate that the production of a specific mature lncRNA molecule is required, we note that splicing of
552 lncRNA transcripts was recently proposed to affect the expression of neighboring protein-coding genes
553 (Engreitz et al. 2016). Thus, while there is evidence for increased functionality for those lncRNA loci
554 that are detected in developmental transcriptomes or in adult somatic organs, our sequence
555 conservation analyses suggest that their biological functions may be carried out in an RNA-
556 independent manner, as exonic sequences are under less constraint than promoter or splice site
557 regions.

558 *Evolutionary divergence of spatio-temporal expression profiles for lncRNAs*

559 We previously established that lncRNA expression patterns evolve rapidly across species in adult
560 organs. Here, we show that this rapid evolution of lncRNA expression is not restricted to adult and
561 aged individuals, but is also true for embryonic and newborn developmental stages. Expression

562 patterns comparisons across species, organs and developmental stages are dominated by differences
563 between species for lncRNAs, while similarities between organs and developmental stages are
564 predominant for protein-coding genes, even across distantly related species. We assessed the extent
565 of expression level conservation by contrasting between-species and within-species expression
566 variations and we showed that lncRNAs have significantly lower levels of conservation than protein-
567 coding genes, for all organs and developmental stages. However, lncRNA expression is significantly
568 more conserved in somatic organs and in early embryonic stages than in the adult testes. Moreover,
569 when orthologous lncRNAs are differentially expressed among developmental stages in both mouse
570 and rat, they generally show parallel profiles of expression variation in both species. This observation
571 is compatible with previous reports indicating that lncRNA expression is often cell type-specific (Liu et
572 al. 2016). The differentially expressed lncRNAs, shared across mouse and rat, may be specific of cell
573 types that change their relative abundance in whole-organ transcriptomes with developmental time.

574

575 Interestingly, when we evaluate expression divergence individually for each orthologous gene pair,
576 and when we correct for the lower lncRNA expression levels, we find that lncRNAs are comparable
577 with protein-coding genes, on average. This observation indicates that much of the between-species
578 differences in lncRNA expression patterns may be due to the low expression levels of lncRNAs. It is not
579 clear however whether this purely an indication of technical biases, that hamper accurate expression
580 estimation for lowly expressed lncRNAs, or whether the low lncRNA expression levels can be
581 interpreted as a sign that these transcripts are non-functional. For those lncRNAs that are cell type-
582 specific, low expression levels in whole organ transcriptomes are expected. This question may be
583 directly addressed in the near future, as single-cell transcriptome assays become more sensitive and
584 allow investigation of lncRNA expression patterns (Liu et al. 2016).

585 Candidate species-specific lncRNAs

586 Finally, we analyzed extreme cases of expression divergence between species, namely situations
587 where transcription can be robustly detected in one species but not in the other, despite the presence

588 of good sequence conservation. We identify more than a thousand candidate species-specific lncRNAs,
589 in both mouse and rat. Interestingly, we observe that candidate mouse-specific lncRNAs are more
590 frequently transcribed from enhancers than lncRNAs conserved between mouse and rat. This
591 observation is consistent with previous reports that enhancers and enhancer-associated lncRNAs
592 evolve rapidly (Villar et al. 2015; Marques et al. 2013). The genetic basis of these extreme transcription
593 pattern changes is still not elucidated, and deserves further detailed investigations. Nevertheless, we
594 show that these lncRNA expression patterns do not occur in an isolated manner. When such species-
595 specific transcription was detected at protein-coding genes bidirectional promoters, the neighboring
596 protein-coding genes also showed increased expression divergence, compared to genes that are
597 transcribed from conserved lncRNA promoters. This observation is compatible with previous reports
598 that lncRNA turnover is associated with changes in neighboring gene expression (Kutter et al. 2012).
599 While lncRNAs changes may be directly affecting gene expression, it is also possible that a common
600 mechanism affects both lncRNAs and protein-coding genes transcribed from bidirectional promoters.

601 **Conclusions**

602 Our comparative transcriptomics approach confirms the established finding that lncRNAs repertoires,
603 sequences and expression patterns evolve rapidly across species, and shows that the accelerated rates
604 of lncRNA evolution are also seen in developmental transcriptomes. These observations are consistent
605 with the hypothesis that the majority of lncRNAs (or at least of those detected with sensitive
606 transcriptome sequencing approaches, in particular in the adult testes) may be non-functional.
607 However, we are able to modulate this conclusion, by showing that there are increased levels of
608 functional constraint on lncRNAs expressed during embryonic development, in particular in the
609 developing brain and kidney. These increased levels of constraint apply to all analyzed aspects of
610 lncRNAs, including sequence conservation for exons, promoter and splice sites, but also expression
611 pattern conservation. For many of these loci, biological function may be RNA-independent, as the
612 highest levels of selective constraint are observed on promoter regions and on splice signals, rather

613 than on lncRNA exonic sequences. Our results are thus compatible with unconventional, RNA-
614 independent functions for lncRNAs expressed during embryonic development.
615

616 **Methods**

617 Biological sample collection

618 We collected samples from three species (mouse C57BL/6J strain, rat Wistar strain and chicken White
619 Leghorn strain), four organs (brain, kidney, liver and testes) and five developmental stages (including
620 two embryonic stages, newborn, young and aged adult individuals). We sampled the following stages
621 in the mouse: embryonic day post-conception (dpc) 13.5 (E13.5 dpc, hereafter mid-stage embryo); E17
622 to E17.5 dpc (late embryo); post-natal day 1 to 2 (newborn); young adult (8-10 weeks old); aged adult
623 (24 months old). For the rat, we sampled the following stages: E15 dpc (mid-stage embryo); E18.5 to
624 E19 dpc (late embryo); post-natal day 1 to 2 (newborn); young adult (8-10 weeks old); aged adult (24
625 months, with the exception of kidney samples and two of four liver samples, derived from 12 months
626 old individuals). The embryonic and neonatal developmental stages were selected for maximum
627 comparability based on Carnegie stage criteria (Theiler 1989). For chicken, we collected samples from
628 Hamburger-Hamilton stages 31 and 36, hereafter termed mid-stage and late embryo. We selected
629 these two stages for comparability with the two embryonic stages in mouse and rat (Hamburger and
630 Hamilton 1951). In general, each sample corresponds to one individual, except for mouse and rat mid-
631 stage embryonic kidney, for which tissue from several embryos was pooled prior to RNA extraction.
632 For adult and aged organs, multiple tissue pieces from the same individual were pooled and
633 homogenized prior to RNA extraction. For brain dissection, we sampled the cerebral cortex. For mouse
634 and rat samples, with the exception of the mid-stage embryonic kidney, individuals were genotyped
635 and males were selected for RNA extraction. Between two and four biological replicates were obtained
636 for each species/organ/stage combination, amounting to 97 samples in total (Supplementary Table 1).

637 RNA-seq library preparation and sequencing

638 We performed RNA extractions using RNeasy Plus Mini kit from Qiagen. RNA quality was assessed
639 using the Agilent 2100 Bioanalyzer. Sequencing libraries were produced using the Illumina TruSeq

640 stranded mRNA protocol with polyA selection, and sequenced as 101 base pairs (bp) single-end reads,
641 at the Genomics Platform of iGE3 and the University of Geneva (<https://ige3.genomics.unige.ch/>).

642 Additional RNA-seq data

643 To improve detection power for lowly expressed lncRNAs, we complemented our RNA-seq collection
644 with samples generated with the same technology for Brown Norway rat adult organs (Cortez et al.
645 2014). We added data generated by the Chickspress project (<http://geneatlas.arl.arizona.edu/>) for
646 adult chicken (red jungle fowl strain UCD001) organs, as well as for embryonic chicken (White Leghorn)
647 organs from two publications (Uebbing et al. 2015; Ayers et al. 2013). Almost all samples were strand-
648 specific, except the chicken adult organs and early embryonic testes. As the data were not perfectly
649 comparable with our own in terms of library preparation and animal strains, the additional rat and
650 chicken samples were only used to increase lncRNA detection sensitivity.

651 RNA-seq data processing

652 We used HISAT2 (Kim et al. 2015) release 2.0.5 to align the RNA-seq data on reference genomes. The
653 genome sequences (assembly versions mm10/GRCm38, rn6/Rnor_6.0 and galGal5/Gallus_gallus-5.0)
654 were downloaded from the Ensembl database (Cunningham et al. 2019). Genome indexes were built
655 using only genome sequence information. To improve detection sensitivity, at the alignment step we
656 provided known splice junction coordinates extracted from Ensembl. We set the maximum intron
657 length for splice junction detection at 1 million base pairs (Mb). To verify the strandedness of the RNA-
658 seq data, we analyzed spliced reads that spanned introns with canonical (GT-AG or GC-AG) splice sites
659 and compared the strand inferred based on the splice site with the one assigned based on the library
660 preparation protocol (Supplementary Table 1). Finally, to estimate the mappability of each genomic
661 region, we generated error-free artificial RNA-seq reads (single-end, 101 bp long, with 5 bp distance
662 between consecutive read starts) from the genome sequence and realigned them to the genome with
663 the same HISAT2 parameters. Regions for which the corresponding reads could be aligned
664 unambiguously were considered “mappable”; the remaining regions were said to be “unmappable”.

665 Transcript assembly and filtering

666 We assembled transcripts for each sample using StringTie (Pertea et al. 2015), release 1.3.5, based on
667 read alignments obtained with HISAT2. We provided genome annotations from Ensembl release 94 as
668 a guide for transcript assembly. We filtered Ensembl annotations to remove transcripts that spanned
669 a genomic length above 2.5 Mb. For protein-coding genes, we kept only protein-coding transcripts,
670 discarding isoforms annotated as “retained_intron”, “processed_transcript” etc. We set the minimum
671 exonic length at 150 bp, the minimum anchor length for splice junctions at 8bp and the minimum
672 isoform fraction at 0.05. We compared the resulting assembled transcripts with Ensembl annotations
673 and we discarded read-through transcripts, defined as overlapping with multiple multi-exonic
674 Ensembl-annotated genes. For strand-specific samples, we discarded transcripts for which the ratio of
675 sense to antisense unique read coverage was below 0.01. We discarded multi-exonic transcripts that
676 were not supported by splice junctions with correctly assigned strands. The filtered transcripts
677 obtained for each sample were assembled into a single dataset *per* species using the merge option in
678 StringTie. For increased sensitivity, we removed the minimum FPKM and TPM thresholds for transcript
679 inclusion. We constructed a combined annotation dataset, starting with Ensembl annotations, to
680 which we added newly-assembled transcripts that had no exonic overlap with Ensembl genes. We also
681 included newly-annotated isoforms for known genes if they had exonic overlap with exactly one
682 Ensembl gene, thus discarding potential read-through transcripts or gene fusions.

683 Protein-coding potential of assembled transcripts

684 To determine whether the newly assembled transcripts were protein-coding or non-coding, we mainly
685 relied on the codon substitution frequency (CSF) score (Lin et al. 2007). As in a previous publication
686 (Necsulea et al. 2014) we scanned whole genome alignments and computed CSF scores in 75 bp sliding
687 windows moving with a 3 bp step. We used pre-computed alignments downloaded from the UCSC
688 Genome Browser (Casper et al. 2018), including the alignment between the mouse genome and 59
689 other vertebrates (for mouse classification), between the human genome and 99 other vertebrates

690 (for rat and chicken classification) and between the rat genome and 19 other vertebrates (for rat
691 classification). For each window, we computed the score in each of the 6 possible reading frames and
692 extracted the maximum score for each strand. We considered that transcripts are protein-coding if
693 they overlapped with positive CSF scores on at least 150 bp. As positive CSF scores may also appear on
694 the antisense strand of protein-coding regions due to the partial strand-symmetry of the genetic code,
695 in this analysis we considered only exonic regions that did not overlap with other genes. In addition,
696 we searched for sequence similarity between assembled transcripts and known protein sequences
697 from the SwissProt 2017_04 (The UniProt Consortium 2017) and Pfam 31.0 (El-Gebali et al. 2019)
698 databases. We kept only SwissProt entries with confidence scores 1, 2 or 3 and we used the Pfam-A
699 curated section of Pfam. We searched for sequence similarity using the blastx utility in the BLAST+
700 2.8.1 package (Camacho et al. 2009; Altschul et al. 1990), keeping hits with maximum e-value $1e-3$ and
701 minimum protein sequence identity 40%, on repeat-masked cDNA sequences. We considered that
702 transcripts were protein-coding if they overlapped with blastx hits over at least 150 bp. Genes were
703 said to be protein-coding if at least one of their isoforms was classified as protein-coding, based on
704 either the CSF score or on sequence similarity with known proteins.

705 Long non-coding RNA selection

706 To construct a reliable lncRNA dataset, we selected newly-annotated genes classified as non-coding
707 based on both the CSF score and on sequence similarity with known proteins and protein domains, as
708 well as Ensembl-annotated genes with non-coding biotypes ("lincRNA", "processed_transcript",
709 "antisense", "TEC", "macro_lncRNA", "bidirectional_promoter_lncRNA", "sense_intronic"). For newly
710 detected genes, we applied several additional filters: we required a minimum exonic length
711 (corresponding to the union of all annotated isoforms) of at least 200 bp for multi-exonic loci and of
712 at least 500 bp for mono-exonic loci; we eliminated genes that overlapped for more than 5% of their
713 exonic length with unmappable regions; we kept only loci that were classified as intergenic and at least
714 5 kb away from Ensembl-annotated protein-coding genes on the same strand; for multi-exonic loci, we
715 required that all splice junctions be supported by reads with correct strand assignment (cf. above). For

716 both *de novo* and Ensembl annotations, we removed transcribed loci that overlapped on at least 50%
717 of their length with retrotransposed gene copies, annotated by the UCSC Genome Browser and from
718 a previous publication (Carelli et al. 2016); we discarded loci that overlapped with UCSC-annotated
719 tRNA genes and with RNA-type elements from RepeatMasker (Smit et al. 2003) on at least 25% of their
720 length. We kept loci supported by at least 10 uniquely mapped RNA-seq reads and for which a ratio of
721 sense to antisense transcription of at least 1% was observed in at least one sample. Although the
722 fraction of reads stemming from the complementary mRNA strand, due to errors in library
723 preparations, is very low in our samples (Supplementary Table 1), we noticed that loci situated on the
724 antisense strand of highly expressed genes can have unreliable expression estimates, due to wrong
725 strand-assignments of RNA-seq reads. Thus, for loci that had sense/antisense exonic overlap with
726 other genes, we computed expression levels either on complete gene annotations, or only on exonic
727 regions that had no overlap with other genes, and computed Spearman's correlation coefficient
728 between the two expression estimates, across all samples. We discarded loci for which the correlation
729 coefficient was below 0.9.

730 *LncRNA and protein-coding gene promoter types*

731 We assessed the proximity between the transcription start sites (TSS) of lncRNA loci and other genes
732 TSS, to determine whether lncRNA promoters are unidirectional or bidirectional. We said that lncRNAs
733 or protein-coding genes have bidirectional promoters if at least one of their annotated TSS is found
734 within 1 kb of a different gene TSS. We also analyzed the proximity between promoter regions and
735 Encode-annotated enhancers, in the mouse (Shen et al. 2012). We combined all enhancer coordinates
736 across all tissues, and converted their coordinates between mm9 and mm10 genome assemblies with
737 liftOver.

738 *Gene expression estimation*

739 We computed the number of uniquely mapping reads unambiguously attributed to each gene using
740 the Rsubread package in R (Liao et al. 2019), discarding reads that overlapped with multiple genes. We

741 also estimated read counts and TPM (transcript *per* million) values *per* gene using Kallisto (Bray et al.
742 2016). To approach absolute expression levels estimates, for better comparisons across samples, we
743 further normalized TPM values using a scaling approach (Brawand et al. 2011). Briefly, we ranked the
744 genes in each sample according to their TPM values, we computed the variance of the ranks across all
745 samples for each gene, and we identified the 100 least-varying genes, found within the inter-quartile
746 range (25%-75%) in terms of average expression levels across samples. We derived normalization
747 coefficients for each sample such that the median of the 100 least-varying genes be identical across
748 samples. We then used these coefficients to normalize TPM values for each sample. We excluded
749 mitochondrial genes from expression estimations and analyses, as these genes are highly expressed
750 and can be variable across samples.

751 Differential expression analyses

752 We used the DESeq2 (Love et al. 2014)(Smedley et al. 2009)(74)(75) package release 1.22.2 in R release
753 3.5.0 (R Core Team 2018) to test for differential expression across developmental stages, separately
754 for each organ and species. We analyzed both protein-coding genes and lncRNAs, selected according
755 to the criteria described above. We first performed a global differential expression analysis, using the
756 likelihood ratio test to contrast a model including an effect of the developmental stage against the null
757 hypothesis of homogeneous expression level across all developmental stages. This analysis was
758 performed on all annotated protein-coding and lncRNA genes for each species, as well as on 1-to-1
759 orthologous genes for mouse and rat. In addition, we down-sampled the numbers of reads assigned
760 to protein-coding genes to obtain identical average numbers of reads for protein-coding genes and
761 lncRNAs. We also contrasted consecutive developmental stages, for each species and organ. For each
762 test, we also computed the expression fold change based on average TPM values for each
763 developmental stage/organ combination. To characterize expression variations across developmental
764 stages, for DE genes shared between mouse and rat, TPM values were averaged across replicates and
765 normalized by dividing by the maximum, for each species. The resulting relative expression profiles
766 were combined across species and clustered with the K-means algorithm.

767 Expression specificity index

768 We used the previously proposed tissue specificity index (Liao et al. 2006) to measure gene expression
769 specificity across organs and developmental stages, provided by the formula: $\tau = \sum (1 - r_i)/(n-1)$,
770 where r_i represents the ratio between the expression level in sample i and the maximum expression
771 level across samples, and n represents the total number of samples. We computed this index on
772 normalized TPM values, averaged across all replicates for a given species / organ / developmental stage
773 combination (Supplementary Dataset 3).

774 Gene markers for organs and developmental stages

775 We extracted protein-coding genes that had high expression specificity indexes ($\tau \geq 0.85$) in both
776 mouse and rat, and for which the organ/stage in which maximum expression is observed is the same
777 for both species. We selected genes that had an expression level (TPM) above 2 in at least one sample,
778 for each species. For this analysis, we combined the young and aged adult samples.

779 Gene ontology enrichment

780 We extracted gene ontology annotations for mouse, rat and chicken from the Ensembl 94 database,
781 using BioMart (Smedley et al. 2015). We evaluated the enrichment of gene ontology categories
782 between a target gene set (e.g., genes that differentially expressed between two developmental
783 stages, in a given organ) and a background gene set (e.g., all genes expressed in that organ), using the
784 hypergeometric test in R. We performed the gene ontology enrichment for the “biological process”
785 category, and set the false discovery rate (FDR) threshold at 0.1. For the developmental transcription
786 factor analysis presented in Figure 2, we selected genes associated with at least one of the following
787 categories: multicellular organism development, system development, embryonic organ development,
788 animal organ development or pattern specification process. We further selected from the resulting list
789 those genes associated with at least one of the following categories: regulation of gene expression,
790 gene expression, positive regulation of gene expression, negative regulation of gene expression,
791 regulation of transcription by RNA polymerase II, regulation of transcription, DNA-templated.

792 Homologous lncRNA family prediction

793 We used existing whole-genome alignments as a guide to predict homologous lncRNAs across species,
794 as previously proposed (Washietl et al. 2014). We first constructed for each gene the union of its exon
795 coordinates across all isoforms, hereafter termed “exon blocks”. We projected exon block coordinates
796 between pairs of species using the liftOver utility and whole-genome alignments generated with blastz
797 (http://www.bx.psu.edu/miller_lab/), available through the UCSC Genome Browser (Casper et al.
798 2018). To increase detection sensitivity, for the initial liftOver projection we required only that 10% of
799 the reference bases remap on the target genome. Projections were then filtered, retaining only cases
800 where the size ratio between the projected and the reference region was between 0.33 and 3 for
801 mouse and rat (0.2 and 5 for comparisons involving chicken). To exclude recent lineage-specific
802 duplications, regions with ambiguous or split liftOver projections were discarded. For genes where
803 multiple exon blocks could be projected across species, we defined the consensus chromosome and
804 strand in the target genome and discarded projected exon blocks that did not match this consensus.
805 We then evaluated the order of the projected exon blocks on the target genes, to identify potential
806 internal rearrangements. If internal rearrangements were due to the position of a single projected
807 exon block, the conflicting exon block was discarded; otherwise, the entire projected gene was
808 eliminated. As the projected reference gene coordinates could overlap with multiple genes in the
809 target genome, we constructed gene clusters based on the overlap between projected exon block
810 coordinates and target annotations, using a single-link clustering approach. We then realigned entire
811 genomic loci for each pair of reference-target genes found within a cluster, using lastz
812 (http://www.bx.psu.edu/miller_lab/) and the threaded blockset aligner (Blanchette et al. 2004). Using
813 this alignment, we computed the percentage of exonic sequences aligned without gaps and the
814 percentage of identical exonic sequence, for each pair of reference-target genes. We then extracted
815 the best hit in the target genome for each gene in the reference genome based on the percentage of
816 identical exonic sequence, requiring that the ratio between the maximum percent identity and the
817 percent identity of the second-best hit be above 1.1. Reciprocal best hits were considered to be 1-to-

818 1 orthologous loci between pairs of species. For analyses across all three species, we constructed
819 clusters of reciprocal best hits from pairwise species comparisons, using a single-link clustering
820 approach. Resulting clusters with more than 1 representative *per* species were discarded. To examine
821 the validity of our procedure for homologous gene family prediction, we compared the resulting gene
822 families with predictions from the Ensembl Compara pipeline (Herrero et al. 2016), extracted from
823 Ensembl release 94, for protein-coding genes.

824 Sequence evolution

825 We evaluated long-term evolutionary sequence conservation based on PhastCons (Siepel et al. 2005)
826 scores, computed for the mouse genome using either a placental mammal or a vertebrate multiple
827 species alignment available from the UCSC Genome Browser (Casper et al. 2018). We attributed a value
828 of 0 to all genomic positions that are not present in the whole-genome alignment used for PhastCons
829 computations. We computed average PhastCons scores on exonic sequences (excluding exonic regions
830 overlapping with other genes), promoter regions (defined as 1 kb immediately upstream of the
831 transcription start site, masking any exonic regions that overlapped in these regions) and splice sites
832 (defined as the first two and last two bases of each intron). For genes with multiple promoters, we
833 computed the average score across all promoters.

834 Gene expression evolution

835 We computed global and *per*-gene expression level conservation between mouse and rat, for 1-to-1
836 orthologous genes. We first measured gene expression conservation for protein-coding genes and
837 lncRNAs as a class. For each organ/developmental stage, we computed the expression level correlation
838 between mouse and rat average TPM levels, across all orthologous pairs. We also computed the
839 correlation between individuals within the same species; for organ/stages with more than two
840 biological replicates we computed the average correlation coefficient across all possible pairs of
841 individuals. We then evaluated the global extent of gene expression conservation through the ratio of
842 the between-species correlation coefficient to the average within-species correlation coefficient.

843 Spearman's rank correlation coefficients were used in all cases. We obtained confidence intervals for
844 expression conservation measures through a bootstrap procedure, resampling 100 times the same
845 number of genes with replacement. In addition to this global measure of expression conservation, we
846 estimated the extent of between-species expression divergence *per gene* by computing Euclidean
847 distances between relative expression profiles for each species. The relative expression profiles were
848 derived from TPM values *per organ/developmental stage*, averaged across biological replicates,
849 divided by the sum of all average TPM values.

850 Statistical analyses and graphical representations

851 All statistical analyses and graphical representations were done with R (R Core Team 2018), version
852 3.5.0. We performed principal component analyses using the *ade4* library (Dray and Dufour 2007) and
853 hierarchical clustering of gene expression matrices using the *hclust* function in the *stats* package in R,
854 on pairwise Euclidean distances. Principal component analyses were performed on log₂-transformed
855 expression levels, and expression profiles were centered and scaled prior to analysis. For all analyses
856 involving multiple statistical tests, false discovery rates were computed with the Benjamini-Hochberg
857 procedure (Benjamini and Hochberg 1995). 95% confidence intervals for median values of distributions
858 were computed with the following formula: median +/- 1.57 x IQR/sqrt(N), where IQR is the inter-
859 quartile range, sqrt denotes the square root and N the number of points.

860 **Availability of data and materials**

861 The raw and processed RNA-seq data were submitted to the NCBI Gene Expression Omnibus (GEO),
862 under accession number GSE108348. Additional processed files and all scripts used to analyze the
863 data are available at the address: ftp://pbil.univ-lyon1.fr/pub/datasets/Darbellay_LncEvoDevo.

864

865 **Author contributions**

866 FD performed organ dissections, RNA extractions, quality control, prepared samples for sequencing
867 and contributed to study design and manuscript preparation. AN designed the study, performed
868 computational analyses and wrote the manuscript. All authors read and approved the final manuscript.

869 **Acknowledgements**

870 We thank Denis Duboule and all members of the laboratory for advice and support, Mylène Docquier,
871 Brice Petit and the Genomics Platform of the University of Geneva for RNA-seq data production,
872 Amanda Cooksey and the Chickspress Team at the University of Arizona
873 (<http://geneatlas.arl.arizona.edu>) for granting us access to chicken RNA-seq data, Ioannis Xenarios and
874 the Vital-IT team for computational support. We thank Jean-Marc Matter (University of Geneva) for
875 providing chicken eggs. This work was performed using the computing facilities of the CC LBBE/PRABI,
876 the Vital-IT Center for high-performance computing of the SIB Swiss Institute of Bioinformatics
877 (<http://www.vital-it.ch>) and the computing center of the French National Institute of Nuclear and
878 Particle Physics (CC-IN2P3). This project was funded by the Swiss National Science Foundation (SNSF
879 Ambizione grant PZ00P3_142636), the Agence Nationale pour la Recherche (ANR JCJC 2017
880 LncEvoSys). FD was supported by a FP7 IDEAL grant (259679).

881

882 **Figure legends**

883 **Figure 1. Comparative transcriptomics across species, organs and developmental stages.**

884 **A.** Experimental design. The developmental stages selected for mouse, rat and chicken are marked on
885 a horizontal axis. Organs sampled for each species and developmental stage are shown below.
886 Abbreviations: br, brain; kd, kidney; lv, liver; ts, testes.

887 **B.** Expression of cell type-specific markers derived from single-cell experiments (full list provided in
888 Supplementary Table 3), in our mouse and rat RNA-seq samples, averaged across biological replicates.
889 The heatmap represents centered and scaled log₂-transformed TPM levels (z-score). Developmental
890 stages are indicated by numeric labels, 1 to 5. Species are color-coded, shown below the heatmap.

891

892 **Figure 2. Protein-coding gene expression patterns are conserved across species.**

893 **A.** First factorial map of a principal component analysis, performed on log₂-transformed TPM values,
894 for 10,363 protein-coding genes with orthologues in mouse, rat and chicken. Colors represent different
895 organs and developmental stages, point shapes represent different species.

896 **B.** Hierarchical clustering, performed on a distance matrix derived from Spearman correlations
897 between pairs of samples, for 10,363 protein-coding genes with orthologues in mouse, rat and chicken.
898 Organ and developmental stages are color-coded, shown below the heatmap. Species of origin is color-
899 coded, shown on the right. Sample clustering is shown on the left.

900 **C.** Same as A, for 289 protein-coding genes with orthologues in mouse, rat and chicken, associated
901 with organism development and regulation of gene expression in mouse gene ontology (Methods).

902 **D.** Same as B, for 289 protein-coding genes associated with organism development and regulation of
903 gene expression.

904

905 **Figure 3. Transcriptome complexity in different species, organs and developmental stages.**

906 **A.** Number of protein-coding genes supported by at least 10 uniquely mapped reads in each sample,
907 after read resampling to homogenize coverage (Methods). Colors represent different organs, point

908 shapes represent different species. Developmental stages are indicated by numeric labels, 1 to 5, on
909 the X-axis. We analyzed a total of 19,356 protein-coding genes in the mouse, 19,274 in the rat and
910 15,509 in the chicken.

911 **D.** Number of lncRNAs supported by at least 10 uniquely mapped reads in each sample, after read
912 resampling to homogenize coverage. We analyzed a total of 18,858 lncRNAs in the mouse, 20,159 in
913 the rat and 5,496 in the chicken.

914

915 **Figure 4. Different expression patterns for protein-coding genes and lncRNAs.**

916 **A.** Distribution of the organ in which maximum expression is observed, for protein-coding genes (pc)
917 and lncRNAs (lnc), for mouse, rat and chicken. Organs are color-coded, shown above the plot.

918 **B.** Distribution of the developmental stage in which maximum expression is observed, for protein-
919 coding genes and lncRNAs, for mouse, rat and chicken. Developmental stages are color-coded, shown
920 above the plot.

921 **C.** Percentage of protein-coding and lncRNA genes that are significantly ($FDR < 0.01$) DE among
922 developmental stages, with respect to the total number of genes tested for each organ. Left panel:
923 differential expression analysis performed with all RNA-seq reads. Right panel: differential expression
924 analysis performed after down-sampling read counts for protein-coding genes, to match those of
925 lncRNAs (Methods).

926 **D.** Distribution of the developmental stage in which maximum expression is observed, for protein-
927 coding genes and lncRNAs that are significantly DE ($FDR < 0.01$) in each organ, for the mouse. The
928 percentages are computed with respect to the total number of DE genes in each organ and gene class.

929

930 **Figure 5. Increased levels of long-term sequence conservation for lncRNAs expressed early in**
931 **development.**

932 **A.** Distribution of the sequence conservation score (PhasCons), for protein-coding and lncRNAs exonic
933 regions, in the mouse. We used precomputed PhastCons score for placental mammals, downloaded

934 from the UCSC Genome Browser. Exonic regions that overlap with exons from other genes were
935 masked. Boxplot notches represent 95% confidence intervals of the medians. Numbers of analyzed
936 genes are shown below the plot. The horizontal dotted line represents the average conservation score
937 computed on intergenic regions, at least 5kb away from transcribed loci.

938 **B.** Distribution of the sequence conservation score, for promoter regions (1kb upstream of
939 transcription start sites) of mouse protein-coding genes and lncRNAs. Exonic sequences were masked
940 in promoter regions. Genes are divided in different classes depending on their promoter type:
941 unidirectional, bidirectional shared with protein-coding genes, bidirectional shared with non-coding
942 genes, overlap with Encode-annotated enhancers.

943 **C.** Distribution of the sequence conservation score, for splice sites (first and last two bases of each
944 intron).

945 **D.** Distribution of the sequence conservation score for protein-coding and lncRNAs exonic regions, for
946 subsets of genes expressed above noise levels (TPM \geq 1) in each organ and developmental stage. Dots
947 represent medians, vertical bars represent 95% confidence intervals. Numbers of analyzed genes are
948 provided in Supplementary Table 5.

949 **E.** Same as A, for promoter regions (1kb upstream of transcription start sites). Exonic sequences were
950 masked before assessing conservation.

951 **F.** Same as B, for splice sites (first and last two bases of each intron).

952

953 **Figure 6. Orthologous lncRNA families for mouse, rat and chicken.**

954 **A.** Number of mouse protein-coding genes and lncRNAs in different classes of evolutionary
955 conservation. From left to right: all loci (with TPM \geq 1 in at least one mouse sample), loci with
956 conserved sequence in the rat, loci for which transcription could be detected (at least 10 unique reads)
957 in predicted orthologous locus in the rat, loci with predicted 1-to-1 orthologues, loci for which the
958 predicted orthologue belonged to the same class (protein-coding or lncRNA) in the rat, loci with
959 conserved sequence in the chicken, loci for which transcription could be detected (at least 10 unique

960 reads) in predicted orthologous locus in the chicken, loci with predicted 1-to-1 orthologues, loci for
961 which the predicted orthologue belonged to the same class (protein-coding or lncRNA) in the chicken.
962 We analyze 19,356 protein-coding genes and 18,858 candidate lncRNAs in the mouse.

963 **B.** Distribution of the organ in which maximum expression is observed, for mouse protein-coding and
964 lncRNA genes that have no orthologues in the rat or chicken, for genes with orthologues in the rat and
965 for genes with orthologues in chicken.

966 **C.** Same as B, for the distribution of the developmental stage in which maximum expression is
967 observed.

968

969 **Figure 7. Global comparison of lncRNA expression patterns across species.**

970 **A.** First factorial map of a principal component analysis, performed on log2-transformed TPM values,
971 for 2,893 orthologous lncRNAs between mouse and rat. Colors represent different organs and
972 developmental stages, point types represent species.

973 **B.** Hierarchical clustering, performed on a distance matrix derived from Spearman correlations
974 between pairs of samples, for 2,893 orthologous lncRNAs between mouse and rat. Organ and
975 developmental stages are shown below the heatmap. Species of origin is shown on the right. Sample
976 clustering is shown on the left.

977

978 **Figure 8. Global estimates of expression conservation across organs and developmental stages.**

979 **A.** Example of between-species and within-species variation of expression levels, for protein-coding
980 genes (left) and lncRNAs (right), for orthologous genes between mouse and rat, for the mid-stage
981 embryonic brain. Spearman's correlation coefficients (ρ) are shown above each plot. We show a
982 smoothed color density representation of the scatterplots, obtained through a (2D) kernel density
983 estimate (smoothScatter function in R).

984 **B.** Expression conservation index, defined as the ratio of the between-species and the within-species
985 expression level correlation coefficients, for protein-coding genes, for each organ and developmental

986 stage. The vertical segments represent minimum and maximum values obtained from 100 bootstrap
987 replicates. We analyzed 15,931 pairs of orthologous genes between mouse and rat.
988 **C.** Same as B, for lncRNAs. We analyzed 2,893 orthologous mouse and rat lncRNAs.

989

990 **Figure 9. Conservation of developmental expression patterns of differentially expressed lncRNAs.**

991 **A.** Comparison of the developmental stage in which maximum expression is observed, for orthologous
992 lncRNAs that are significantly differentially expressed ($FDR < 0.01$) among developmental stages, for
993 both mouse and rat. Genes are divided based on the developmental stage where maximum expression
994 is observed in mouse organs (X-axis). The Y axis represents the percentage of orthologous genes that
995 reach maximum expression in each developmental stage, in the rat. Numbers of analyzed genes are
996 shown below the plot.

997 **B.** Expression profiles of orthologous lncRNAs that are significantly differentially expressed ($FDR < 0.01$)
998 among developmental stages, for both mouse and rat, in the brain. TPM values were averaged across
999 replicates and normalized by dividing by the maximum, for each species. The resulting relative
1000 expression profiles were combined across species and clustered with the K-means algorithm. The
1001 average profiles of the genes belonging to each cluster are shown. Gray lines represent profiles of
1002 individual genes from a cluster. Numbers of genes in each cluster are shown in the plot.

1003 **C.** Same as B, for the kidney.

1004 **D.** Same as B, for the liver.

1005 **E.** Same as B, for the testes. For this organ, we searched for only 4 clusters with the K-means algorithm.

1006

1007 **Figure 10. Per-gene estimates of expression pattern divergence between species.**

1008 **A.** Relationship between the per-gene expression divergence measure (Euclidean distance of relative
1009 expression profiles among organs/stages, between mouse and rat), and the average expression values
1010 (\log_2 -transformed TPM) across all mouse and rat samples. We show a smoothed color density

1011 representation of the scatterplots, obtained through a (2D) kernel density estimate (smoothScatter
1012 function in R). Red line: linear regression.

1013 **B.** Distribution of the expression divergence value for all protein-coding and lncRNA genes with
1014 predicted 1-to-1 orthologues in mouse and rat.

1015 **C.** Distribution of the residual expression divergence values, after regressing the average expression
1016 level, for protein-coding genes and lncRNAs.

1017 **D.** Relationship between expression divergence and exonic sequence conservation (% exonic sequence
1018 aligned without gaps between mouse and rat), for protein-coding genes and lncRNAs.

1019 **E.** Average contribution of each organ/developmental stage combination to expression divergence, for
1020 protein-coding genes and lncRNAs.

1021

1022

1023 **References**

- 1024 Altschul SF, Gish W, Miller W, Myers EW, Lipman DJ. 1990. Basic local alignment search tool. *J Mol Biol*
1025 **215**: 403–410.
- 1026 Amândio AR, Necsulea A, Joye E, Mascrez B, Duboule D. 2016. Hotair is dispensible for mouse
1027 development. *PLoS Genet* **12**: e1006232.
- 1028 Anders S, Huber W. 2010. Differential expression analysis for sequence count data. *Genome Biol* **11**:
1029 R106.
- 1030 Anderson KM, Anderson DM, McAnally JR, Shelton JM, Bassel-Duby R, Olson EN. 2016. Transcription
1031 of the non-coding RNA upperhand controls Hand2 expression and heart development. *Nature*
1032 **539**: 433–436.
- 1033 Arendt D, Musser JM, Baker CVH, Bergman A, Cepko C, Erwin DH, Pavlicev M, Schlosser G, Widder S,
1034 Laubichler MD, et al. 2016. The origin and evolution of cell types. *Nat Rev Genet* **17**: 744–757.
- 1035 Ayers KL, Davidson NM, Demiyah D, Roeszler KN, Grützner F, Sinclair AH, Oshlack A, Smith CA. 2013.
1036 RNA sequencing reveals sexually dimorphic gene expression before gonadal differentiation in
1037 chicken and allows comprehensive annotation of the W-chromosome. *Genome Biol* **14**.
- 1038 Bassett AR, Akhtar A, Barlow DP, Bird AP, Brockdorff N, Duboule D, Ephrussi A, Ferguson-Smith AC,
1039 Gingeras TR, Haerty W, et al. 2014. Considerations when investigating lncRNA function in vivo.
1040 *eLife* **3**: e03058.
- 1041 Benjamini Y, Hochberg Y. 1995. Controlling the false discovery rate: a practical and powerful approach
1042 to multiple testing. *J Roy Stat Soc B* **57**: 289+300.
- 1043 Ben-Tabou de-Leon S, Davidson EH. 2007. Gene regulation: gene control network in development.
1044 *Annu Rev Biophys Biomol Struct* **36**: 191.
- 1045 Blanchette M, Kent WJ, Riemer C, Elnitski L, Smit AFA, Roskin KM, Baertsch R, Rosenbloom K, Clawson
1046 H, Green ED, et al. 2004. Aligning multiple genomic sequences with the threaded blockset
1047 aligner. *Genome Res* **14**: 708–715.
- 1048 Brannan CI, Dees EC, Ingram RS, Tilghman SM. 1990. The product of the H19 gene may function as an
1049 RNA. *Mol Cell Biol* **10**: 28–36.
- 1050 Brawand D, Soumillon M, Necsulea A, Julien P, Csárdi G, Harrigan P, Weier M, Liechti A, Aximu-Petri A,
1051 Kircher M, et al. 2011. The evolution of gene expression levels in mammalian organs. *Nature*
1052 **478**: 343–348.
- 1053 Bray NL, Pimentel H, Melsted P, Pachter L. 2016. Near-optimal probabilistic RNA-seq quantification.
1054 *Nat Biotechnol* **34**: 525–527.
- 1055 Brown CJ, Ballabio A, Rupert JL, Lafreniere RG, Grompe M, Tonlorenzi R, Willard HF. 1991. A gene from
1056 the region of the human X inactivation centre is expressed exclusively from the inactive X
1057 chromosome. *Nature* **349**: 38–44.
- 1058 Camacho C, Coulouris G, Avagyan V, Ma N, Papadopoulos J, Bealer K, Madden TL. 2009. BLAST+:
1059 architecture and applications. *BMC Bioinformatics* **10**: 421.

- 1060 Carelli FN, Hayakawa T, Go Y, Imai H, Warnefors M, Kaessmann H. 2016. The life history of retrocopies
1061 illuminates the evolution of new mammalian genes. *Genome Res* **26**: 301–314.
- 1062 Casper J, Zweig AS, Villarreal C, Tyner C, Speir ML, Rosenbloom KR, Raney BJ, Lee CM, Lee BT, Karolchik
1063 D, et al. 2018. The UCSC Genome Browser database: 2018 update. *Nucleic Acids Res* **46**: D762–
1064 D769.
- 1065 Cesana M, Cacchiarelli D, Legnini I, Santini T, Sthandier O, Chinappi M, Tramontano A, Bozzoni I. 2011.
1066 A long noncoding RNA controls muscle differentiation by functioning as a competing
1067 endogenous RNA. *Cell* **147**: 358–369.
- 1068 Cortez D, Marin R, Toledo-Flores D, Froidevaux L, Liechti A, Waters PD, Grützner F, Kaessmann H. 2014.
1069 Origins and functional evolution of Y chromosomes across mammals. *Nature* **508**: 488–93.
- 1070 Cunningham F, Achuthan P, Akanni W, Allen J, Amode MR, Armean IM, Bennett R, Bhai J, Billis K, Boddu
1071 S, et al. 2019. Ensembl 2019. *Nucleic Acids Res* **47**: D745–D751.
- 1072 Doolittle WF. 2018. We simply cannot go on being so vague about “function.” *Genome Biol* **19**: 223.
- 1073 Dray S, Dufour AB. 2007. The ade4 package: implementing the duality diagram for ecologists. *J Stat*
1074 *Softw* **22**: 1–20.
- 1075 El-Gebali S, Mistry J, Bateman A, Eddy SR, Luciani A, Potter SC, Qureshi M, Richardson LJ, Salazar GA,
1076 Smart A, et al. 2019. The Pfam protein families database in 2019. *Nucleic Acids Res* **47**: D427–
1077 D432.
- 1078 Engreitz JM, Haines JE, Perez EM, Munson G, Chen J, Kane M, McDonel PE, Guttman M, Lander ES.
1079 2016. Local regulation of gene expression by lncRNA promoters, transcription and splicing.
1080 *Nature* **539**: 452–455.
- 1081 Gendrel A-V, Heard E. 2014. Noncoding RNAs and epigenetic mechanisms during X-chromosome
1082 inactivation. *Annu Rev Cell Dev Biol* **30**: 561–580.
- 1083 Goudarzi M, Berg K, Pieper LM, Schier AF. 2019. Individual long non-coding RNAs have no overt
1084 functions in zebrafish embryogenesis, viability and fertility. *eLife* **8**.
- 1085 Graur D, Zheng Y, Price N, Azevedo RBR, Zufall RA, Elhaik E. 2013. On the immortality of television sets:
1086 “function” in the human genome according to the evolution-free gospel of ENCODE. *Genome*
1087 *Biol Evol* **5**: 578–590.
- 1088 Green CD, Ma Q, Manske GL, Shami AN, Zheng X, Marini S, Moritz L, Sultan C, Gurczynski SJ, Moore BB,
1089 et al. 2018. A comprehensive roadmap of murine spermatogenesis defined by single-cell RNA-
1090 Seq. *Dev Cell* **46**: 651-667.e10.
- 1091 Groff AF, Sanchez-Gomez DB, Soruco MML, Gerhardinger C, Barutcu AR, Li E, Elcavage L, Plana O,
1092 Sanchez LV, Lee JC, et al. 2016. In vivo characterization of Linc-p21 reveals functional cis-
1093 regulatory DNA elements. *Cell Rep* **16**: 2178–2186.
- 1094 Grote P, Herrmann BG. 2015. Long noncoding RNAs in organogenesis: making the difference. *Trends*
1095 *Genet TIG* **31**: 329–335.

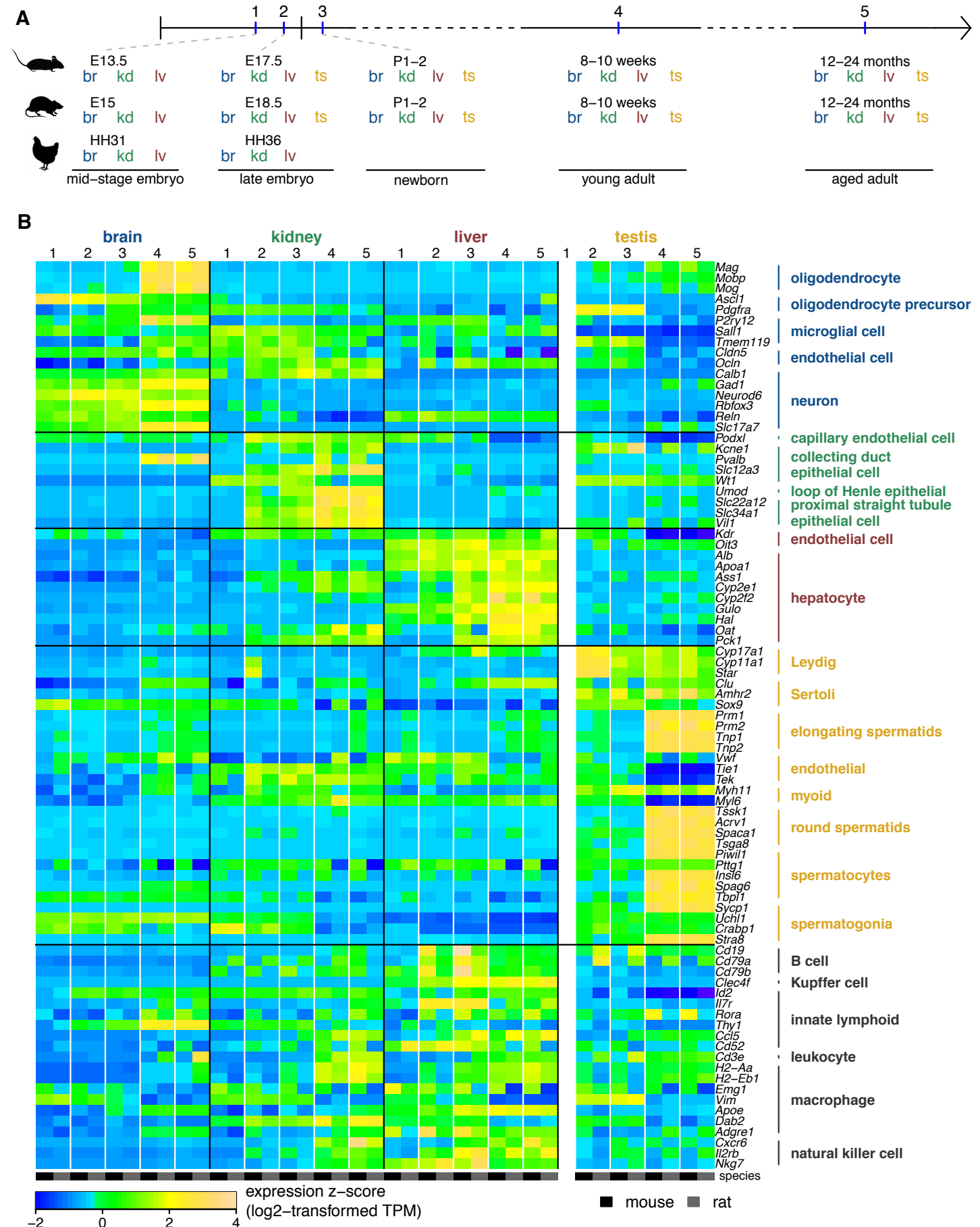
- 1096 Grote P, Wittler L, Hendrix D, Koch F, Währisch S, Beisaw A, Macura K, Bläss G, Kellis M, Werber M, et
1097 al. 2013. The tissue-specific lncRNA Fendrr is an essential regulator of heart and body wall
1098 development in the mouse. *Dev Cell* **24**: 206–214.
- 1099 Guttman M, Amit I, Garber M, French C, Lin MF, Feldser D, Huarte M, Zuk O, Carey BW, Cassady JP, et
1100 al. 2009. Chromatin signature reveals over a thousand highly conserved large non-coding RNAs
1101 in mammals. *Nature* **458**: 223–227.
- 1102 Haerty W, Ponting CP. 2013. Mutations within lncRNAs are effectively selected against in fruitfly but
1103 not in human. *Genome Biol* **14**: R49.
- 1104 Haerty W, Ponting CP. 2014. No gene in the genome makes sense except in the light of evolution. *Annu*
1105 *Rev Genomics Hum Genet* **15**: 71–92.
- 1106 Haerty W, Ponting CP. 2015. Unexpected selection to retain high GC content and splicing enhancers
1107 within exons of multiexonic lncRNA loci. *RNA N Y N* **21**: 333–346.
- 1108 Hamburger V, Hamilton HL. 1951. A series of normal stages in the development of the chick embryo. *J*
1109 *Morphol* **88**: 49–92.
- 1110 Herrero J, Muffato M, Beal K, Fitzgerald S, Gordon L, Pignatelli M, Vilella AJ, Searle SMJ, Amode R, Brent
1111 S, et al. 2016. Ensembl comparative genomics resources. *Database J Biol Databases Curation*
1112 **2016**.
- 1113 Hezroni H, Koppstein D, Schwartz MG, Avrutin A, Bartel DP, Ulitsky I. 2015. Principles of long noncoding
1114 RNA evolution derived from direct comparison of transcriptomes in 17 species. *Cell Rep* **11**:
1115 1110–1122.
- 1116 Iyer MK, Niknafs YS, Malik R, Singhal U, Sahu A, Hosono Y, Barrette TR, Prensner JR, Evans JR, Zhao S,
1117 et al. 2015. The landscape of long noncoding RNAs in the human transcriptome. *Nat Genet* **47**:
1118 199–208.
- 1119 Kaessmann H. 2010. Origins, evolution, and phenotypic impact of new genes. *Genome Res* **20**: 1313–
1120 1326.
- 1121 Kathleen Baxter K, Uittenbogaard M, Yoon J, Chiaramello A. 2009. The neurogenic basic helix-loop-
1122 helix transcription factor NeuroD6 concomitantly increases mitochondrial mass and regulates
1123 cytoskeletal organization in the early stages of neuronal differentiation. *ASN Neuro* **1**.
- 1124 Khalil AM, Guttman M, Huarte M, Garber M, Raj A, Rivea Morales D, Thomas K, Presser A, Bernstein
1125 BE, van Oudenaarden A, et al. 2009. Many human large intergenic noncoding RNAs associate
1126 with chromatin-modifying complexes and affect gene expression. *Proc Natl Acad Sci U S A* **106**:
1127 11667–11672.
- 1128 Kim D, Langmead B, Salzberg SL. 2015. HISAT: a fast spliced aligner with low memory requirements.
1129 *Nat Methods* **12**: 357–60.
- 1130 Kutter C, Watt S, Stefflova K, Wilson MD, Goncalves A, Ponting CP, Odom DT, Marques AC. 2012. Rapid
1131 turnover of long noncoding RNAs and the evolution of gene expression. *PLoS Genet* **8**:
1132 e1002841.

- 1133 Latos PA, Pauler FM, Koerner MV, Şenergin HB, Hudson QJ, Stocsits RR, Allhoff W, Stricker SH, Klement
1134 RM, Warczok KE, et al. 2012. Airn transcriptional overlap, but not its lncRNA products, induces
1135 imprinted Igf2r silencing. *Science* **338**: 1469–1472.
- 1136 Liao B-Y, Scott NM, Zhang J. 2006. Impacts of gene essentiality, expression pattern, and gene
1137 compactness on the evolutionary rate of mammalian proteins. *Mol Biol Evol* **23**: 2072–2080.
- 1138 Liao Y, Smyth GK, Shi W. 2019. The R package Rsubread is easier, faster, cheaper and better for
1139 alignment and quantification of RNA sequencing reads. *Nucleic Acids Res.*
- 1140 Lin MF, Carlson JW, Crosby MA, Matthews BB, Yu C, Park S, Wan KH, Schroeder AJ, Gramates LS, St
1141 Pierre SE, et al. 2007. Revisiting the protein-coding gene catalog of *Drosophila melanogaster*
1142 using 12 fly genomes. *Genome Res* **17**: 1823–1836.
- 1143 Lin MF, Jungreis I, Kellis M. 2011. PhyloCSF: a comparative genomics method to distinguish protein
1144 coding and non-coding regions. *Bioinforma Oxf Engl* **27**: i275-282.
- 1145 Liu SJ, Nowakowski TJ, Pollen AA, Lui JH, Horlbeck MA, Attenello FJ, He D, Weissman JS, Kriegstein AR,
1146 Diaz AA, et al. 2016. Single-cell analysis of long non-coding RNAs in the developing human
1147 neocortex. *Genome Biol* **17**: 67.
- 1148 Love MI, Huber W, Anders S. 2014. Moderated estimation of fold change and dispersion for RNA-seq
1149 data with DESeq2. *Genome Biol* **15**: 550.
- 1150 Marques AC, Hughes J, Graham B, Kowalczyk MS, Higgs DR, Ponting CP. 2013. Chromatin signatures at
1151 transcriptional start sites separate two equally populated yet distinct classes of intergenic long
1152 noncoding RNAs. *Genome Biol* **14**: R131.
- 1153 McMahon AP. 2016. Development of the Mammalian Kidney. *Curr Top Dev Biol* **117**: 31–64.
- 1154 Nakagaki BN, Mafra K, de Carvalho É, Lopes ME, Carvalho-Gontijo R, de Castro-Oliveira HM, Campolina-
1155 Silva GH, de Miranda CDM, Antunes MM, Silva ACC, et al. 2018. Immune and metabolic shifts
1156 during neonatal development reprogram liver identity and function. *J Hepatol* **69**: 1294–1307.
- 1157 Necsulea A, Soumillon M, Warnefors M, Liechti A, Daish T, Grutzner F, Kaessmann H. 2014. The
1158 evolution of lncRNA repertoires and expression patterns in tetrapods. *Nature* **505**: 635–640.
- 1159 Ørom UA, Derrien T, Beringer M, Gumireddy K, Gardini A, Bussotti G, Lai F, Zytnicki M, Notredame C,
1160 Huang Q, et al. 2010. Long noncoding RNAs with enhancer-like function in human cells. *Cell*
1161 **143**: 46–58.
- 1162 Perteau M, Perteau GM, Antonescu CM, Chang T-C, Mendell JT, Salzberg SL. 2015. StringTie enables
1163 improved reconstruction of a transcriptome from RNA-seq reads. *Nat Biotechnol* **33**: 290–5.
- 1164 Perteau M, Shumate A, Perteau G, Varabyou A, Breitwieser FP, Chang Y-C, Madugundu AK, Pandey A,
1165 Salzberg SL. 2018. CHES: a new human gene catalog curated from thousands of large-scale
1166 RNA sequencing experiments reveals extensive transcriptional noise. *Genome Biol* **19**: 208.
- 1167 Ponjavic J, Ponting CP, Lunter G. 2007. Functionality or transcriptional noise? Evidence for selection
1168 within long noncoding RNAs. *Genome Res* **17**: 556–65.
- 1169 R Core Team. 2018. *R: A Language and Environment for Statistical Computing*. [https://www.R-](https://www.R-project.org/)
1170 [project.org/](https://www.R-project.org/).

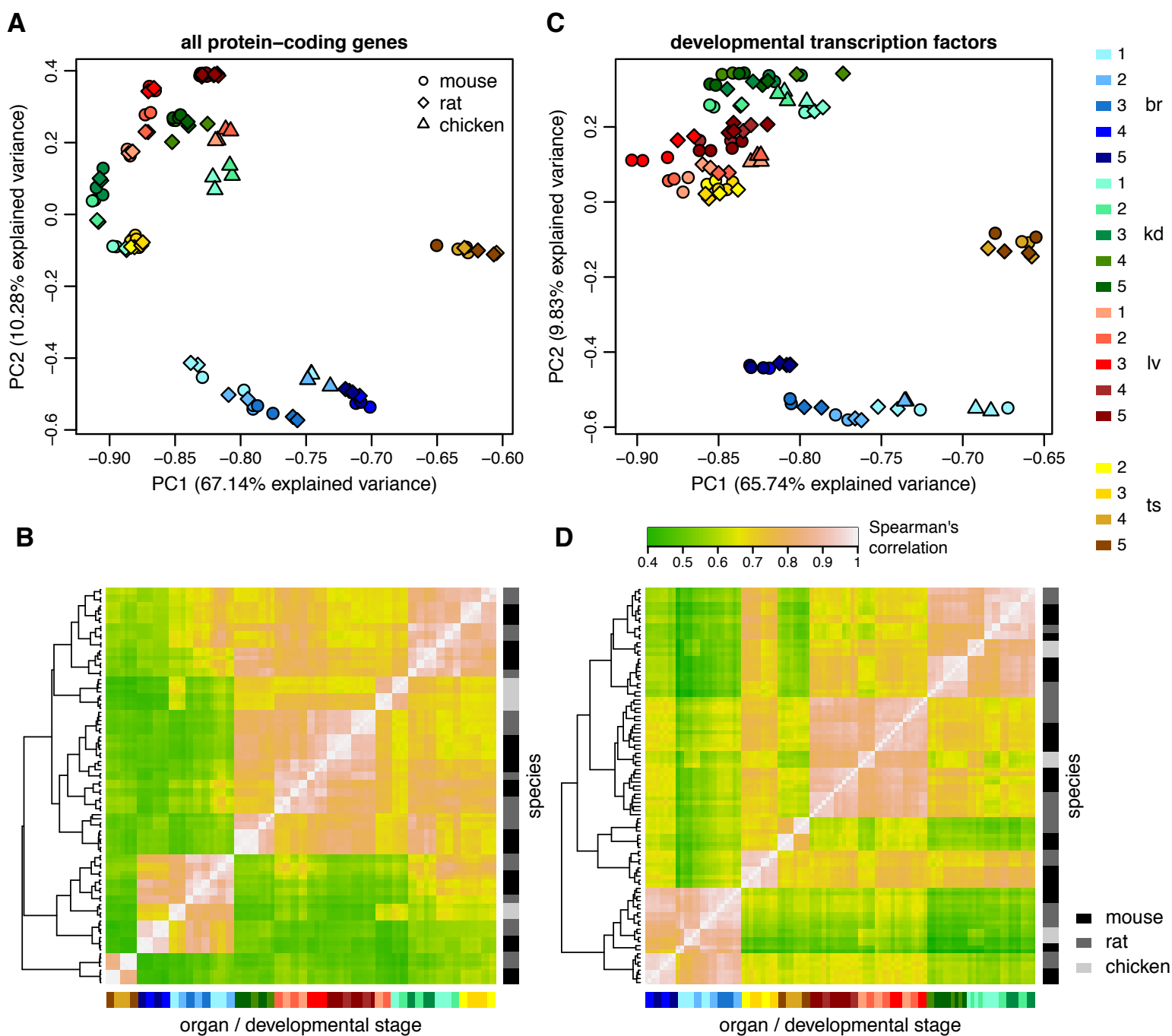
- 1171 Ramsköld D, Wang ET, Burge CB, Sandberg R. 2009. An abundance of ubiquitously expressed genes
1172 revealed by tissue transcriptome sequence data. *PLoS Comput Biol* **5**: e1000598.
- 1173 Rinn JL, Kertesz M, Wang JK, Squazzo SL, Xu X, Bruggmann SA, Goodnough LH, Helms JA, Farnham PJ,
1174 Segal E, et al. 2007. Functional demarcation of active and silent chromatin domains in human
1175 HOX loci by noncoding RNAs. *Cell* **129**: 1311–1323.
- 1176 Sauvageau M, Goff LA, Lodato S, Bonev B, Groff AF, Gerhardinger C, Sanchez-Gomez DB, Hacısuleyman
1177 E, Li E, Spence M, et al. 2013. Multiple knockout mouse models reveal lincRNAs are required
1178 for life and brain development. *eLife* **2**: e01749.
- 1179 Schüler A, Ghanbarian AT, Hurst LD. 2014. Purifying selection on splice-related motifs, not expression
1180 level nor RNA folding, explains nearly all constraint on human lincRNAs. *Mol Biol Evol* **31**: 3164–
1181 3183.
- 1182 Shen Y, Yue F, McCleary DF, Ye Z, Edsall L, Kuan S, Wagner U, Dixon J, Lee L, Lobanenkov VV, et al. 2012.
1183 A map of the cis-regulatory sequences in the mouse genome. *Nature* **488**: 116–120.
- 1184 Siepel A, Bejerano G, Pedersen JS, Hinrichs AS, Hou M, Rosenbloom K, Clawson H, Spieth J, Hillier LW,
1185 Richards S, et al. 2005. Evolutionarily conserved elements in vertebrate, insect, worm, and
1186 yeast genomes. *Genome Res* **15**: 1034–50.
- 1187 Smedley D, Haider S, Ballester B, Holland R, London D, Thorisson G, Kasprzyk A. 2009. BioMart--
1188 biological queries made easy. *BMC Genomics* **10**: 22.
- 1189 Smedley D, Haider S, Durinck S, Pandini L, Provero P, Allen J, Arnaiz O, Awedh MH, Baldock R, Barbiera
1190 G, et al. 2015. The BioMart community portal: an innovative alternative to large, centralized
1191 data repositories. *Nucleic Acids Res* **43**: W589-598.
- 1192 Smit AF., Hubley R, Green P. 2003. *RepeatMasker Open-4.0*. <http://www.repeatmasker.org>.
- 1193 Soumillon M, Necsulea A, Weier M, Brawand D, Zhang X, Gu H, Barthès P, Kokkinaki M, Nef S, Gnirke
1194 A, et al. 2013. Cellular source and mechanisms of high transcriptome complexity in the
1195 mammalian testis. *Cell Rep* **3**: 2179–2190.
- 1196 Tabula Muris Consortium. 2018. Single-cell transcriptomics of 20 mouse organs creates a Tabula Muris.
1197 *Nature* **562**: 367–372.
- 1198 Theiler K. 1989. *The house mouse: atlas of embryonic development*. Springer-Verlag, Berlin Heidelberg
1199 <https://www.springer.com/la/book/9783642884207>.
- 1200 The UniProt Consortium. 2017. UniProt: the universal protein knowledgebase. *Nucleic Acids Res* **45**:
1201 D158–D169.
- 1202 Uebbing S, Konzer A, Xu L, Backström N, Brunström B, Bergquist J, Ellegren H. 2015. Quantitative mass
1203 spectrometry reveals partial translational regulation for dosage compensation in chicken. *Mol*
1204 *Biol Evol* **32**: 2716–2725.
- 1205 Ulitsky I. 2016. Evolution to the rescue: using comparative genomics to understand long non-coding
1206 RNAs. *Nat Rev Genet* **17**: 601–614.
- 1207 Ulitsky I, Shkumatava A, Jan CH, Sive H, Bartel DP. 2011. Conserved function of lincRNAs in vertebrate
1208 embryonic development despite rapid sequence evolution. *Cell* **147**: 1537–1550.

- 1209 Villar D, Berthelot C, Aldridge S, Rayner TF, Lukk M, Pignatelli M, Park TJ, Deaville R, Erichsen JT,
1210 Jasinska AJ, et al. 2015. Enhancer evolution across 20 mammalian species. *Cell* **160**: 554–566.
- 1211 Washietl S, Kellis M, Garber M. 2014. Evolutionary dynamics and tissue specificity of human long
1212 noncoding RNAs in six mammals. *Genome Res* **24**: 616–28.
- 1213 Zakany J, Darbellay F, Mascrez B, Necsulea A, Duboule D. 2017. Control of growth and gut maturation
1214 by HoxD genes and the associated lncRNA Haglr. *Proc Natl Acad Sci U S A* **114**: E9290–E9299.
- 1215

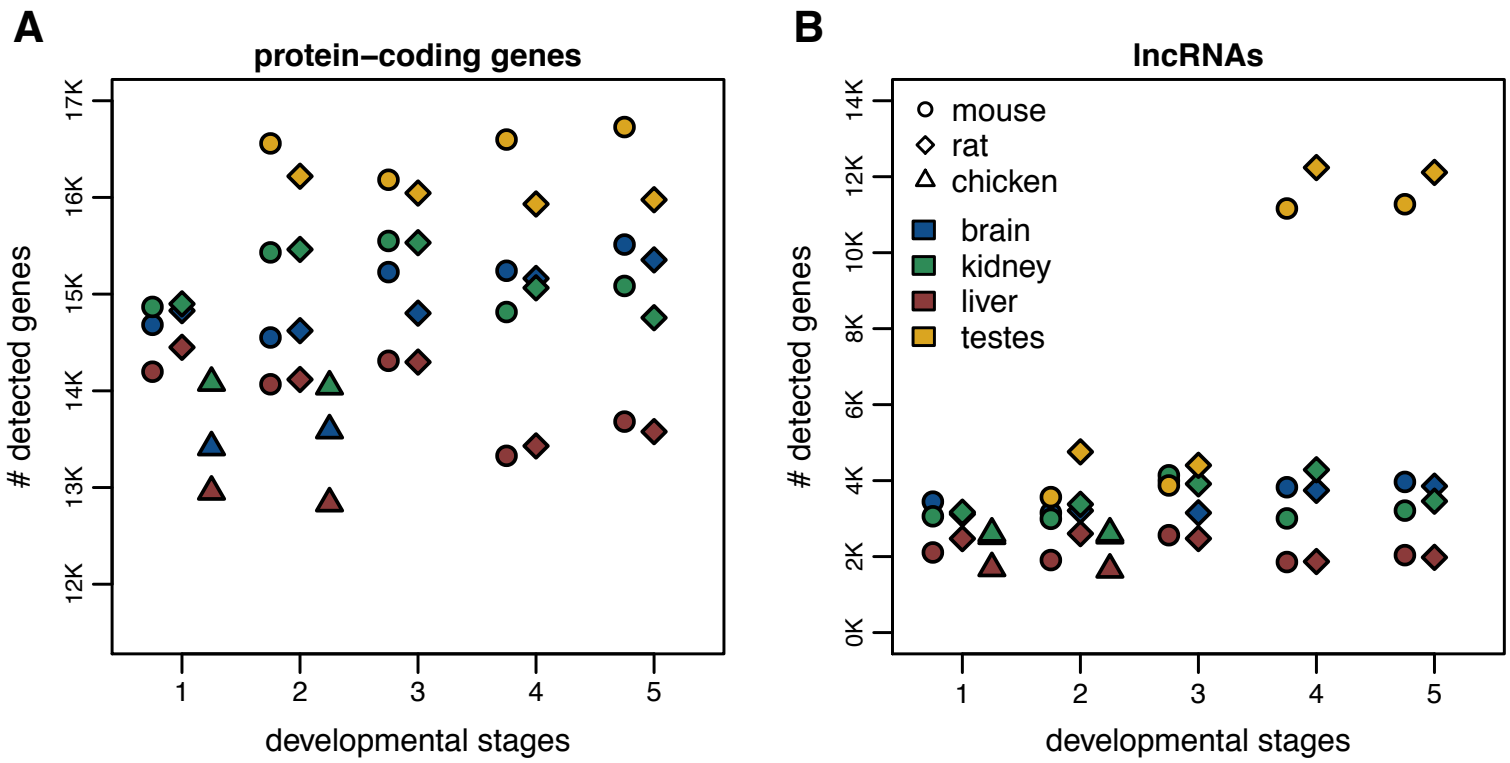
Darbelay and Necsulea, Figure 1



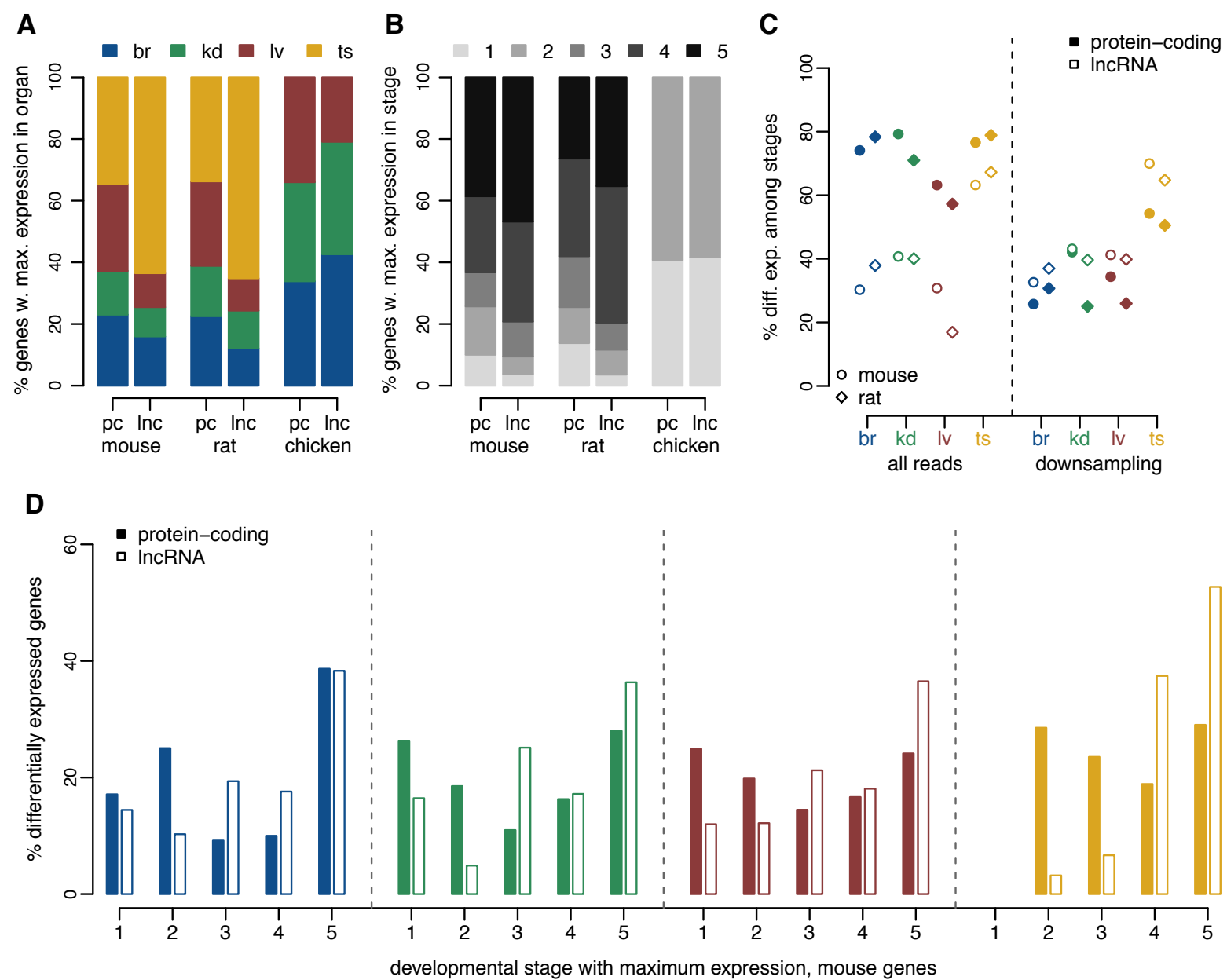
Darbellay and Necsulea, Figure 2



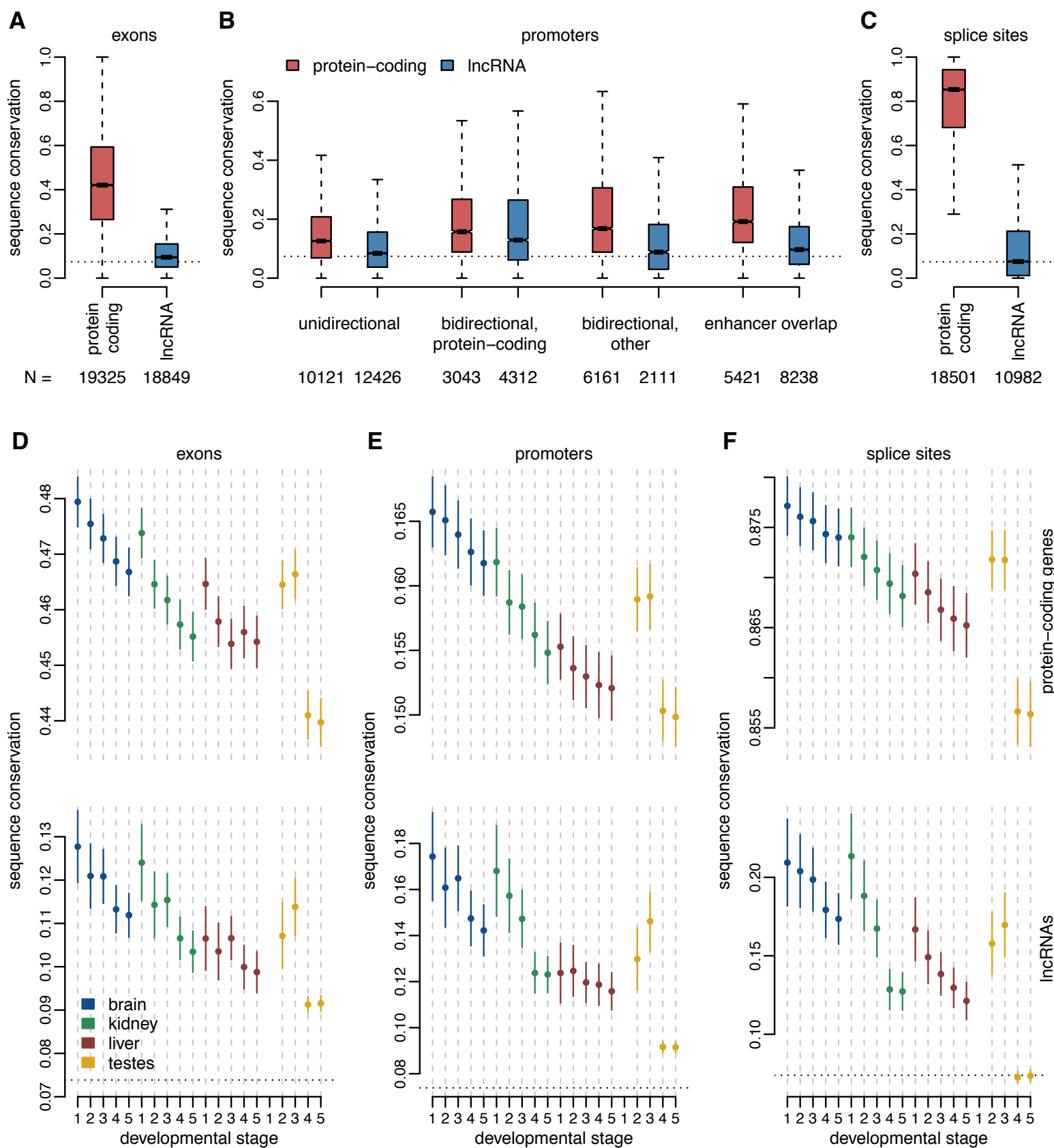
Darbellay and Necsulea, Figure 3



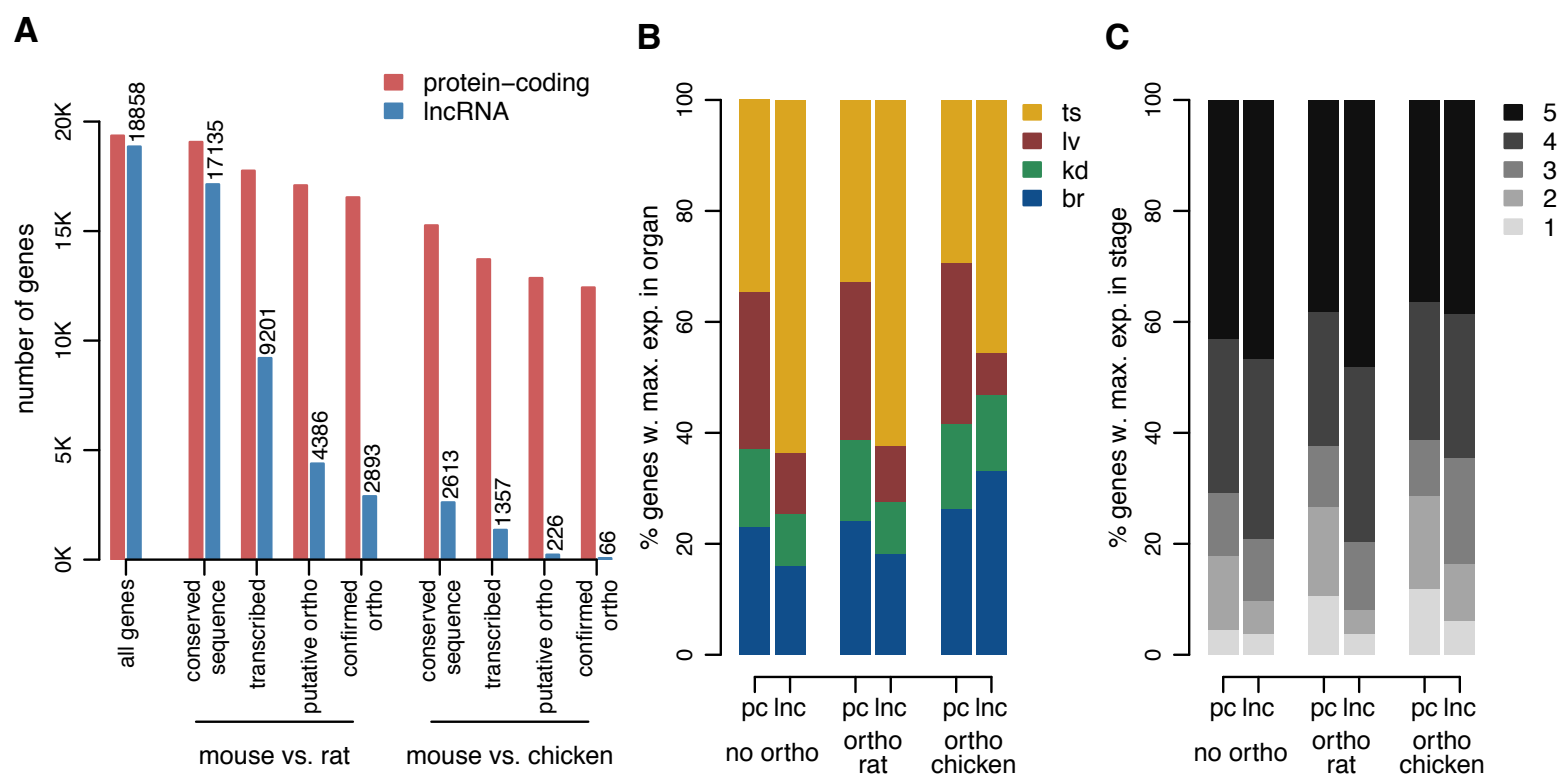
Darbellay and Necsulea, Figure 4



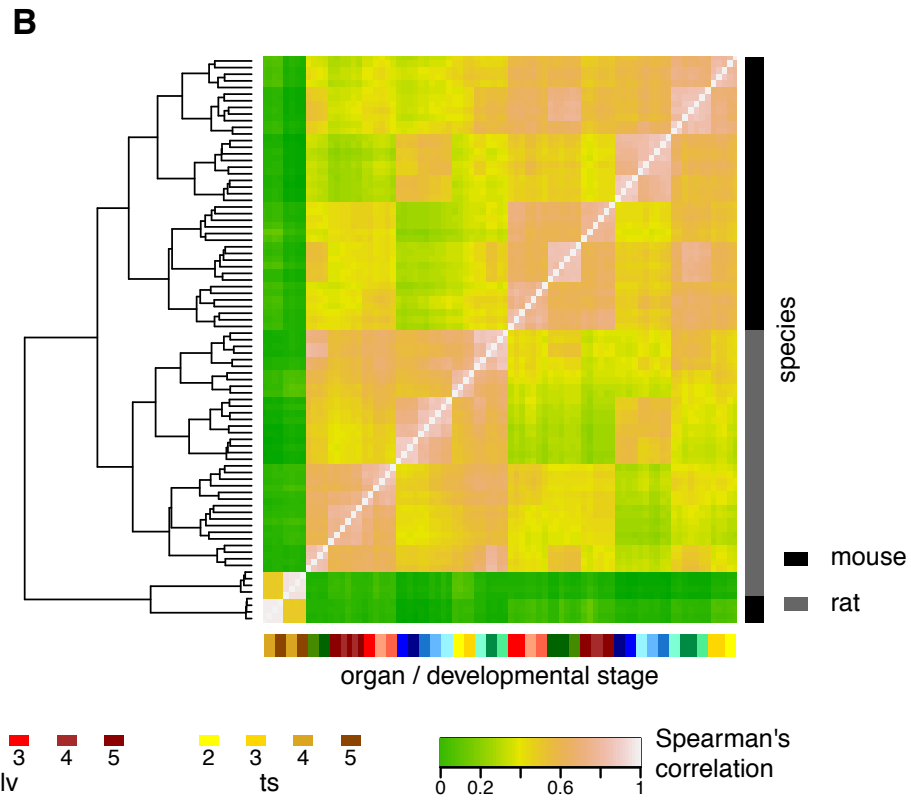
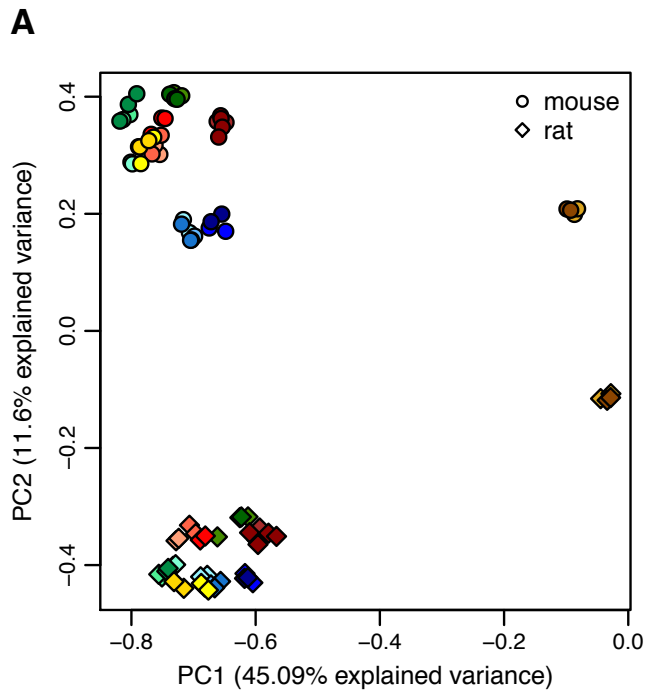
Darbelay and Necsulea, Figure 5



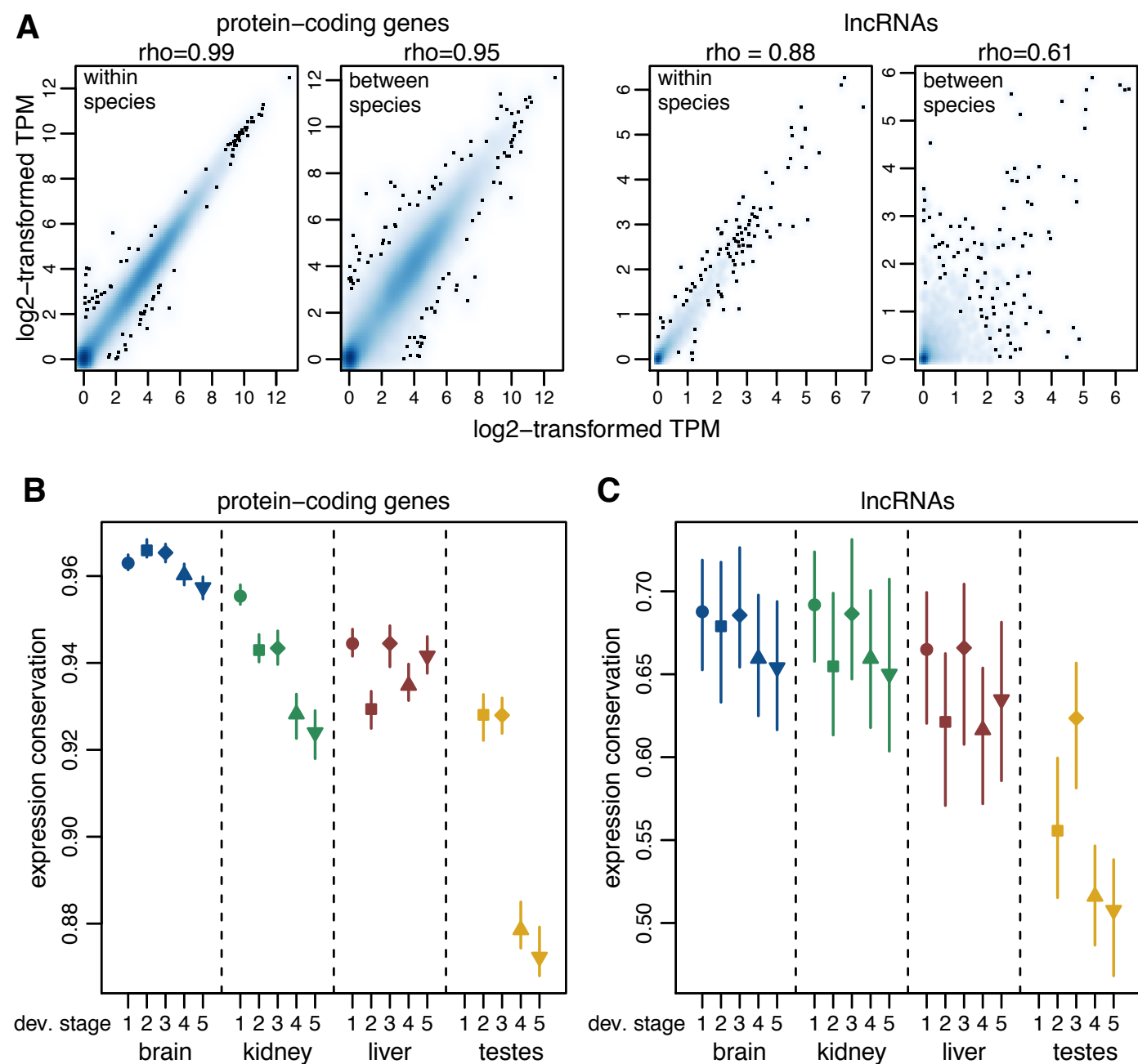
Darbellay and Necsulea, Figure 6



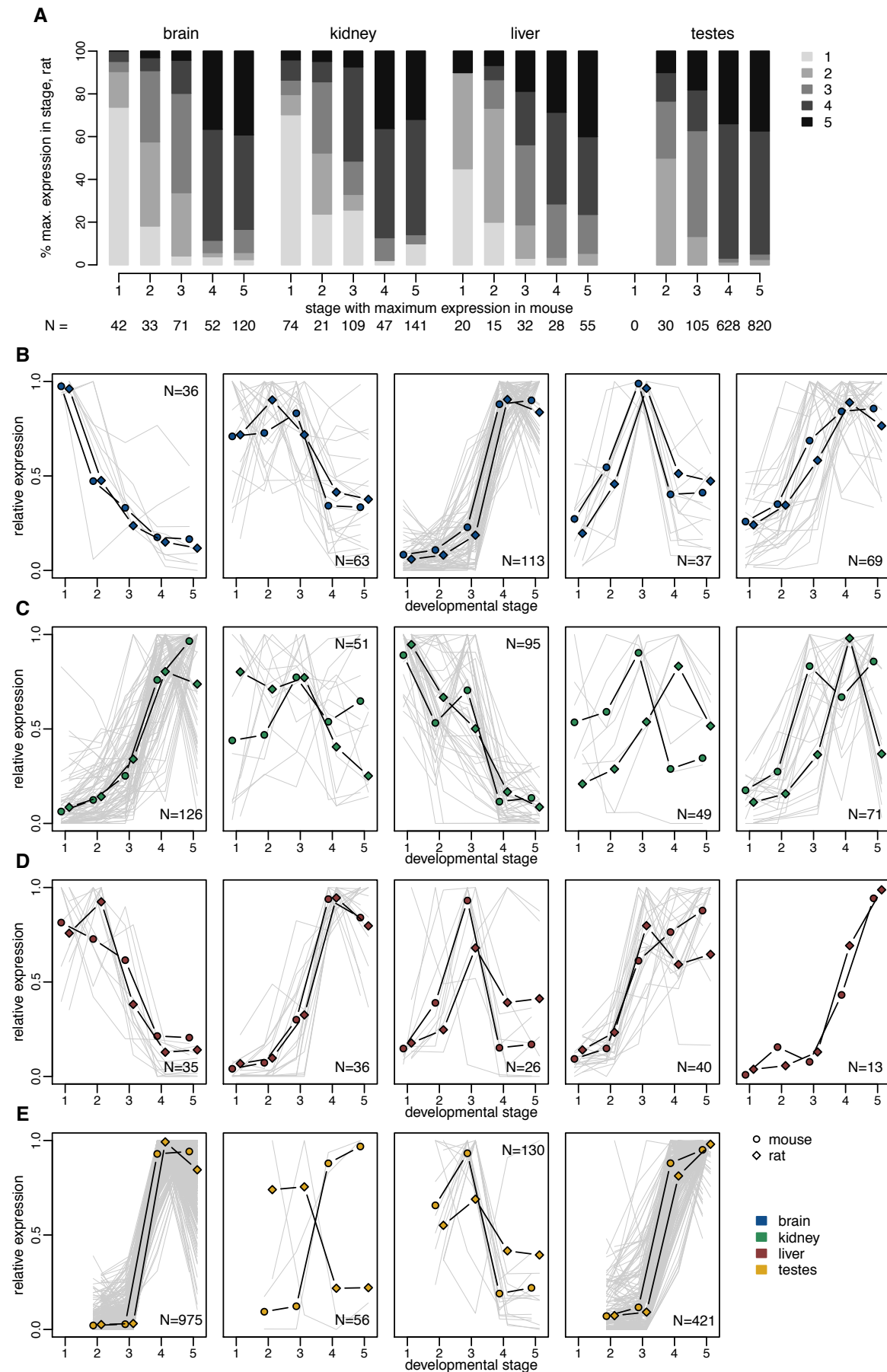
Darbellay and Necsulea, Figure 7



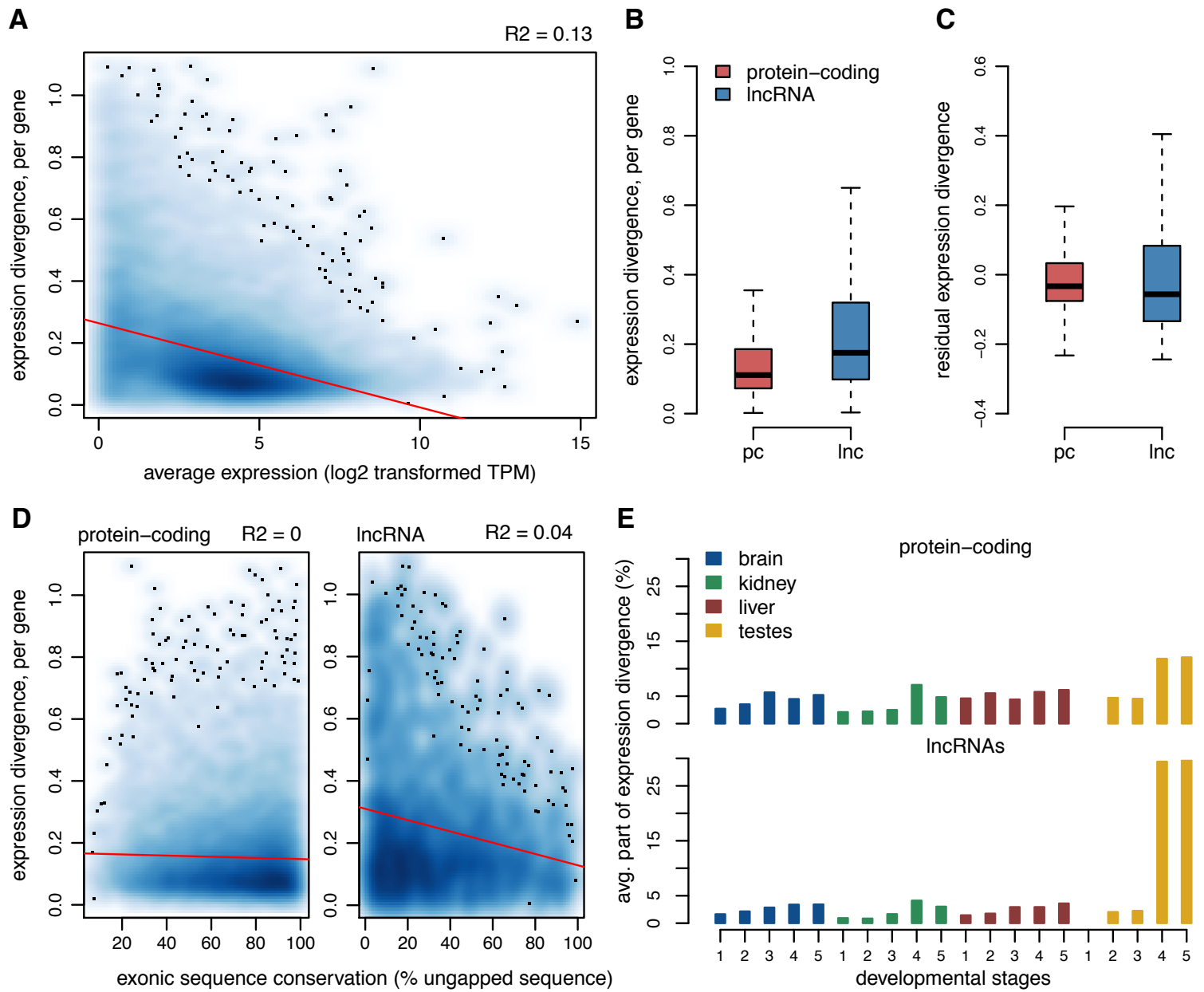
Darbellay and Necsulea, Figure 8



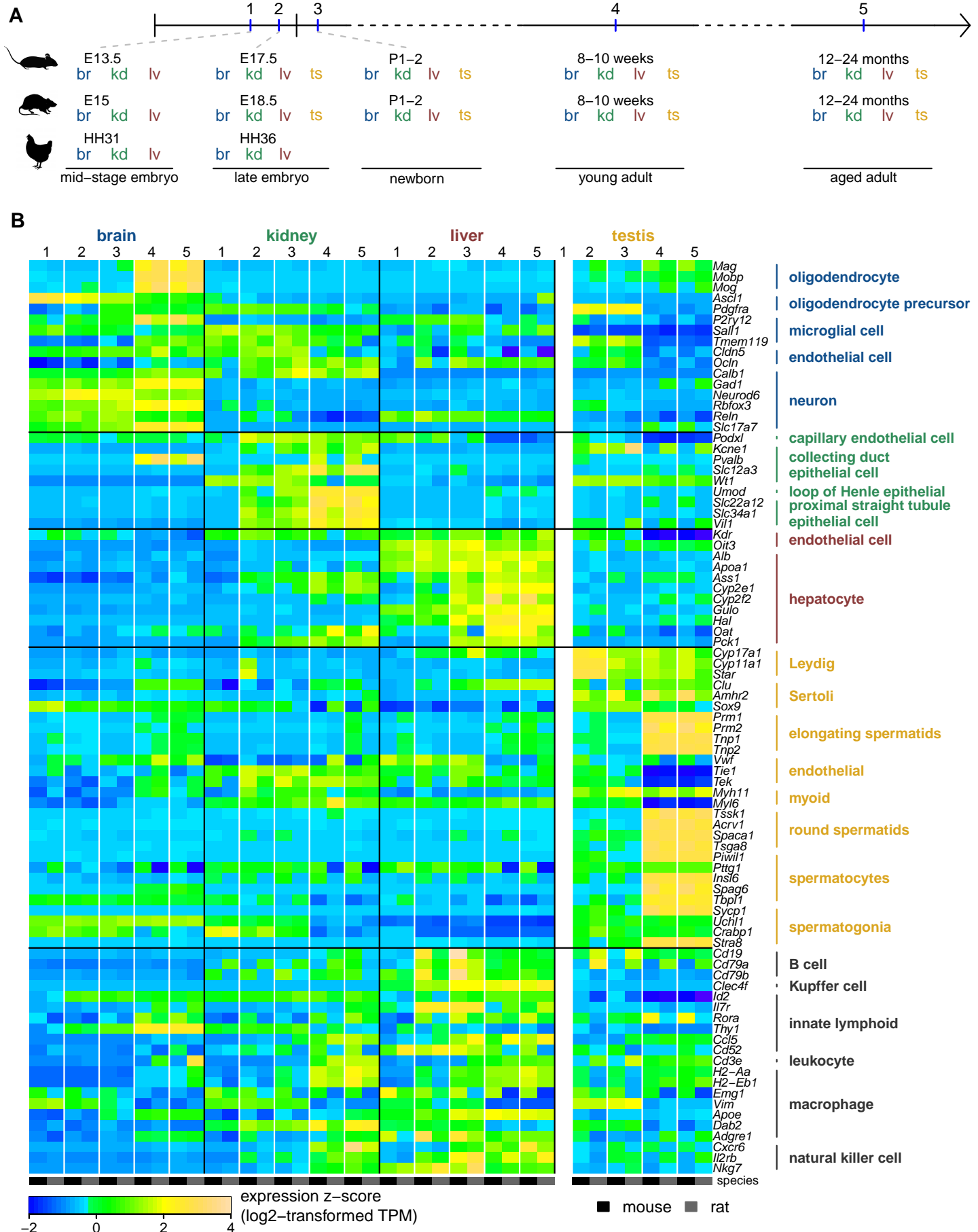
Darbellay and Necsulea, Figure 9



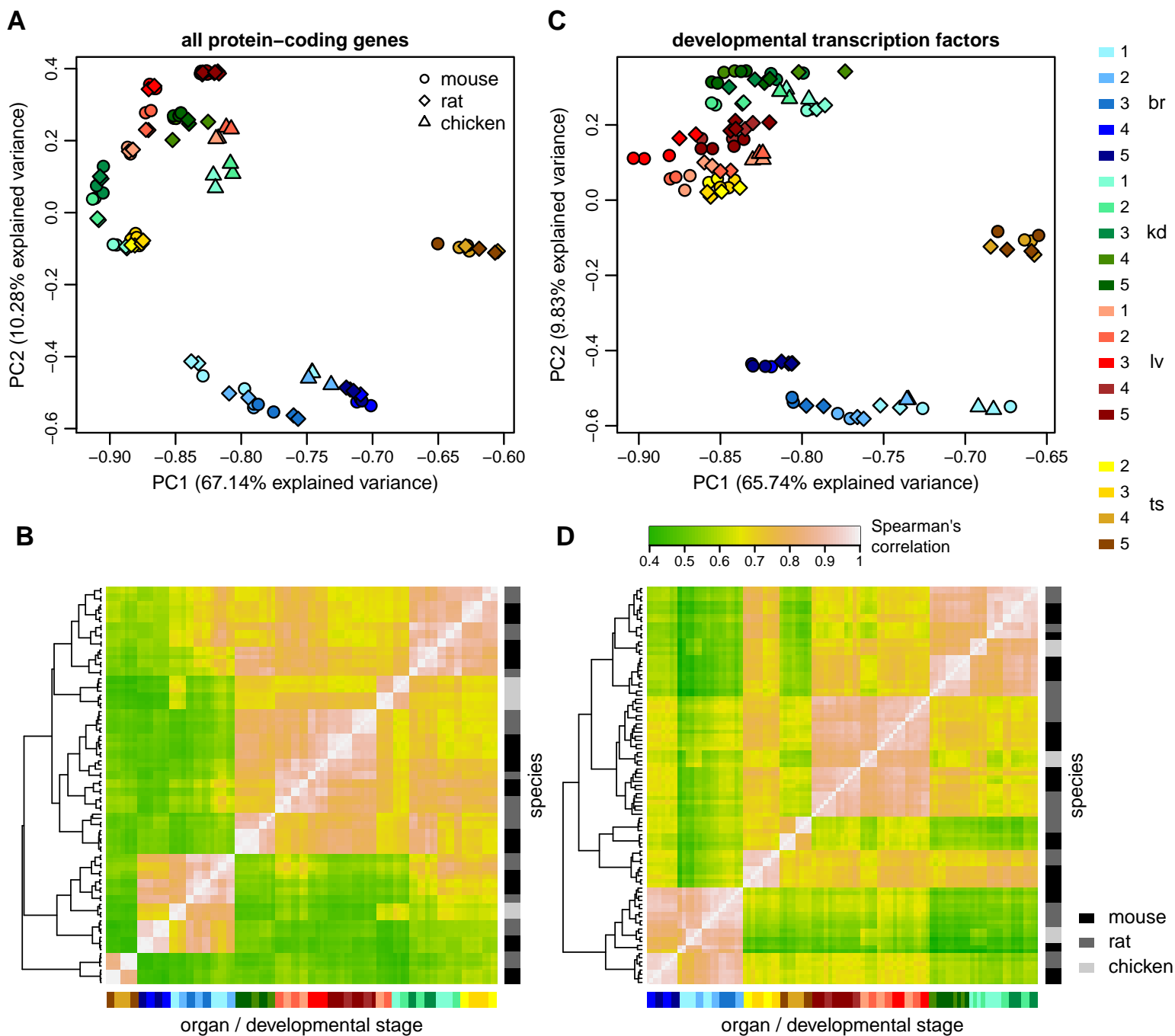
Darbelay and Necsulea, Figure 10



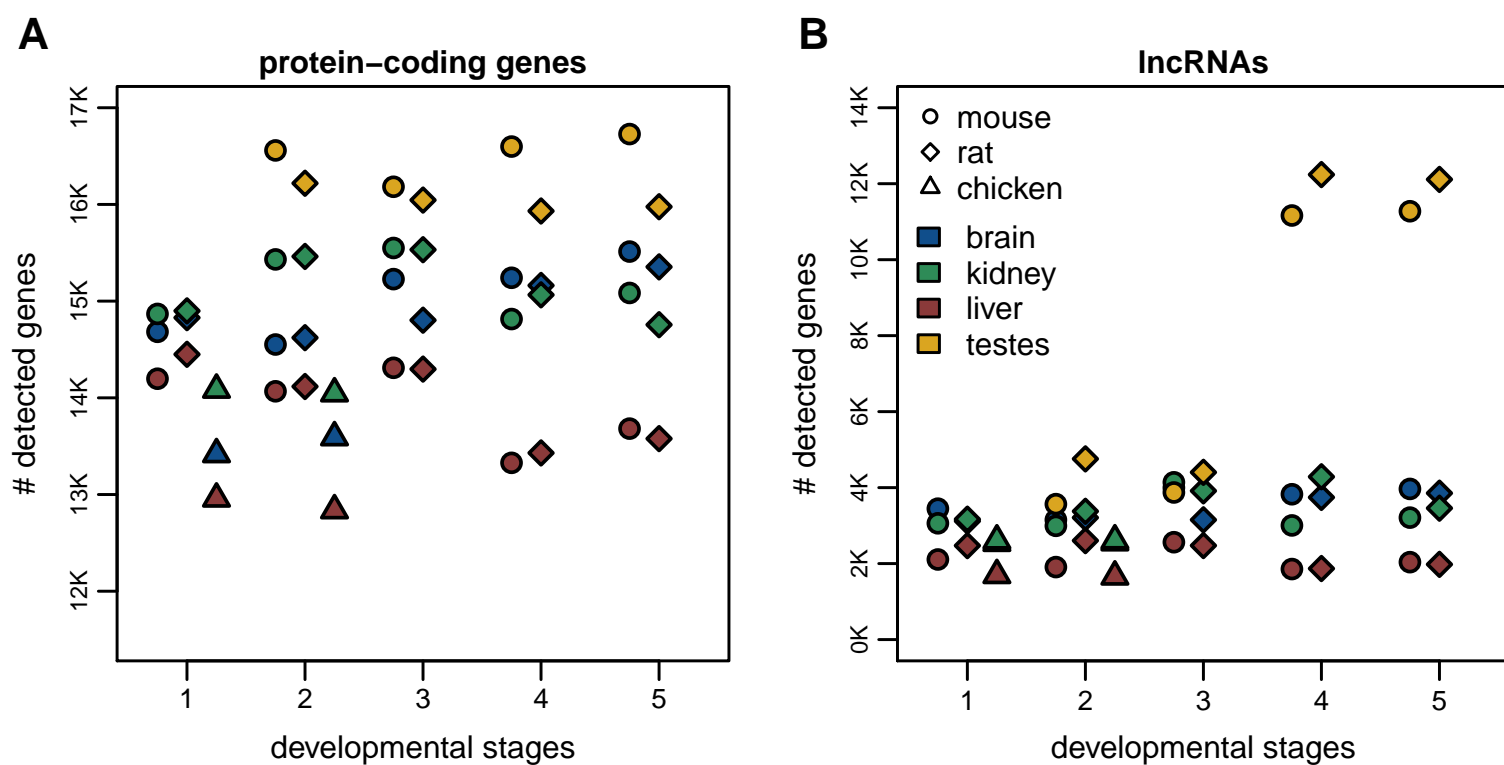
Darbelay and Necsulea, Figure 1



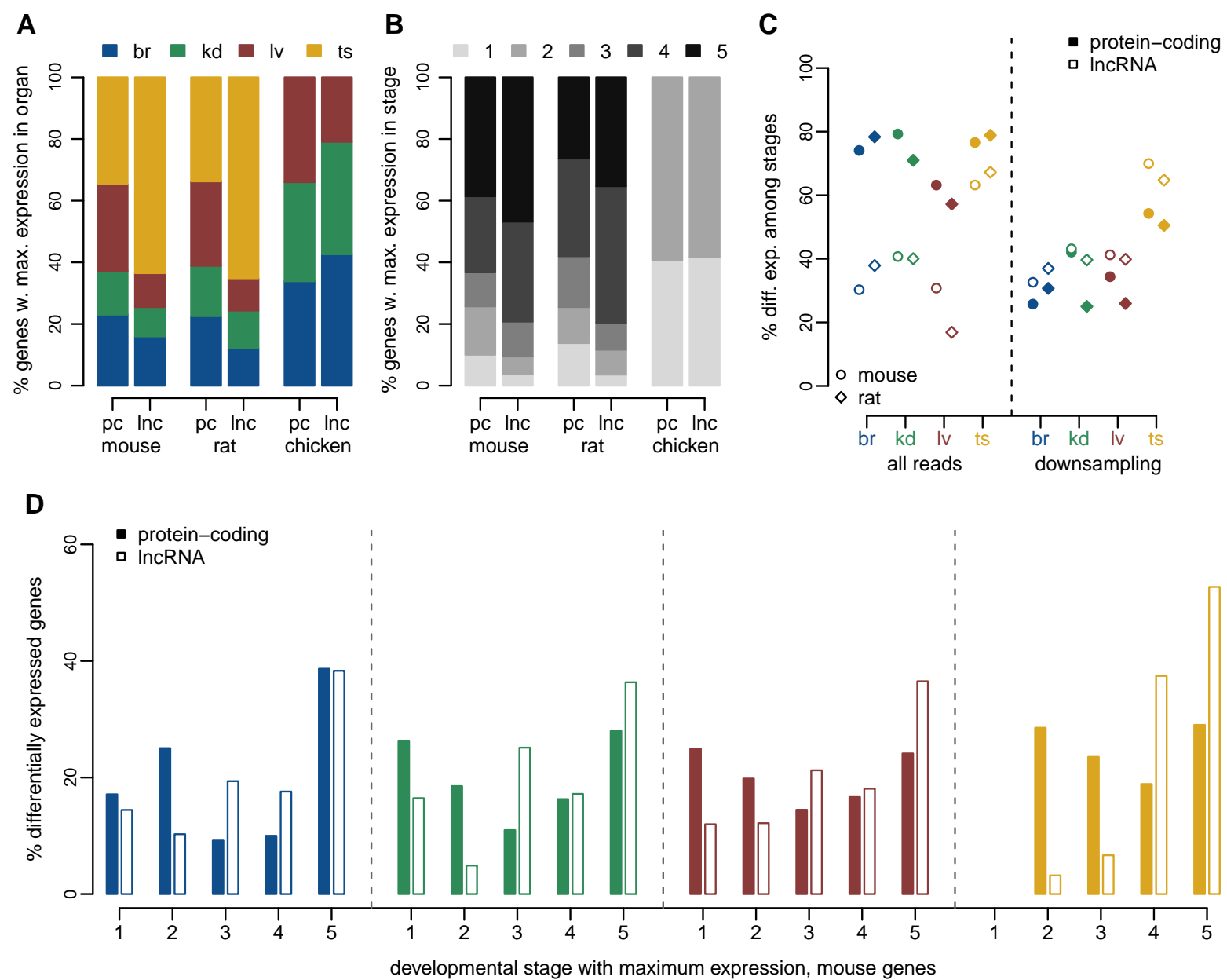
Darbellay and Necsulea, Figure 2



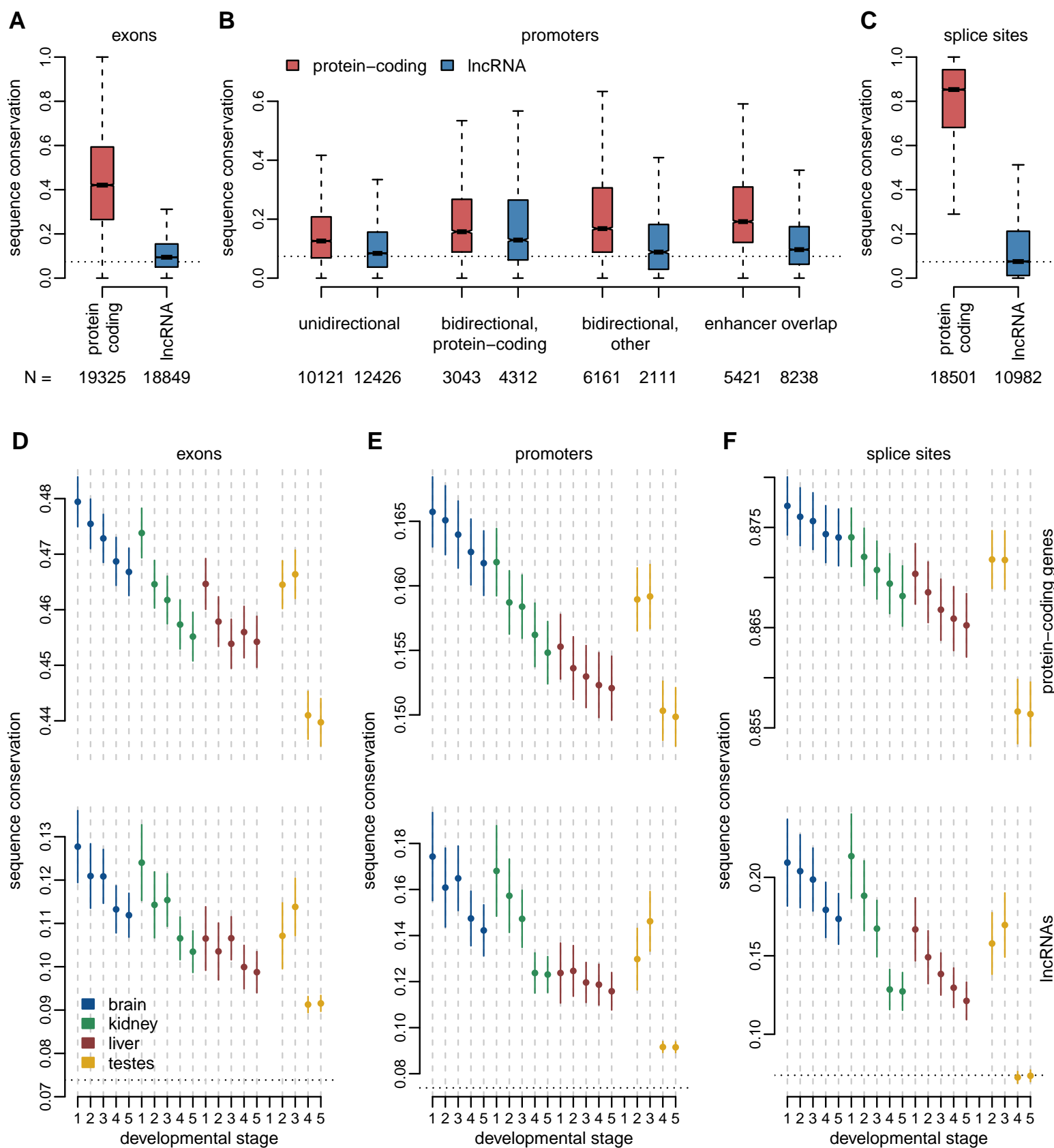
Darbellay and Necsulea, Figure 3



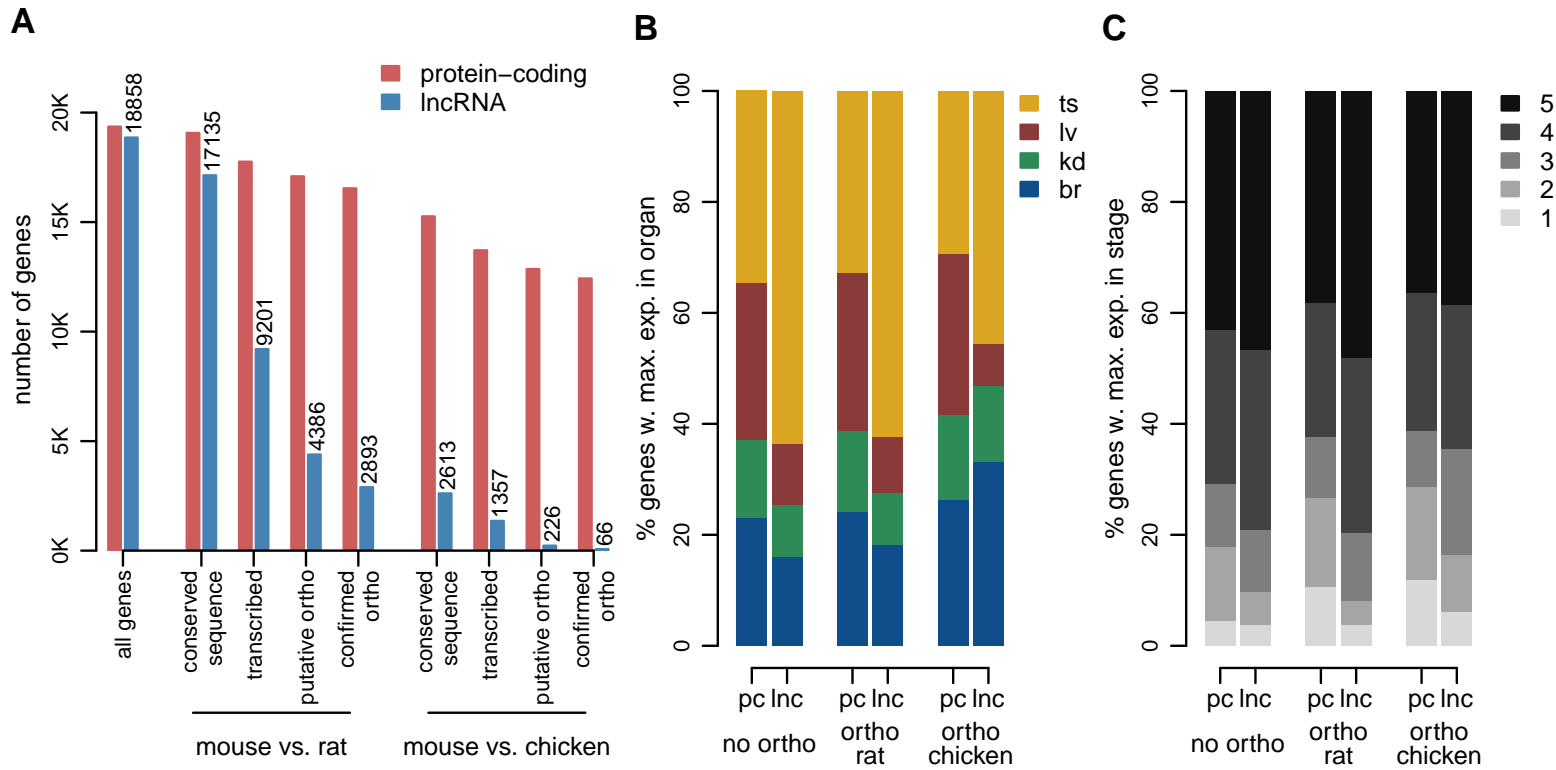
Darbellay and Necsulea, Figure 4



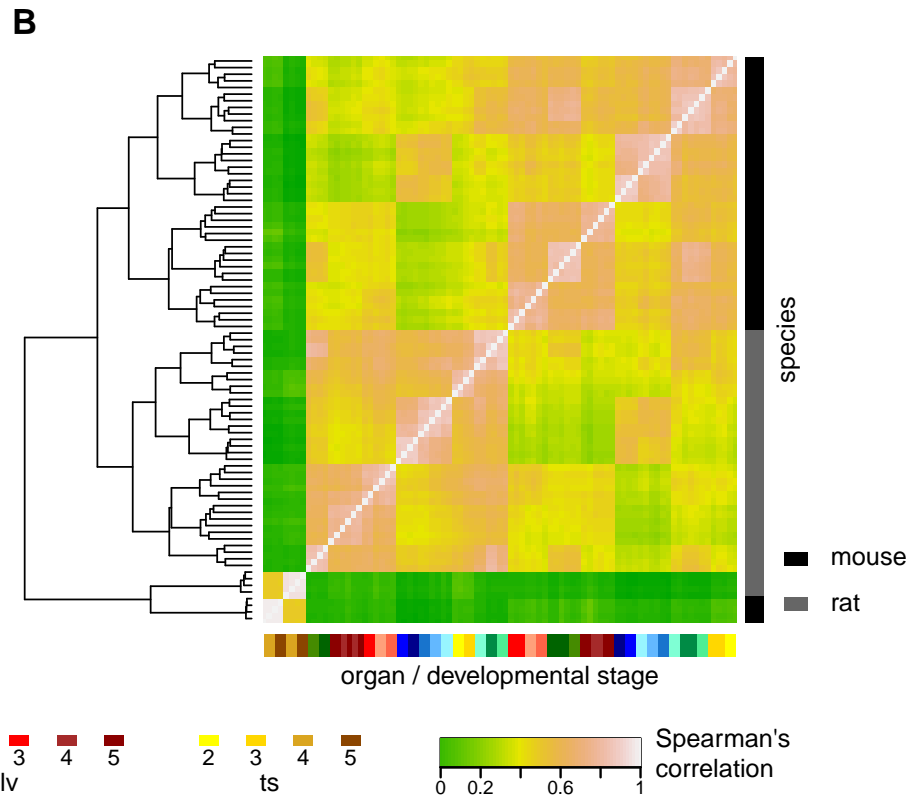
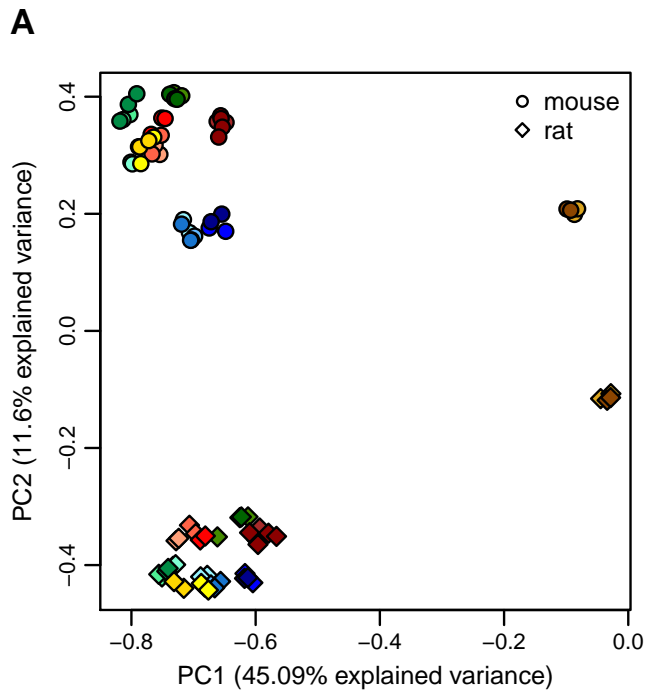
Darbelay and Necsulea, Figure 5



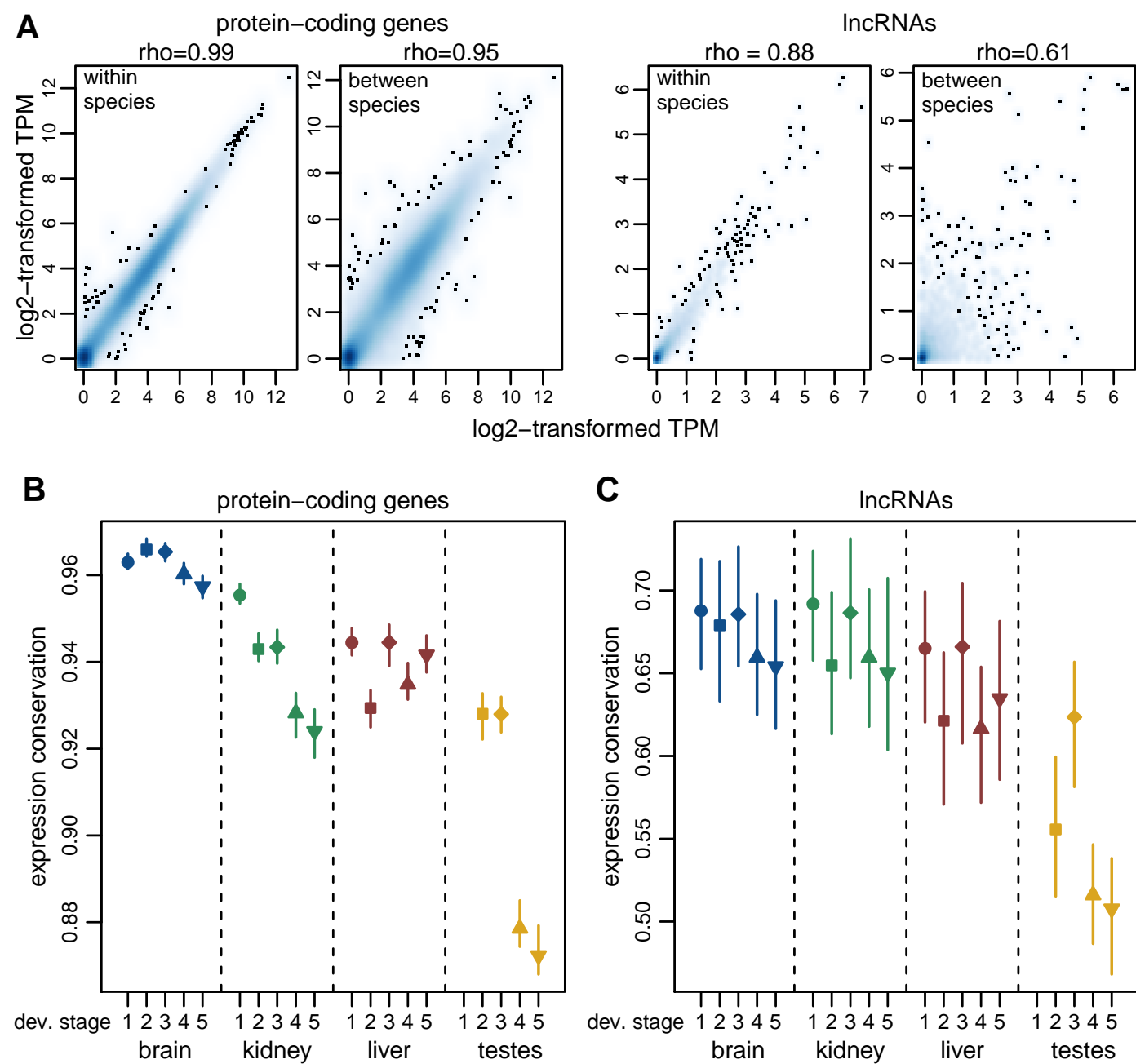
Darbellay and Necsulea, Figure 6



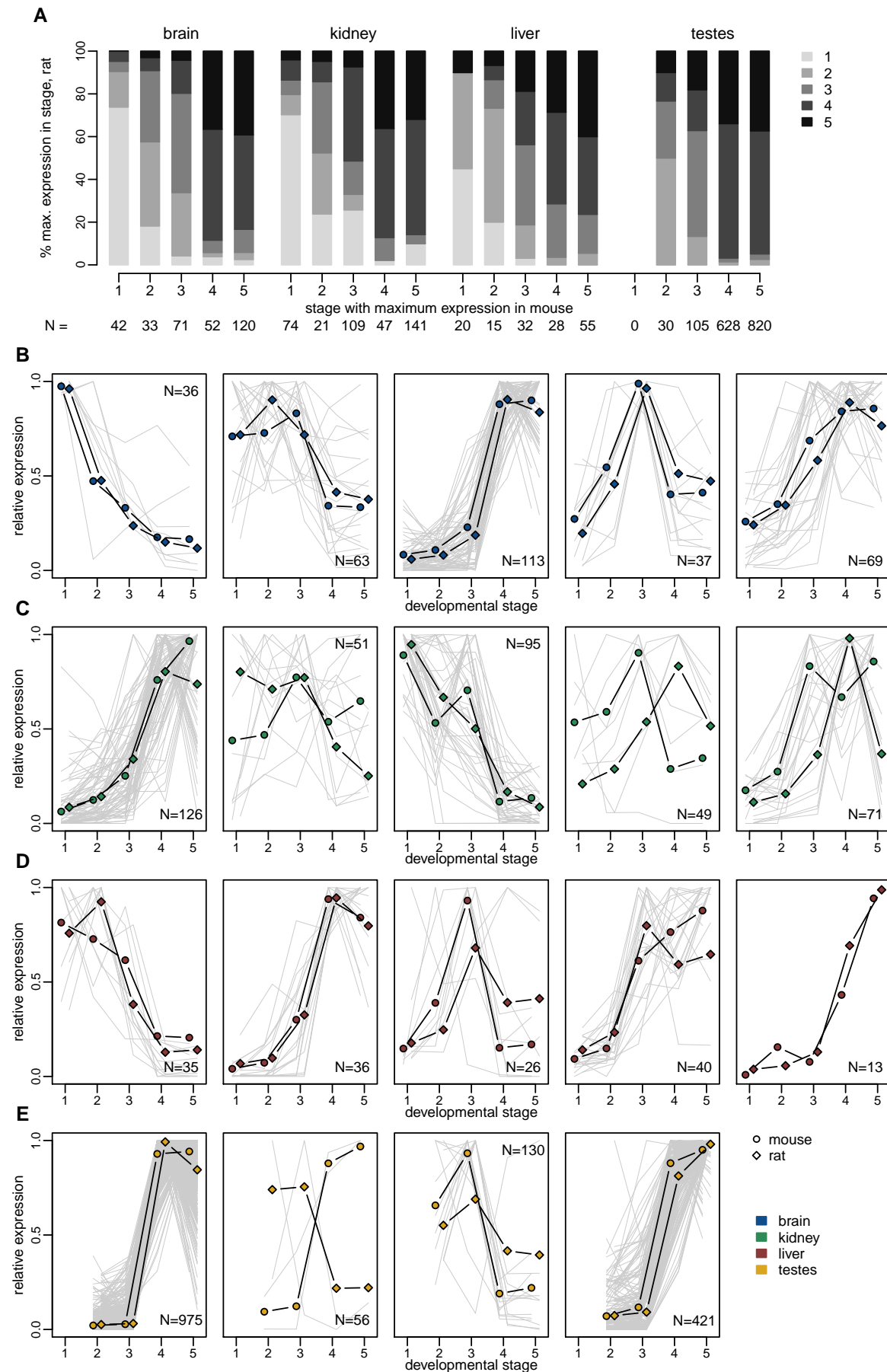
Darbellay and Necsulea, Figure 7



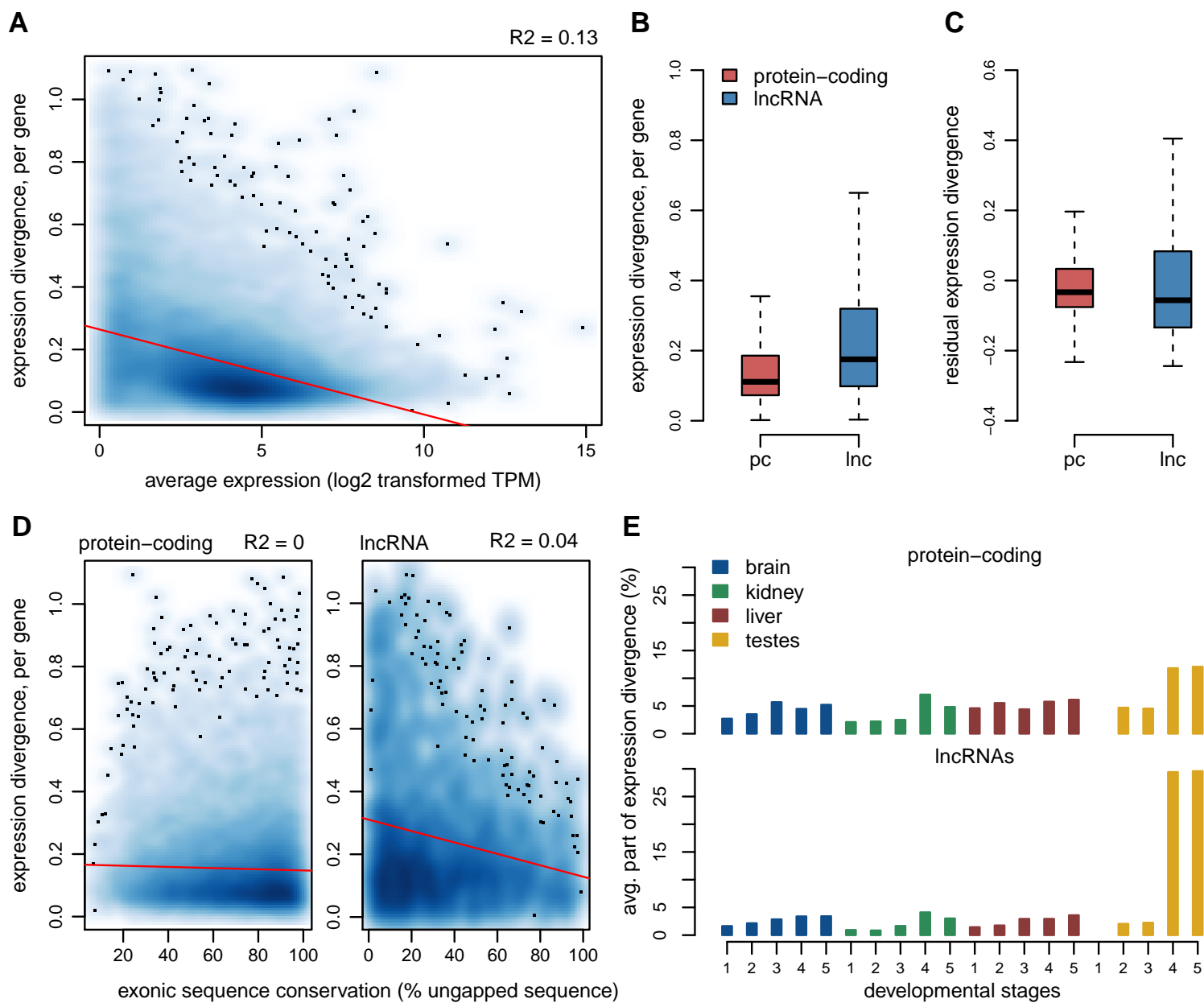
Darbellay and Necsulea, Figure 8



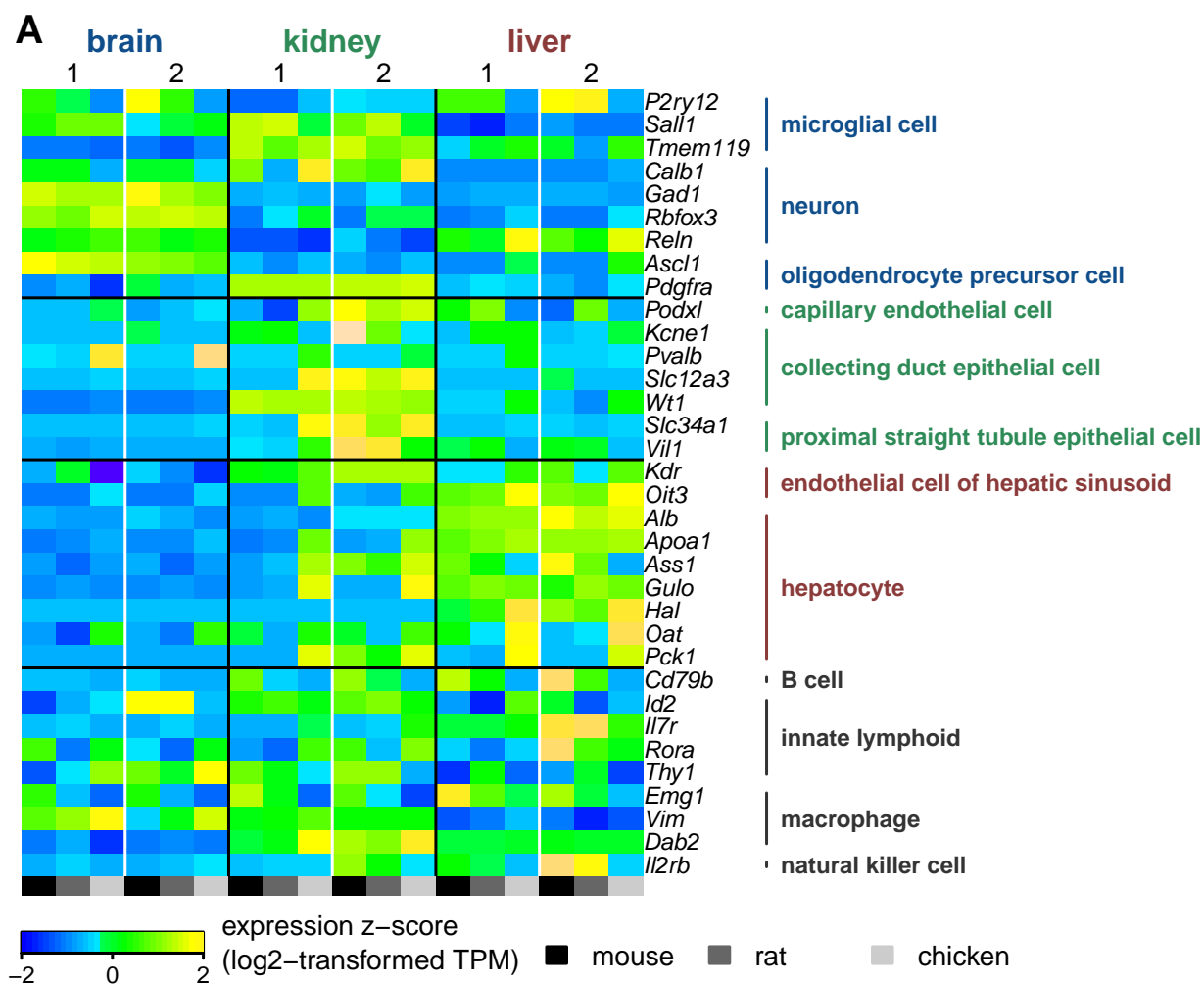
Darbelay and Necsulea, Figure 9



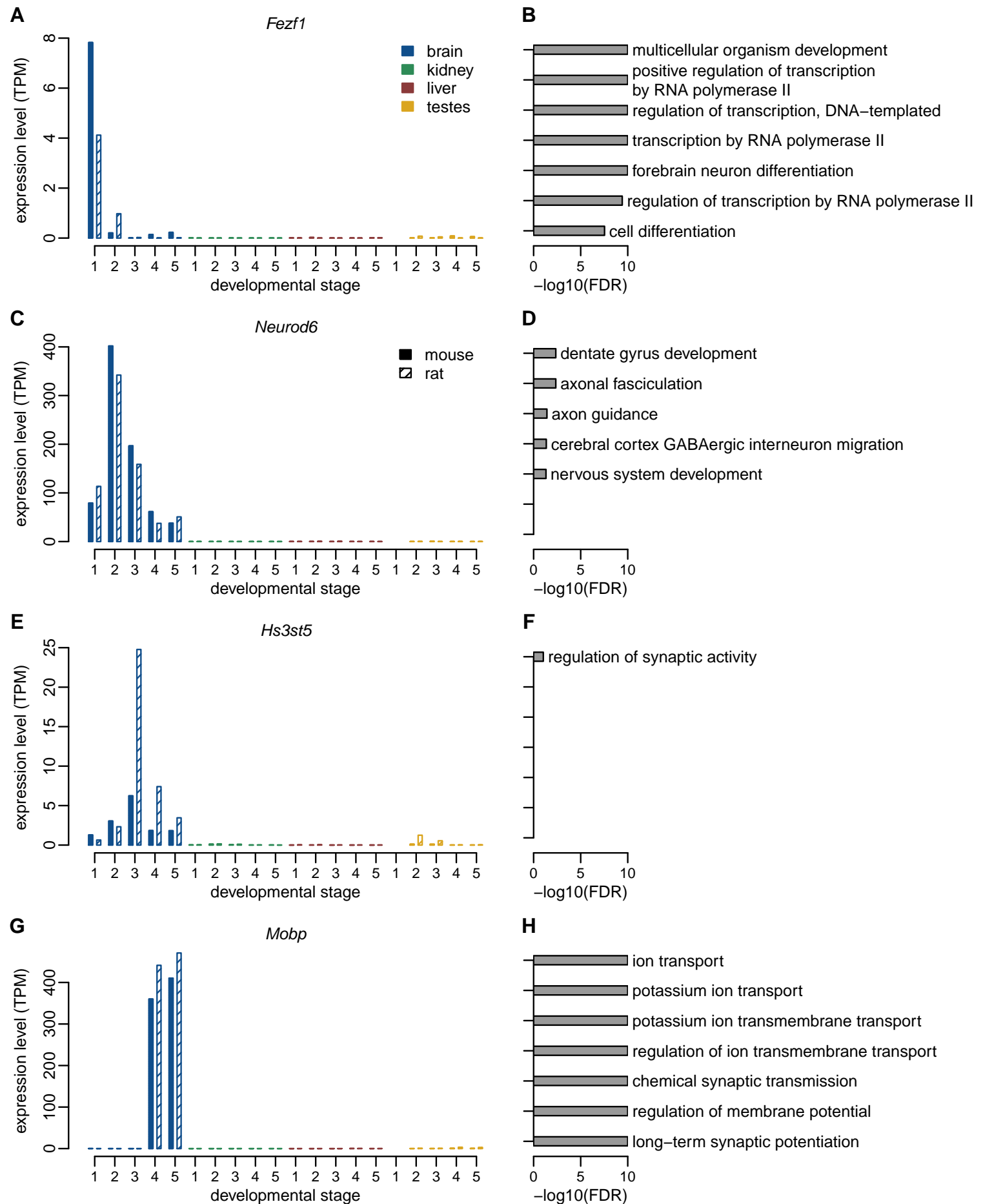
Darbelay and Necsulea, Figure 10



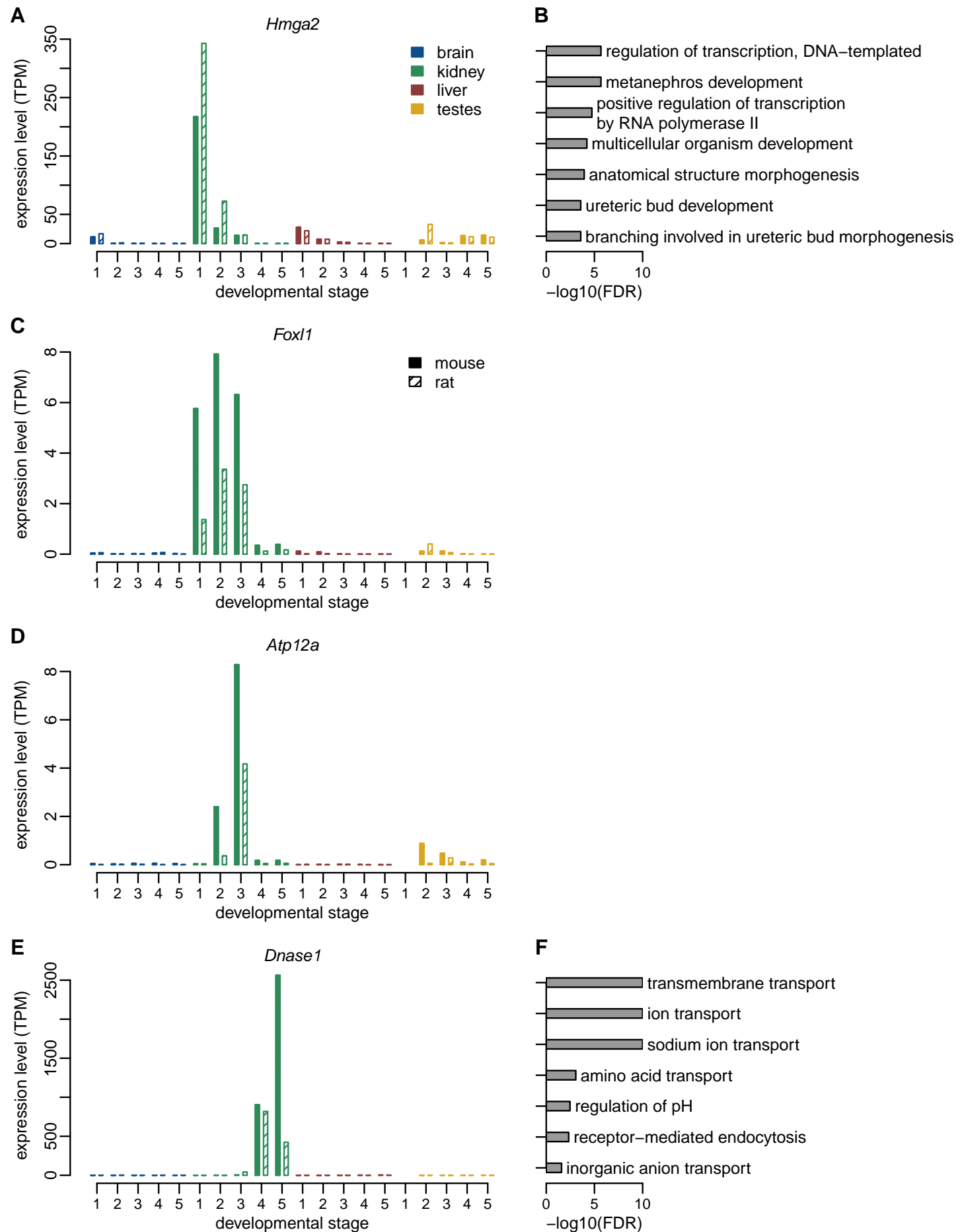
Darbelay and Necsulea, Supplementary Figure 1



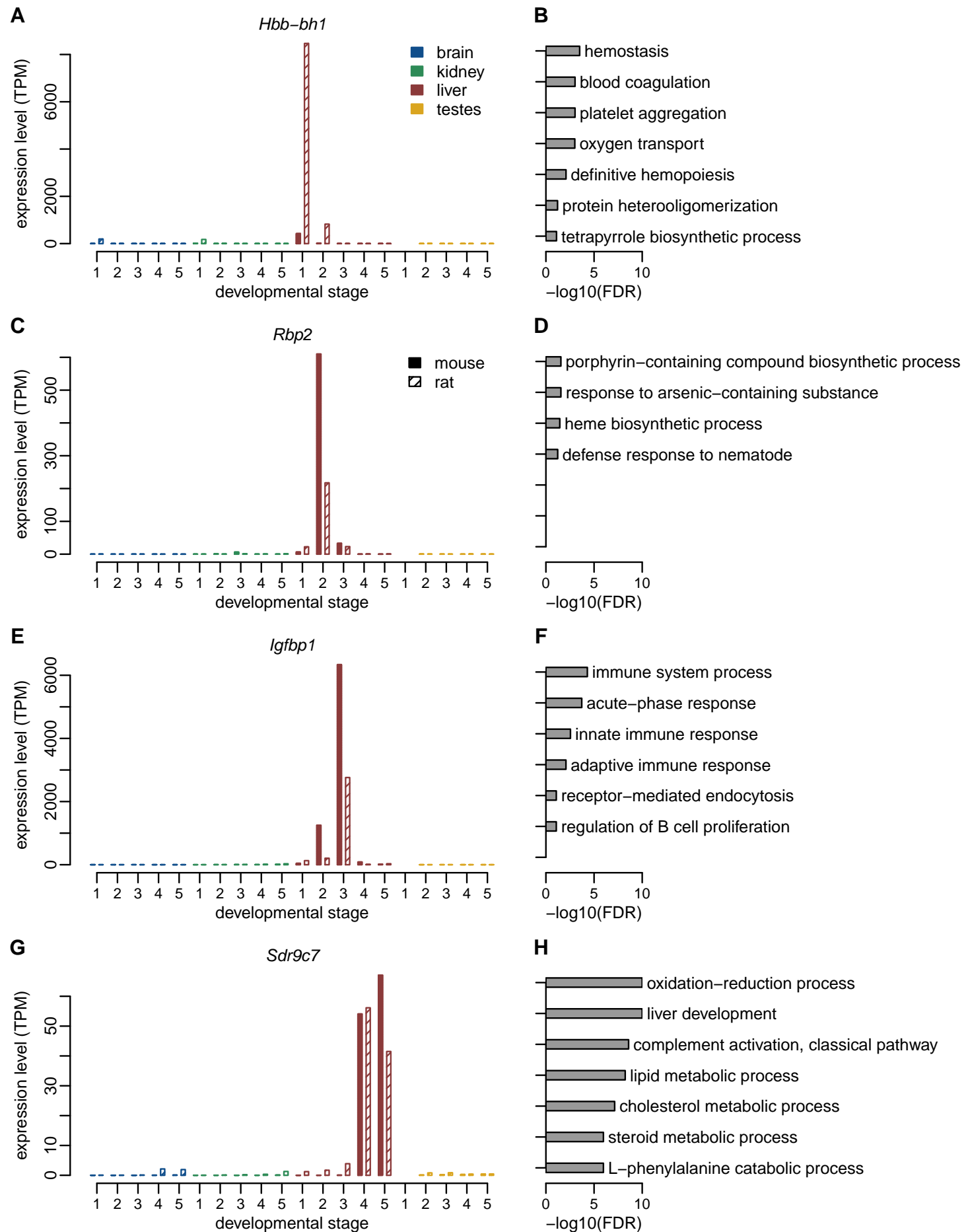
Darbelay and Necsulea, Supplementary Figure 2



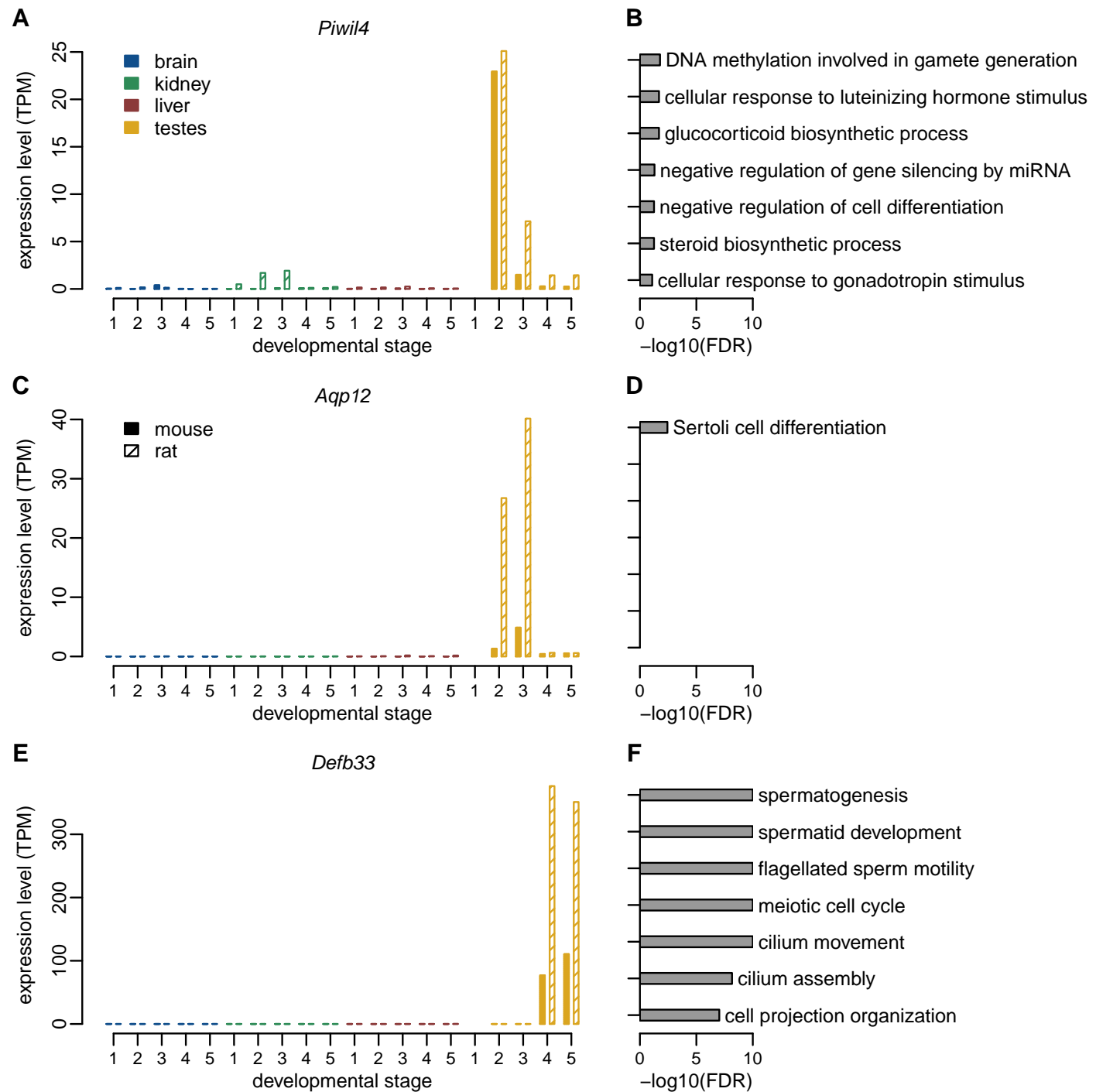
Darbelay and Necsulea, Supplementary Figure 3



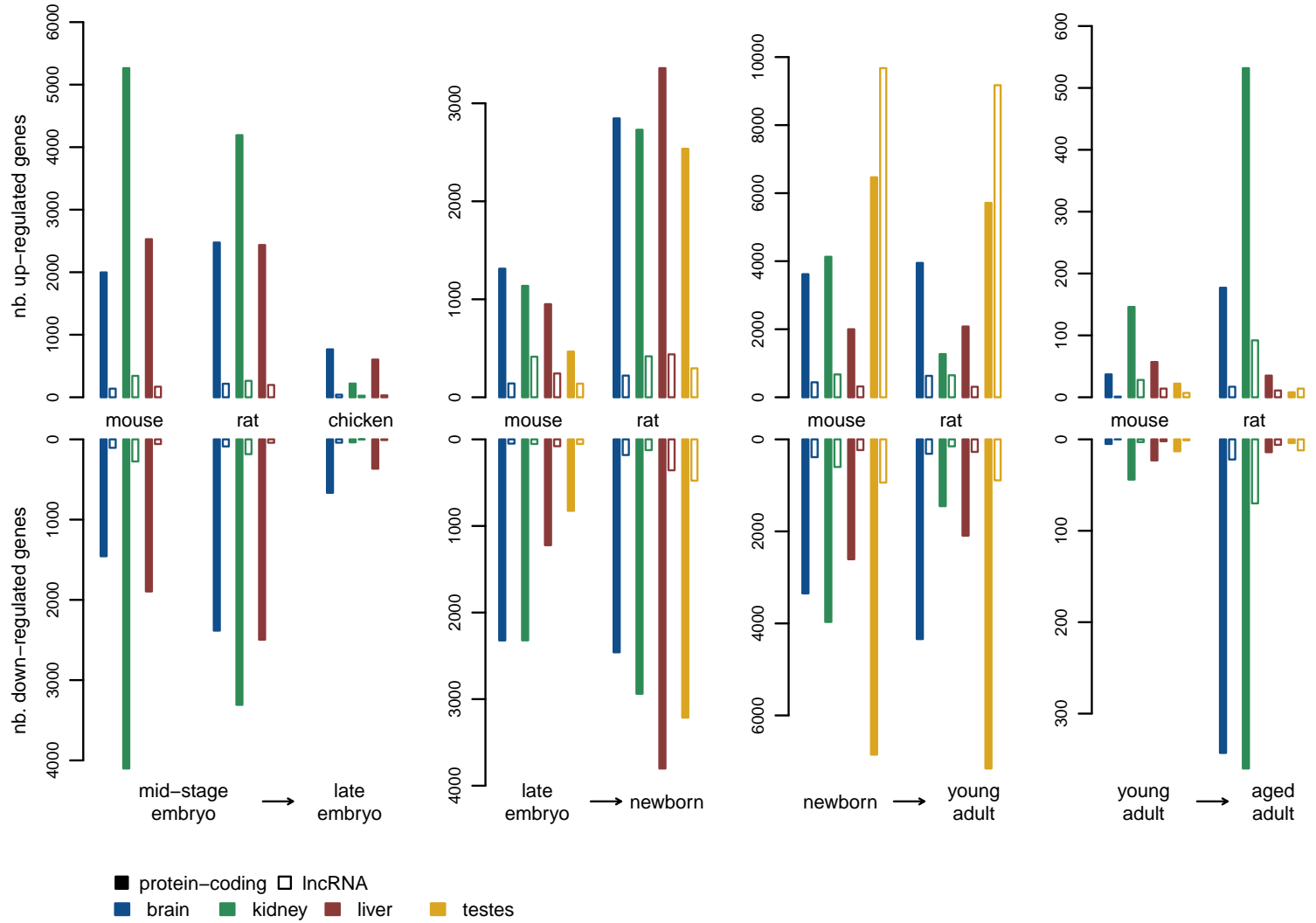
Darbelay and Necsulea, Supplementary Figure 4



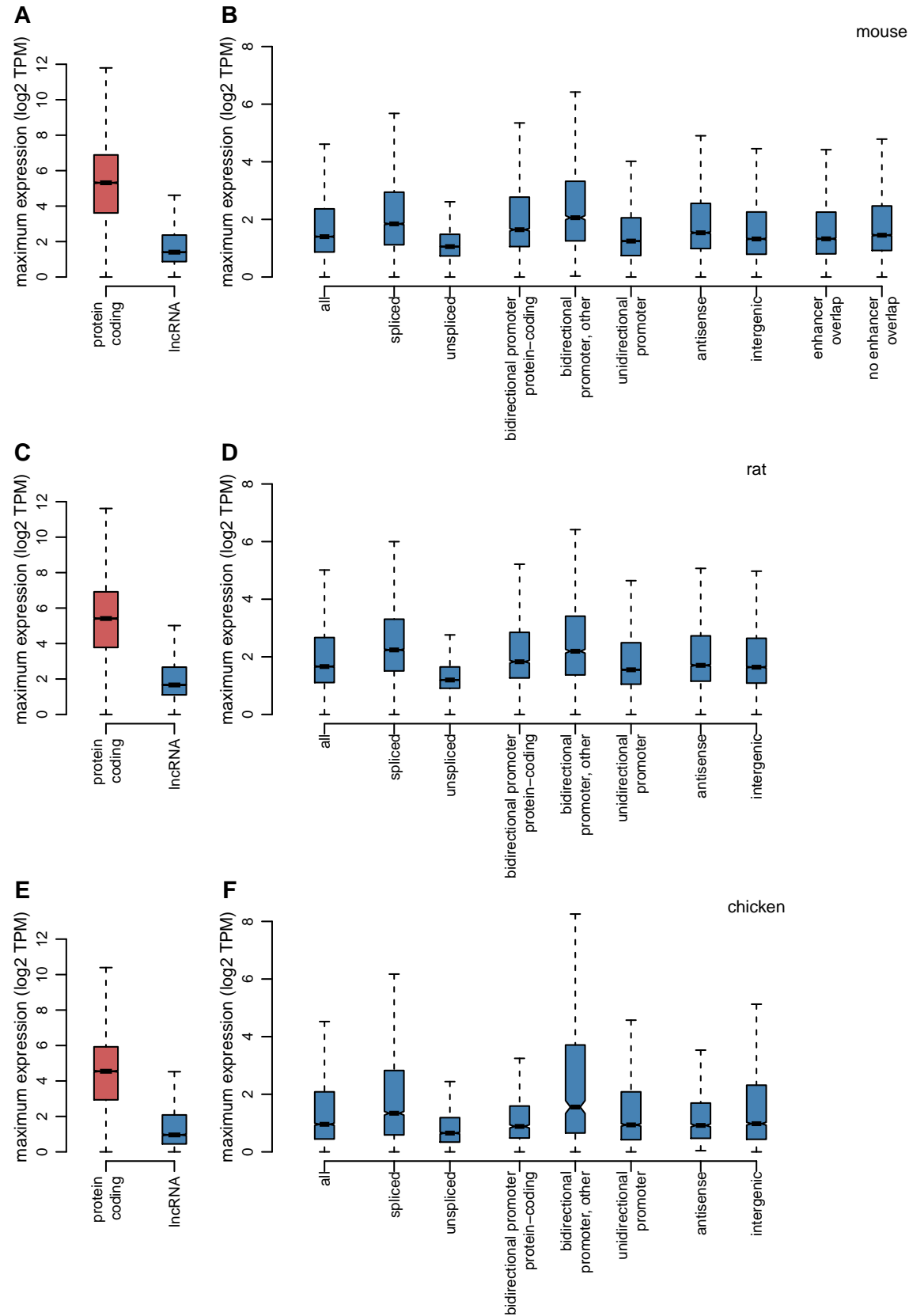
Darbelay and Necsulea, Supplementary Figure 5



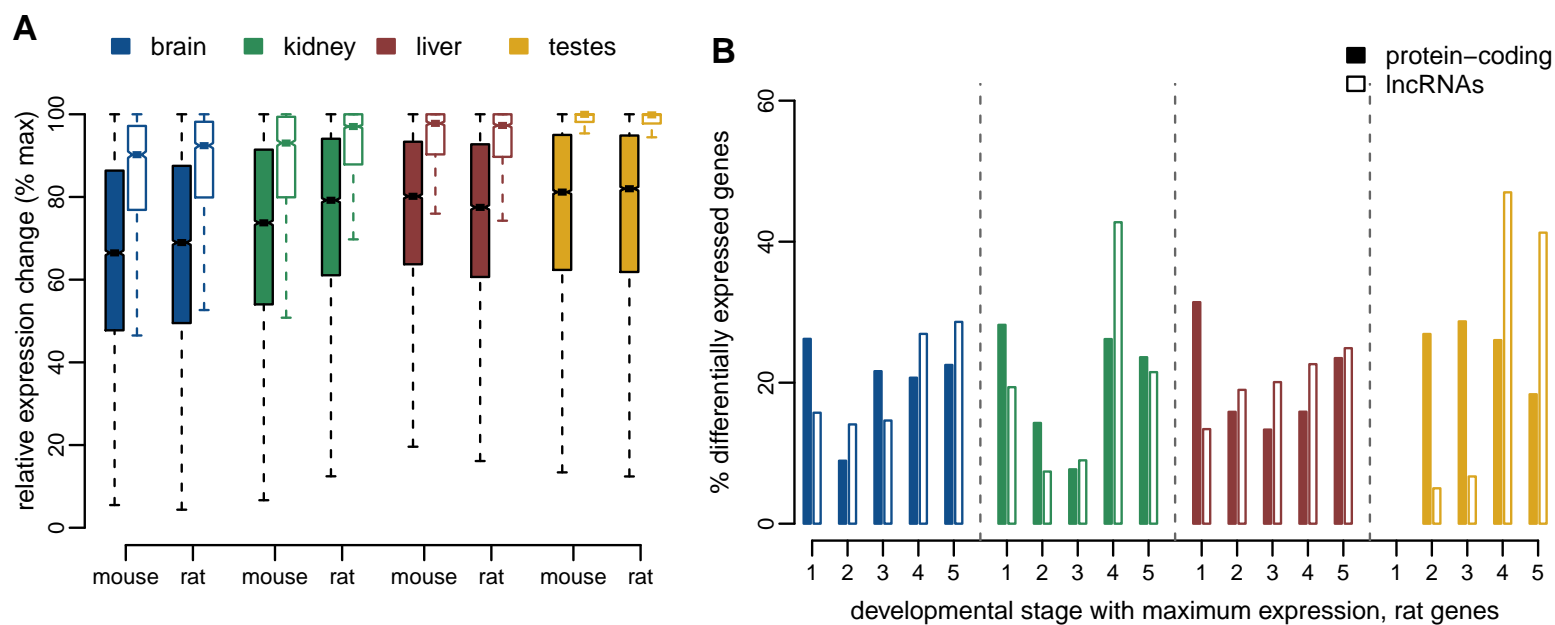
Darbellay and Necsulea, Supplementary Figure 6



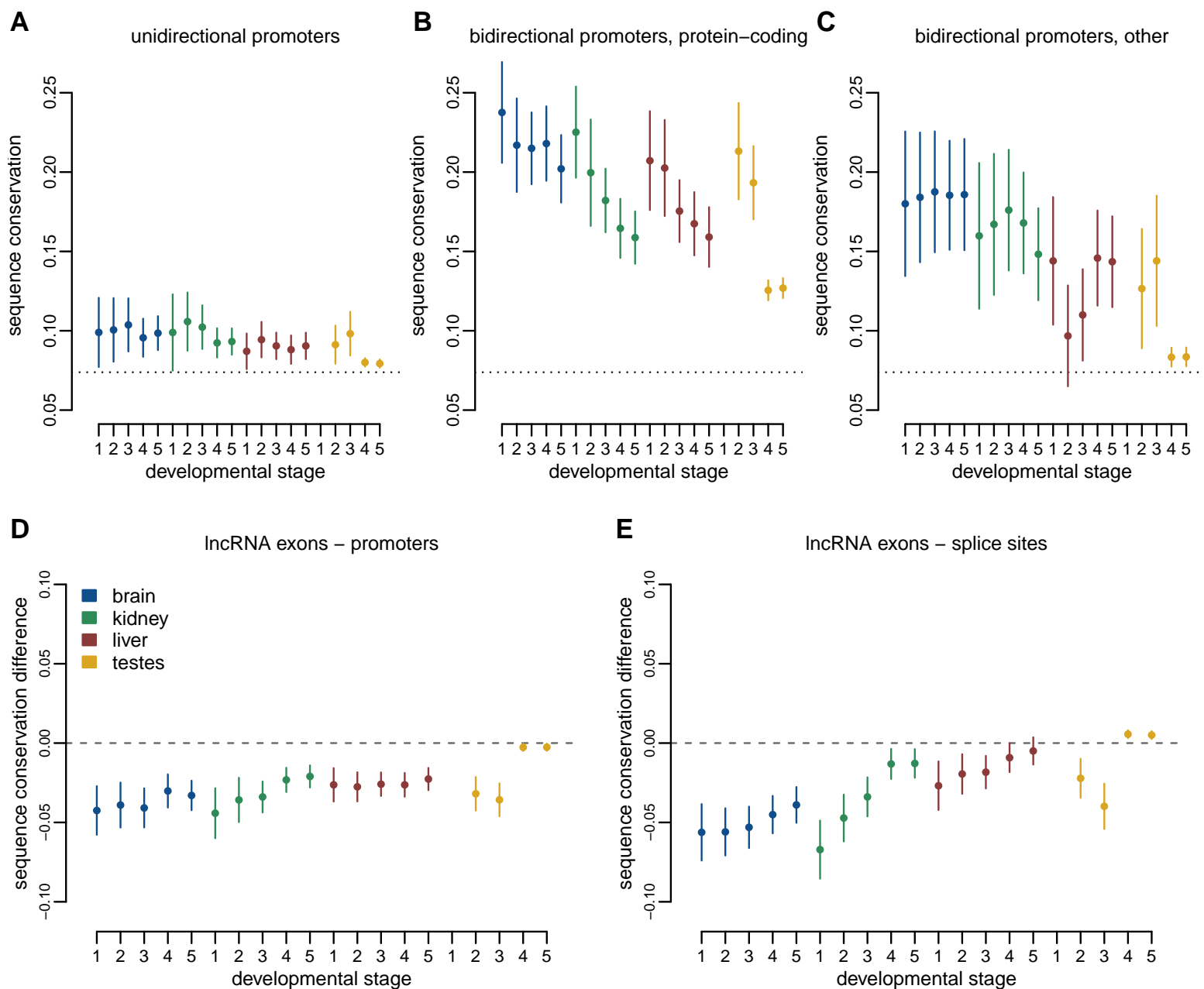
Darbellay and Necsulea, Supplementary Figure 7



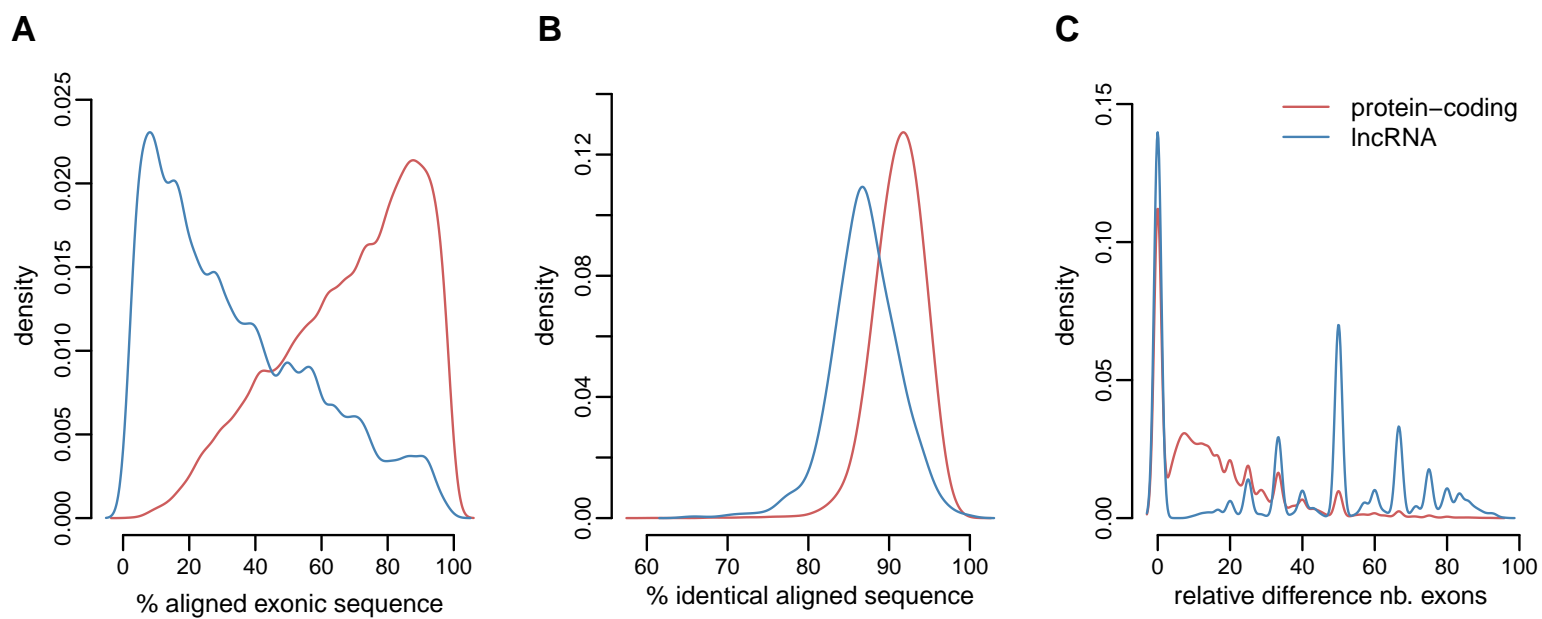
Darbellay and Necsulea, Supplementary Figure 8



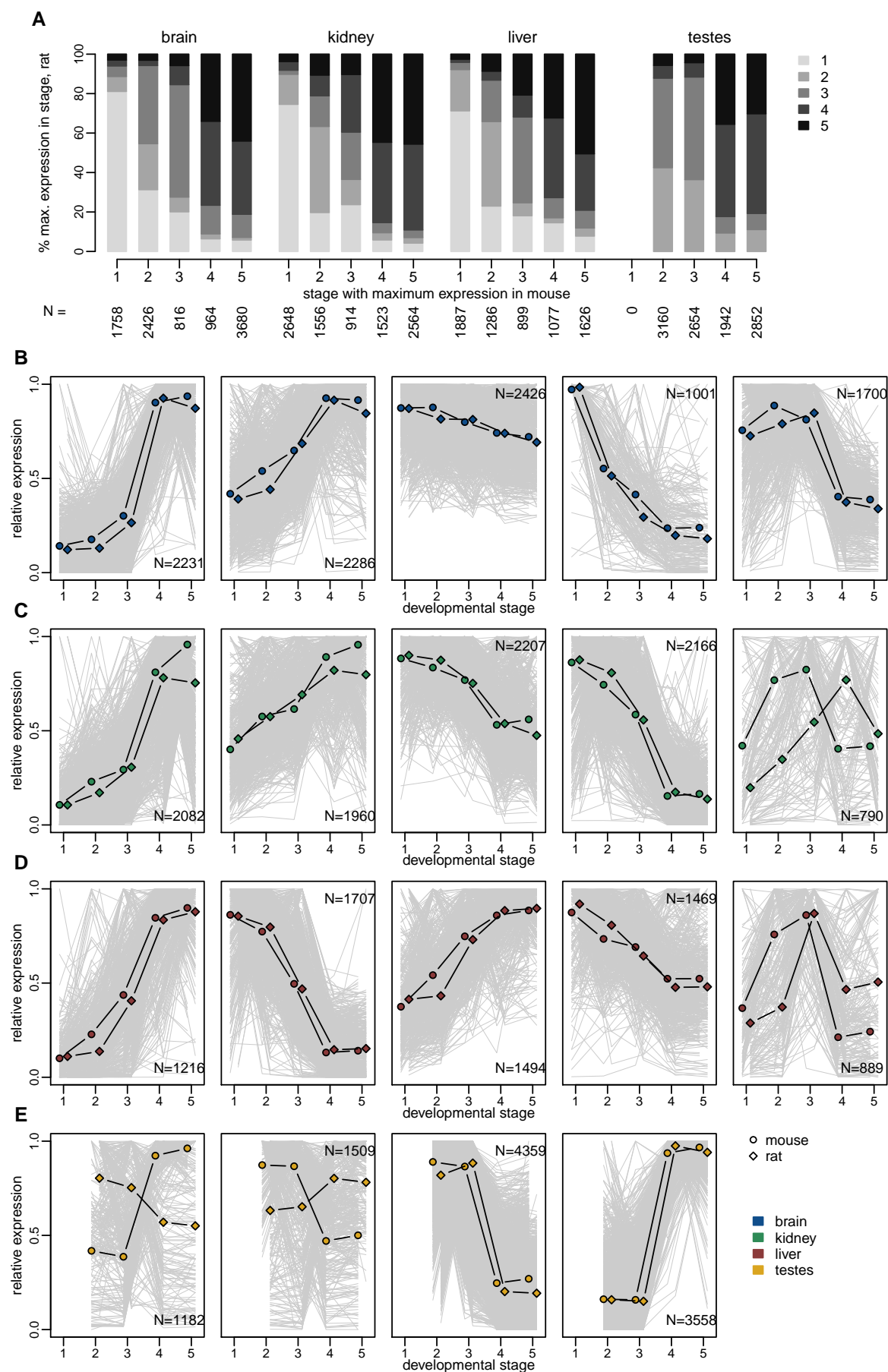
Darbelay and Necsulea, Supplementary Figure 9



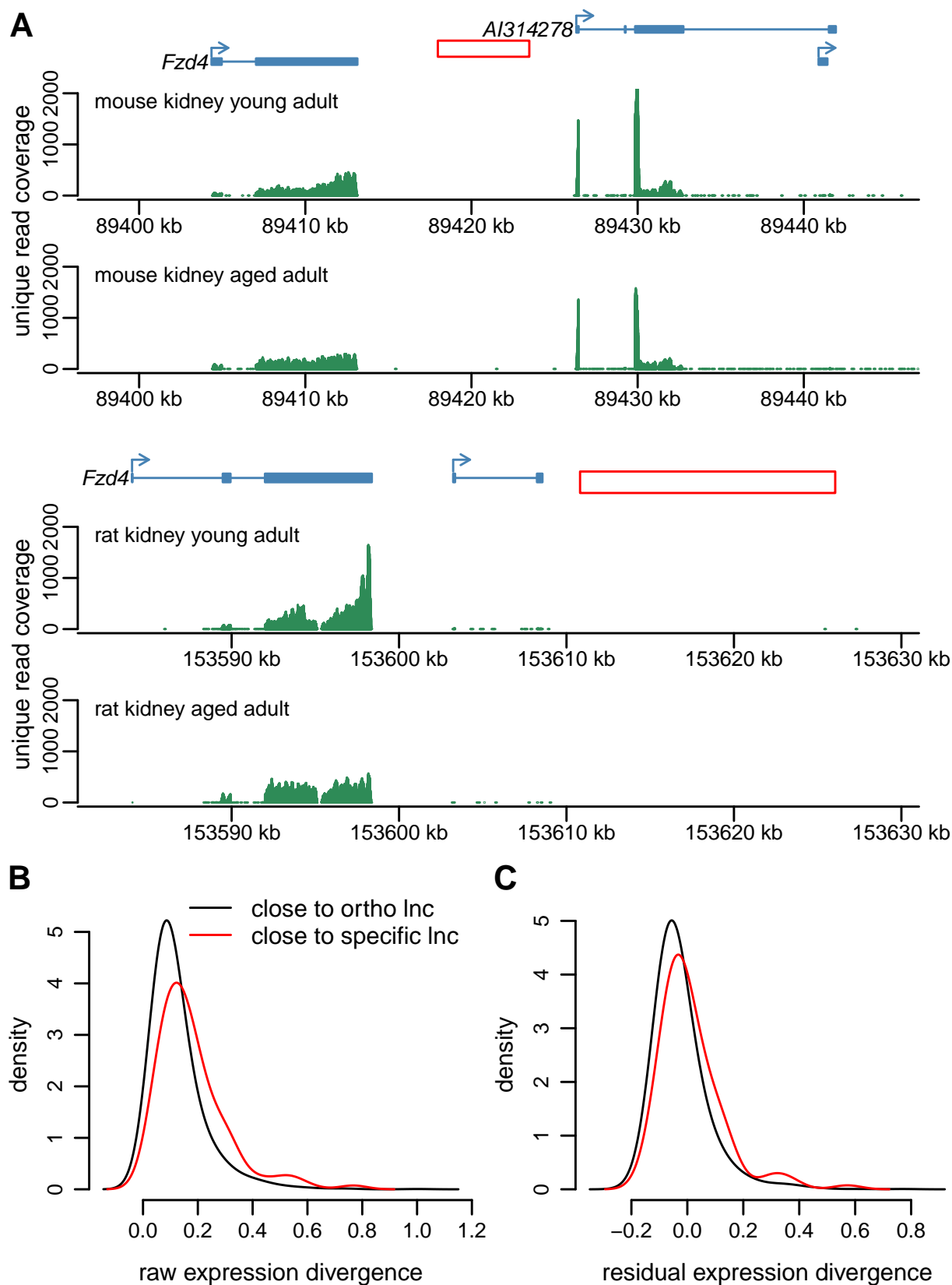
Darbellay and Necsulea, Supplementary Figure 10



Darbellay and Necsulea, Supplementary Figure 11



Darbelay and Necsulea, Supplementary Figure 13



Darbellay and Necsulea, Supplementary Figure 14

